

**WA School of Mines: Minerals, Energy and Chemical Engineering
Department of Petroleum Engineering**

**New Analyses Methods to Improve the Understanding of Shale
Hydration and Dispersion in Drilling Fluids**

Prabhu Elango

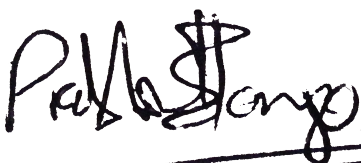
**This thesis is presented for the Degree of
Master of Philosophy (Petroleum Engineering)
of
Curtin University**

November 2018

Declaration

To the best of my knowledge and belief this thesis contains no material previously published by any other person except where due acknowledgement has been made. This thesis contains no material which has been accepted for the award of any other degree or diploma in any university.

Prabhu Elango


Prabhu Elango

Signature: Prabhu Elango

Date: 11 November 2018

This thesis is dedicated to my parents, Elango Ganapathi and Bala Ilango, for their infinite love and support.

Acknowledgements

I would first like to thank my thesis advisor and research supervisor Dr. Masood Mostofi. I am indebted to him for initiating my interest in this area of research. He consistently allowed this thesis to be my own work, but steered me in the right direction whenever he thought I needed it. He welcomed all my questions with a smile and I am deeply grateful for his guidance.

I am grateful to my co-supervisors Dr. Phillip Fawell, Dr. Frank Samani and Dr. Alton Grabsch. Their expertise in this area of research and guidance really made a difference and it was an honour to work with them.

I would like to thank Dr. Ryan Noble and Dr. Michael Verrall for their assistance with the automated particle analyzers that were used in this research project.

And finally, last but by no means least, a big thank you to everyone in building 619. It was great sharing the laboratory with all of you during the last two years.

Table of Contents

Abstract	1
Chapter 1	2
Introduction	2
1.1 Background.....	2
1.2 Objectives	6
1.3 Significance	7
1.4 Organisation of Thesis	7
Chapter 2	8
Literature Review	8
2.1 Shale swelling mechanisms.....	8
2.2 Shale instability	13
2.3 Shale inhibition	19
2.4 Analysing shale reactivity with laboratory methods.....	20
2.4.1 Sample Description.....	23
2.4.2 X-ray Diffraction.....	25
2.4.3 Cation Exchange Capacity	26
2.4.4 Scanning Electron Microscopy	28
2.4.5 Swelling Test	29
2.4.6 Dispersion Test	31
2.4.7 Capillary Suction Time Test.....	32
2.4.8 Bulk Hardness Test	33
2.4.9 Bentonite Inhibition test	34
2.4.10 Fracture Development Test and Immersion Test.....	35
Review of laboratory tests	36
2.5 Particle analysis.....	36
2.6 Clay/Shale particle inhibition test	38
ii. Particle size distribution	41
iii. Rheology measurements.....	42
Chapter 3	44
Research Methodology	44
3.1 Introduction	44
3.2 Experimental Program	45
3.2.1 Testing with shale rock	51

3.2.2 Extended test.....	55
3.2.3 Materials used in testing	56
Chapter 4	58
Results and Discussion	58
4.1 Introduction	58
4.2 Experimental results	59
4.2.1 Effect of potassium chloride	59
Particle count.....	59
Particle size distribution.....	61
4.2.2 Field application studies.....	64
Effect of using shale core rock on particle size distribution.....	64
4.2.3 Effect of time on.....	67
Particle count.....	67
Particle size distribution.....	68
Rheology	69
4.2.4 Industrial additives	70
i. AMC Xtrahib	72
ii. Low Molecular Weight PHPA.....	75
iii. High Molecular Weight PHPA.....	78
iv. Kla-stop	81
v. Xanthan Gum	84
Chapter 5	89
Conclusion	89
5.1 Contribution	89
5.2 Field Implications	91
5.3 Recommendations and future work	92
Appendix	95
Bibliography	127

List of Figures

Figure 1. Schematic of circulation of drill cuttings from petroleum drilling operations.	4
Figure 2. Impact of solids content on drilling rate	5
Figure 3. Operating rig days increase with increase in solids content	6
Figure 4. (Left) SEM image of Wavy subhedral montmorillonite crystal ; (Right) SEM image of Illitic clay	8
Figure 5. (Left) SEM image of smectite clay ; (Right) SEM image of authigenic kaolinite packet	9
Figure 6. Simplified schematic of the DDL in the surface of clay minerals indicating pressure generated by forced overlap of the DDL.....	10
Figure 7. (Left) Osmotic clay swelling; (Right) Inner-crystalline clay swelling	11
Figure 8. Simplified diagram of all the forces acting downhole on a shale rock.	12
Figure 9. Simple diagram of the onset of several fronts around a borehole over a period.	13
Figure 10. Shale Instability causing Stuck Pipe.....	14
Figure 11. Schematic of a Shale Shaker.....	15
Figure 12. Hydrocyclone Efficiency increasing with increasing Cutting Particle Diameter	16
Figure 13. Shale Swelling Indicator.....	17
Figure 14. Shale Disintegration.....	19
Figure 15. Process of test selection based on shared shale sample features	21
Figure 16. Types of testing.....	22
Figure 17. Fracture propagation from shale to limestone	25
Figure 18. Sample diffraction powder patterns	26
Figure 19. Sample XRD test result showing how each different phase produces a different combination of peaks	26
Figure 20. Filter paper showing the end point in CEC determination by titration with methylene blue: a light blue halo around the drop.....	27
Figure 21. Typical results for CEC ranges of soil materials	28
Figure 22. SEM photograph of a Kaolinite sample	29
Figure 23. Swelling test apparatus	30
Figure 24. Sample swelling test results of shale capsules in different brines	31
Figure 25. Sample dispersion test results involving industrial additives	32
Figure 26. Sample CST results of how increasing the swelling clay percentage or decreasing the average particle size of a sample will result in increased CST times	33
Figure 27. (Left) Bulk hardness tester; (Right) sample results using shale cuttings with additives	34
Figure 28. Sample bentonite inhibition test results with apparent viscosity variation vs bentonite content	34
Figure 29. Time-lapse images showing changes in the microstructure of sandstones before and after injection of CO ₂ aqueous solution	35
Figure 30. (Left) Sample particle count result from FBRM ; (Right) Sample particle size distribution result from Mastersizer	37
Figure 31. (Left) FRM electronics box and purge unit; (Right) FBRM apparatus and pipe-mounting adapter	38

Figure 32. (Left) FBRM Probe Schematic; (Right) Chord Length of particle schematic.....	39
Figure 33. (Left) Schematic drawing of probe position relative to the overhead stirrer; (Right) Sample photo.	40
Figure 34. Results of the use of FBRM as a tool for real-time measurement of solid particles.....	40
Figure 35. (Left) Malvern Mastersizer 3000; (Right) Laser Diffraction Schematic. ...	42
Figure 36. Shear stress and deformation rate relationship of different fluids	43
Figure 37. Shear stress vs. shear rate of whole mud systems	43
Figure 38. General procedure chart.	47
Figure 39. Experimental setup.	48
Figure 40. Sample FBRM results of a triplicate of tests.....	49
Figure 41. Sample result showing how the average is obtained from 12 tests.....	50
Figure 42. Sample bubble peak in an aqueous dispersion	51
Figure 43. Exact location of drill hole (MSDP02), ~52 km west of Port Augusta	52
Figure 44. Red and green, finely laminated shale with minor sandstone, Tregolana Shale Member	52
Figure 45. Real-time XRF geochemistry and XRD mineralogy on drill cuttings.....	53
Figure 46. (Top) Port Augusta shale rock sample; pulverized shale; (Bottom) Pulverizer/Grinder; Motorized sieve shaker.....	53
Figure 47. PSD of dry shale sample.....	54
Figure 48. Field trial of RoXplorer Coiled Tubing rig at Port Augusta - Photo courtesy of DET CRC.	54
Figure 49. (Left) Ofite Model 900 Viscometer; (Right) Sample Viscometer results of a simple additive solution.	55
Figure 50. (Left) Sack of API Bentonite used for testing; (Right) PSD of dry Sodium Montmorillonite sample.	56
Figure 51. The variation of particle count during 2hr degradation experiments performed at various concentrations of KCl.	60
Figure 52. The effect of KCl on the size distribution of clay particles.	61
Figure 53. The variation of particle size distribution of clay particles after 2 hours of mixing at various KCl concentrations.	63
Figure 54. Variation of two group sizes of clay particles at different KCl concentrations after two hours of mixing.	64
Figure 55. Coiled tube drilling system, RoXplorer, used in the drilling trials in South Australia	65
Figure 56. Variation of size distribution of shale formation at different KCl concentrations.	66
Figure 57. The effect of KCl concentration on the particles in the range of 0.1-1 μm , 1-10 μm and 10-100 μm	66
Figure 58. Sample FBRM test results.....	67
Figure 59. Variation of clay particle distribution in water during a 47 hr experiment.	68
Figure 60. Variation of volumetric percentage of particles in groups of 0.1-1 μm , 1-10 μm and 10-100 μm at different times.....	69
Figure 61. Variation of apparent viscosity during the 47 hr test.....	70

Figure 62. Variation of apparent viscosity at shear rate of 1020 1/s during the 47 hr test.	70
Figure 63. AMC Xtrahib particle count results.	72
Figure 64. AMC Xtrahib normalized count results.	73
Figure 65. AMC Xtrahib particle size results	74
Figure 66. AMC Xtrahib particle size distribution.....	75
Figure 67. LMwPHPA particle count results.	75
Figure 68. LMwPHPA normalized count results.	76
Figure 69. LMwPHPA particle size results.	77
Figure 70. LMwPHPA particle size distribution.....	78
Figure 71. HMwPHPA particle count results.	79
Figure 72. HMwPHPA normalized count results.	79
Figure 73. HMwPHPA particle size results.....	80
Figure 74. HMwPHPA particle size distribution.....	81
Figure 75. Kla-stop particle count results.	82
Figure 76. Kla-stop normalized count results.	82
Figure 77. Kla-stop particle size results.....	83
Figure 78. Kla-stop particle size distribution.....	84
Figure 79. Xanthan Gum particle count results.	85
Figure 80. Xanthan Gum normalized count results.	85
Figure 81. Xanthan Gum particle size results.....	86
Figure 82. Xanthan Gum particle size distribution.....	87
Figure 83. Conceptual variation of particle size distribution during the chemical degradation of cuttings: (a) variation of total size distribution; (b) variation of the proportion of fine and coarse particles.	90
Figure 84. The variation of suspension fluid during the cutting degradation: (a) variation of viscosity; (b) variation of filtration rate.....	91

Abstract

Encountering shale intervals during drilling operations can become a challenge due to the swelling tendencies of shale when interacting with water. This sensitivity to water and the resulting swelling mechanisms that occur are complicated subjects. The important question of how shales hydrate and swell is difficult to clarify as the term 'shales' applies to a broad group of laminated rocks where clay mineralogy and physio-chemical properties can vary widely. Incorporating shale inhibiting additives into the drilling mud has been a commonly used technique to minimize and possibly mitigate this swelling of shale.

Synthetic muds are widely used on a majority of shale oil/gas drilling operations in the United States which is ultimately a large portion of the worldwide drilling count. Water-based muds that give comparable performance to synthetic muds are increasingly growing in demand, primarily due to the growing concern placed on the environmental impact of operations, with water-based alternatives ultimately being more environmentally friendly.

This work details novel experimental methods that were applied to investigate shale and clay mineral reactivity as they come in contact with water-based drilling fluids and gain new information about the dynamics of the inhibitory process. A conventional additive, Potassium Chloride, and a few other commercial additives were tested and their shale stabilizing potential was investigated through the use of two advanced particle analyzers. The first was the Focused Beam Reflectance Measurement (FBRM) M500 - a probe-based tool that is inserted directly into a medium to track the particle size and count in real time in that particular medium. The second tool that was used was the Malvern Mastersizer 3000, which uses laser diffraction to obtain particle size distributions for wet and dry dispersions. These tools were also used to monitor changes caused by several industrial additives to the particle count and particle size distribution of the shale and clay samples. A benchmark and comparison of results were completed that concluded that these modern pieces of equipment can indeed be used to analyze the process of shale hydration and dispersion and add another dimension to this field of study by linking clay swelling and breakdown with particle characteristics.

Chapter 1

Introduction

1.1 Background

Economic infrastructures worldwide are dependent on resource extraction activities such as mineral and hydrocarbon drilling production. In these operations, drilling plays a dynamic and crucial role. It is one of the most crucial operations in all mineral exploration procedures and often can be the most expensive. An area of research that remains evergreen and popular is in the improvement of drilling technologies that lower the cost of drilling and increase the probability of finding and extracting oil and gas reserves.

Drilling in the mining industry has been centred on two main purposes - exploration drilling and production drilling, while drilling in the petroleum industry has been focussed on targeting larger reservoirs traditionally, but most drilling operations nowadays involve discovering smaller, less readily detectable reservoirs. The development of fields nowadays requires overcoming significant challenges as these fields are usually more geologically complex. Efficient exploration and production techniques are required to guarantee the quality of life in many parts of the world.

Improvements in drilling technologies, including the development and usage of highly effective drilling fluids, has allowed wells to be drilled deeper, longer and under more challenging conditions. Figure 1 shows a simplified schematic of a general drilling operation. An important part of any drilling operation - drilling fluids, perform numerous functions during the drilling operation such as cooling and lubricating the bit, controlling formation pressures, providing shale stability, suspending drill cuttings, minimizing formation damage and facilitate cementing and completion. The drilling mud is pumped down the drill string and flows back up the annulus, carrying cuttings up to the surface. The cuttings are then filtered out by the various solids control equipment at the surface. Ensuring that the mud performs all its tasks is a 24-hour operation usually involving a team of mud engineers. Efficient mud management includes a profound understanding of the chemicals and solids used to create muds and fully comprehending how each element behaves individually as well as part of a solution [3].

Drilling fluids represent on average 15 to 18% of the total cost (about \$1 million) of the entire petroleum well drilling operation [4]. Drilling fluids are water or oil-based or synthetic-based and depending upon the requirement of the drilling operation, the type of drilling fluid varies. Water-based fluids usually tend to impact the environment less than oil-based muds which are usually used for very deep drilling and for difficult depth drilling operations. Synthetic muds were developed by the oil and gas industry with synthetic and non-synthetic oleaginous (similar to oil) materials as the base fluid to provide the drilling performance features of traditional oil-based fluids but with lower environmental impact and in some cases less drilling waste [5]. At this time of writing, synthetic muds are widely used on a majority of shale oil/gas drilling operations in the United States which is ultimately a large portion of the worldwide drilling count. Water-based muds that give comparable performance to synthetic muds are certainly still demanded by operators due to increasing concern placed on environmental impact of operations, with water-based alternatives being more environmentally friendly. The environmental impact must be taken into account when designing the drilling fluid necessary besides considering the chemical structure and properties of the well. The disposal of drilling fluids after they have been used can pose a severe environmental challenge as the drilling fluid is, in varying degrees, toxic. The US Environmental Protection Agency has imposed strict global environmental regulations, standards, and guidelines and thus it has become compulsory for the drilling industry to develop a trend of producing environmentally friendly drilling practices [6].

As a result, non-environmentally friendly drilling fluids such as oil-based muds (OBM) are decreasing in popularity and researchers have been more focussed on developing novel drilling fluid systems that are environmentally acceptable [7-10].

Geologists define "Shale" as a fine-grained sedimentary rock composed of clay and silt-size particles with diameters of less than or equal to 62.5 microns [11]. Shale's constitute 60%-70% of Earth's sedimentary rocks [12] and the two common characteristics of all shales is that they all usually tend to have a high composition of clay minerals and possess extremely low permeability [13]. There are various classifications for the types of shales but the sampling used in the testing phase of this research work was limited to Black Shale as it was readily available.

One of the most critical aspects of Shale is their sensitivity to water. This is because the contact between clay-rich shale formations and water is directly related to causing wellbore instability and represents a tremendous challenge for the drilling industry. Clay-water interactions have been the subject of research in various disciplines. The study of shale and its properties is imperative because a significant proportion of all drilled formations are composed of shales, and these shales contribute heavily to wellbore-instability challenges that occur within the lifespan of a drilling operation [14]. Such shale-instability related problems are reported to cause over 1.5 billion U.S dollars per year to the drilling cost operations worldwide [15].

In total, for this research project, the type of clay samples being tested were limited to two - Sodium Montmorillonite and a Shale core sample. This shale sample was obtained from near Port Augusta, South Australia. It was obtained from field trials in the consolidated cover rocks of the Gawler Crator and is representative of the type of shale that are typically drilled in South Australia [16].

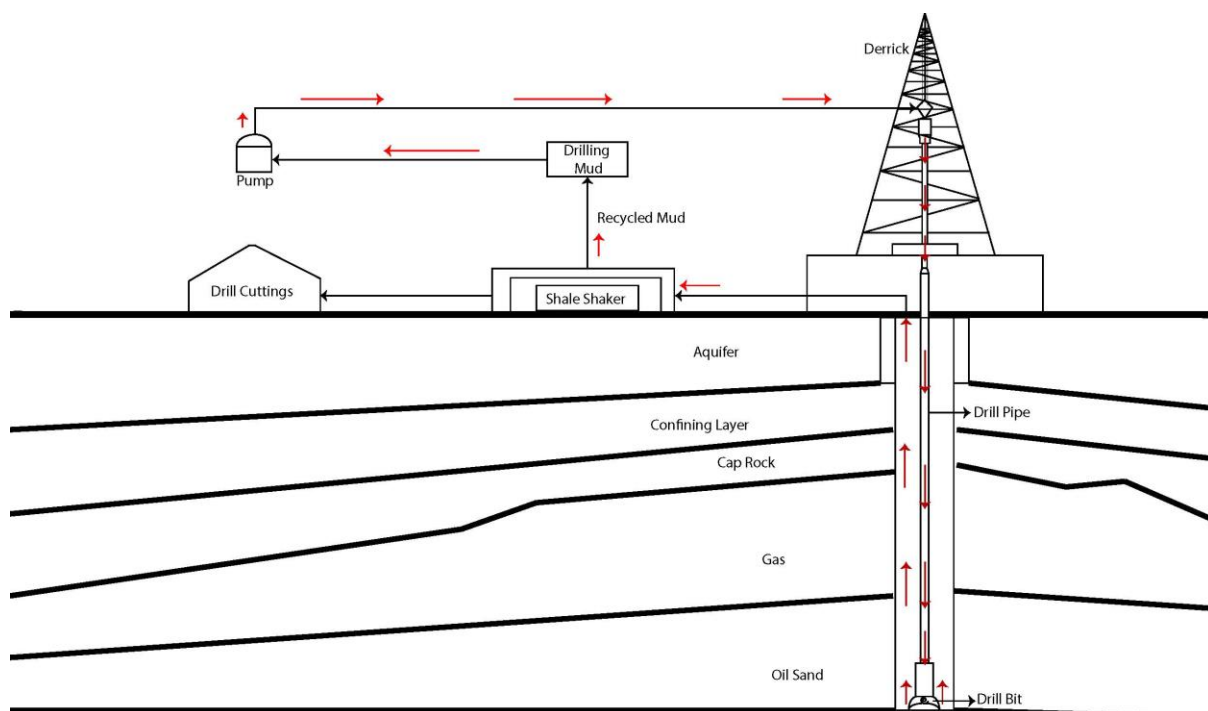


Figure 1. Schematic of circulation of drill cuttings from petroleum drilling operations.

One of the challenges in any drilling operation is the successful removal and separation of solid particles from the drilling fluid. The following key points can summarize the advantages and importance of removing drilled solids -

1. Reduction in bit wear.
2. Thinner filter cakes which allow for a lower risk of stuck pipe.
3. Lower viscosity and drilled solid content which leads to faster drilling rates can be observed in Figure 2.

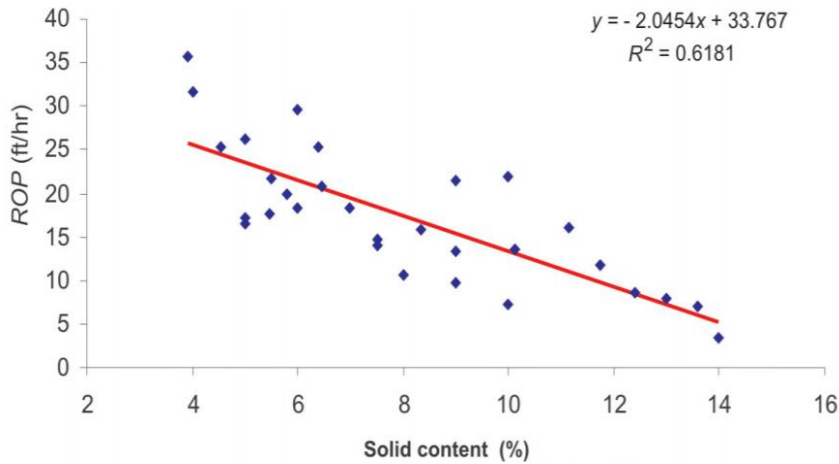


Figure 2. Impact of solids content on drilling rate [13].

Finer cuttings are usually harder to remove and are mostly formed due to size degradation of larger cuttings as they come in contact with the drilling fluid. These cuttings are mostly clay-rich cuttings produced from drilling shale formations. The increase in the concentration of these small cuttings eventually make the drilling fluid too viscous, leading to an increase in rig days and thus rig costs. The correlation between solids content and rig costs is provided by field study results shown in Figure 3 [17].

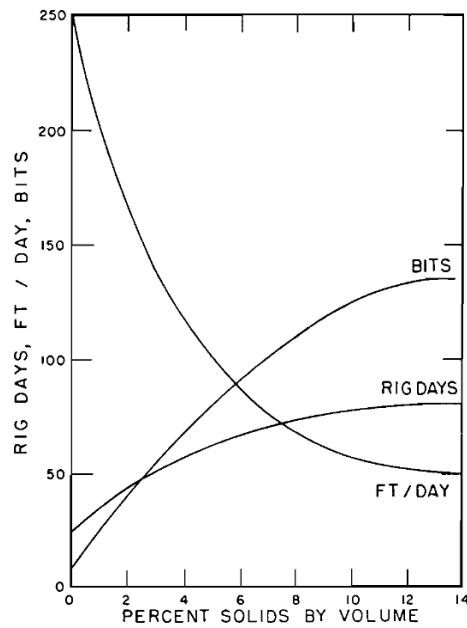


Figure 3. Operating rig days increase with increase in solids content [17].

Significant work has been done to better understand the reaction of drilling fluid with shale formations and many test protocols have been proposed and applied to benchmark the reactivity of different drilling fluids with shale formations. The effect of drilling fluid on degradation/dispersion of clay particles has not been thoroughly studied before.

1.2 Objectives

The goal of this thesis is to characterize the disintegration of clay/shale cuttings and analyse the effect that different chemical additives have on the cuttings. This is achieved by proposing a new approach to gain information about the inhibition mechanism through the use of advanced particle analyzing equipment, namely, the FBRM M500 and the Malvern Mastersizer 3000. These tools were used to study particle size distributions and particle counts of the clay samples after submersion in water and with exposure to numerous additives. A test protocol is proposed to study the breakdown of cuttings as they are exposed to an aqueous environment, and specific laboratory tests are followed. The type of clay samples being tested are limited to two – Sodium Montmorillonite and a Shale core sample which will be detailed in further pages. These samples were tested under similar conditions to ensure the procedure can be replicated.

1.3 Significance

A substantial proportion of drilling fluid properties are adversely impacted by the solids entrained during the drilling process. An effective drilling mud monitoring tool at the rig site is needed to observe and ultimately control the impact of low gravity solids and suspended cuttings on the fluid properties. Present day equipment used for solid control mainly rely on shale shakers for efficient filtration of solids. Shale shakers are critical and often effective at removing unwanted cuttings from the drilling operation. However, having an in-situ drilling mud monitoring tool working in conjunction with the shale shaker or other solids control equipment would serve an additional advantage of allowing the cuttings samples to be analysed and determine the consequence of a particular type of drilling fluid on the cuttings. The use of such a system would facilitate efficient solids control which ultimately leads to improvements in well quality, controls costs and limits the environmental impact of the drilling process.

1.4 Organisation of Thesis

This thesis comprises a total of five chapters. In Chapter 2, a summary of the relevant contribution in the literature on the area of shale-rock interaction is provided.

Chapter 3 describes the methodology used to test several inhibitive additives with particle analyzers. First, the use of traditional Potassium chloride is detailed, and then the usage of various industrial additives is explained. The methodology involves a foundational step-by-step procedure with some variable parameters that can be changed based on the requirements of the researcher.

In Chapter 4, the framework and results of testing are discussed through the study and analysis of particle size and particle count results. A benchmark of the additives tested is provided based on their performance under identical conditions.

Finally, Chapter 5 discusses the conclusions that were derived from this research and the experimental study. Recommendations for future testing are provided based on the strengths and fallacies done in this work of research.

Chapter 2

Literature Review

2.1 Shale swelling mechanisms

A significant part of subsurface formations are comprised of shale rocks that swell and disintegrate once they come in contact with the water present in drilling fluids. This reaction of shales is caused by their composition and structure. The bulk of all shales contain chemically active, flattened clays and the predominant clay minerals are namely Kaolinite, Chlorite, Illite, and Smectite or Montmorillonite. These clay minerals are often studied using Scanning Electron Microscopy (SEM) and example SEM images are shown in Figure 4 and Figure 5. Of these, the group of clays that are known to expand due to a change of ionic conditions and ultimately scatter and travel with the flow of fluid are the Smectite clays. In reservoir engineering, such swelling clays cause significant challenges as they reduce the permeability of the rock formation thus reducing the area of flow [18]. In drilling engineering, the reaction of clay with drilling fluid results in borehole instability, drilling problems such as stuck pipe, and an increase in fine suspended solid particles in drilling fluid.

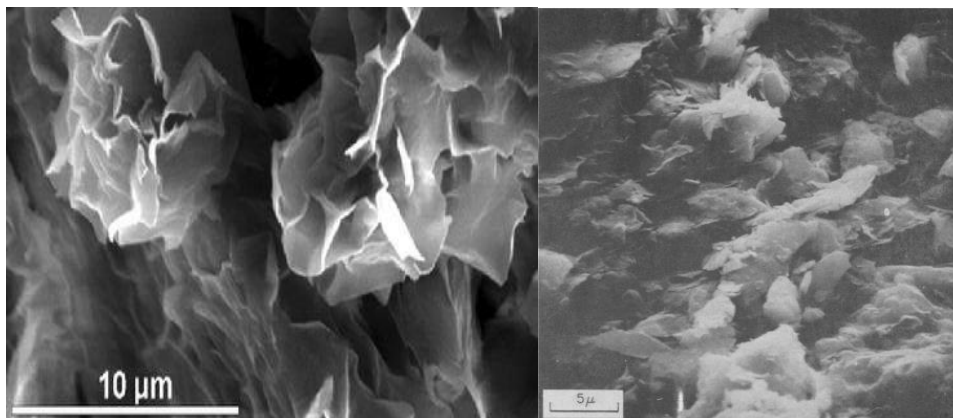


Figure 4. (Left) SEM image of Wavy subhedral montmorillonite crystal [1]; (Right) SEM image of Illitic clay [2].

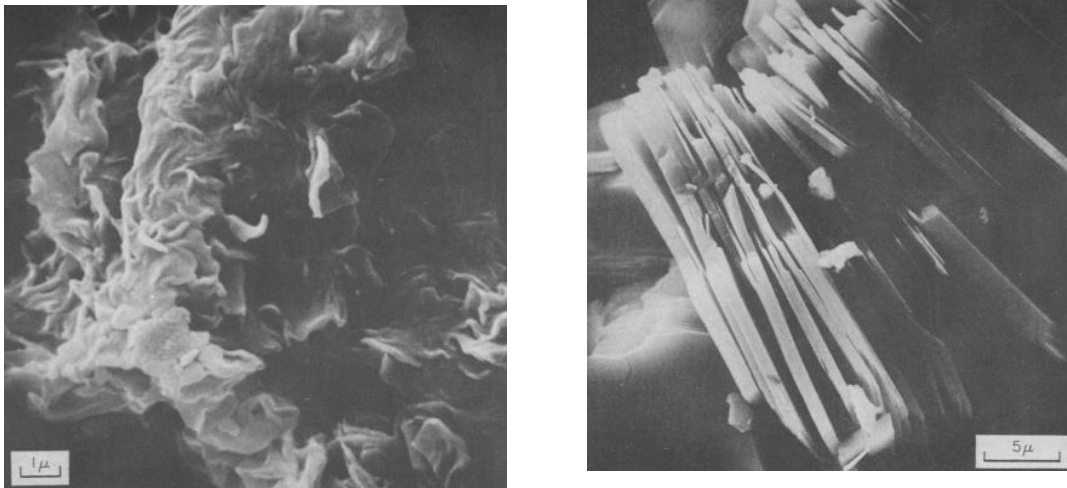


Figure 5. (Left) SEM image of smectite clay [2]; (Right) SEM image of authigenic kaolinite packet [2].

The instability of shales and clays when in contact with water has been known for well over 80 years. In the literature and the drilling industry, there is a general agreement on the clay swelling mechanism, but the mechanism of shale swelling and degradation is imprecise as the material is laminated and composite including silica and carbonate materials. There is no real understanding of the mechanism, but it is widely recognized that the nature of the shale is the primary source of instability. What is repeatedly mentioned in the literature is that the proposed causes of shale instability are not conclusive and merely proposed theories. The study of shale swelling and mechanisms involved is not yet completely understood, but a common reoccurrence in the literature is the conclusion that the presence of a more substantial volume of Smectite clays leads to an overall more considerable swelling degree of clays. Water and other polar substances are allowed into the Smectite structure resulting in the increased interlayer distance due to the moderately weak intercrystalline bonds in the clay structure [19]. In addition to water activity and salinity, the hydration of clays is controlled by a few other factors – External pressure, temperature and the location of the interlayer charge [20].

Important areas that are of key relevance include:

1. Clay scale mechanics
2. Wellbore and geomechanical considerations
3. Thermal considerations – outside the scope of this research work

4. Geochemical and physiochemical responses based on the physical and chemical organization of the shale material (being laminated and a composite material)

There are numerous theories and research papers published as possible explanations for the mechanism of shale instability, but in general, there are three main theories that are prevalent and widely cited in the literature. The first theory that has been popular amongst researchers is known as the diffuse double-layer (DDL) theory [21-23]. The DDL theory proposes that the surface of a clay particle attracts positive ions because the clay surface is negatively charged. The diffuse double layer is this area of attracted positive ions in solution and the negatively charged surface of the clay. The diffuse double layer's thickness surrounding outer clay mineral surfaces is around a similar amount or even more significant than the majority of pores found in shales. Thus, the quoted studies claim that electrostatic repulsion that leads to amplified pore pressure in all forms of shale occurs due to the overlap of DDL associated with water immersed clays as can be observed from Figure 6 [24].

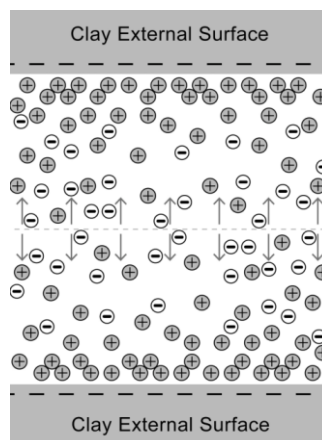


Figure 6. Simplified schematic of the DDL in the surface of clay minerals indicating pressure generated by forced overlap of the DDL.

The second widely accepted theory behind the cause of shale instability is advocated by Wilson and Wilson [24] who pointed out that the universal cause of shale instability cannot be solely due to their clay mineral composition as many problem shales are not composed of expandable clays. They then argued that the instability is due to the general hydrophilic nature of shales in combination with the overall texture, structure, and fabric of shales. This meant that shales that are composed chiefly of Illite and Kaolinite, which are considered non-reactive clay

minerals, may also be unstable to aqueous fluids during drilling operations. Osmotic swelling, described in Figure 7, ensues in the interlamellar region of Smectites, and this is considered to be another instability trigger by many researchers [25-27]. Lower valence cations are absorbed amongst adjacent layers or platelets to recoup for the subsequent remaining negative charge of the platelet faces. On wetting, these cations are released to the water which results in a net negative charge on the surface that is neutralized by double layer ions [28]. So in summary, when immersed in water, the interlayer cations get hydrated and equilibrate with the surrounding suspension. The electrical double-layer repulsion causes a net negative charge on the platelets and induces the layers away from each other and if unhindered, will cause complete separation [29]. The platelets randomly orient themselves into a structure, similar to a card house and form a space-filling, thixotropic gel, even at low volume fraction [28, 30]. This system that is produced is challenging to dewater due to the resulting complex and vast environment of the clay platelet network. To retard this whole process, the simple addition of salts does a great job as the salts restrict the double-layer repulsion.

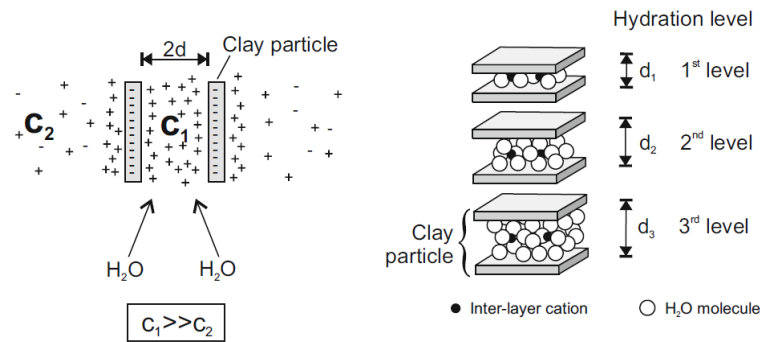


Figure 7. (Left) Osmotic clay swelling [31]; (Right) Inner-crystalline clay swelling [32].

Figure 8 illustrates a simple model of balance of forces that are imposed on a shale rock that contains clays. All the forces can be divided into two types:

1. Mechanical forces:
 - a. Pore pressure;
 - b. Overburden stresses;
 - c. The stress acting in between granular contact points;

2. Physio-chemical forces:

- a. Van der Waals attraction forces;
- b. Hydration/solvation of clay surfaces that cause short-range repulsive/attractive forces;
- c. Electrostatic Born repulsion

The physio-chemical forces are typically taken collectively to create “swelling stress/pressure” which is also considered to be one of the sources for the swelling behavior of clays and shales. It is commonly used in the oil/gas industry, and it is important to note that the phrase “swelling pressure” is always influencing clay platelets as a tensile force. It does not merely instigate due to shale coming in contact with an aqueous solution. It must also be noted that swelling stresses are dependent on the type of clay and that the magnitude of the swelling pressure can be affected by the chemical changes caused by shale and water-based drilling fluid contact [33].

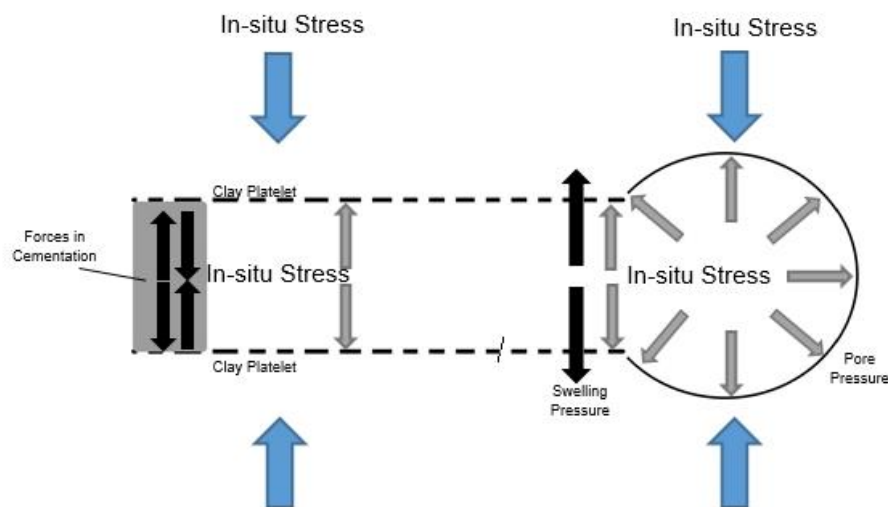


Figure 8. Simplified diagram of all the forces acting downhole on a shale rock.

The third dominant theory is cited in a few research studies [34, 35] whereby new information was published proving that shale-aqueous structures might behave as “leaky osmotic membranes” that withstand the flow of water driven by chemical osmosis. The lack of freedom of movement in the clay-rich, low-permeability matrices of shales causes a membrane to be formed. In shales, ion diffusion coefficients have been shown to be typically in the range of $1-10 \cdot 10^{-10} \text{ m}^2/\text{s}$ [14]. For shales with nano-darcy range permeability ($k=10^{-9}D-10^{-21} \text{ m}^2$), ion diffusion is then

quicker than hydraulic flow. Finally, there exists an additional significant operation which occurs quicker than ion diffusion in shales, which is the Darcy flow of practically incompressible water into a high-stiffness shale matrix that then has a significant impact on pore pressure. This shown in Equation 1. Due to their low base permeability, shales cannot dispel pore pressures rapidly enough to long distances. As a result, the pore pressure will be raised to a stretched out zone around the wellbore as a result of the water influx.

$$\text{Hydraulic flow} < \text{Ion diffusion} < \text{Darcy flow}$$

Equation 1. Speed of flows in shales with nano-darcy range permeability

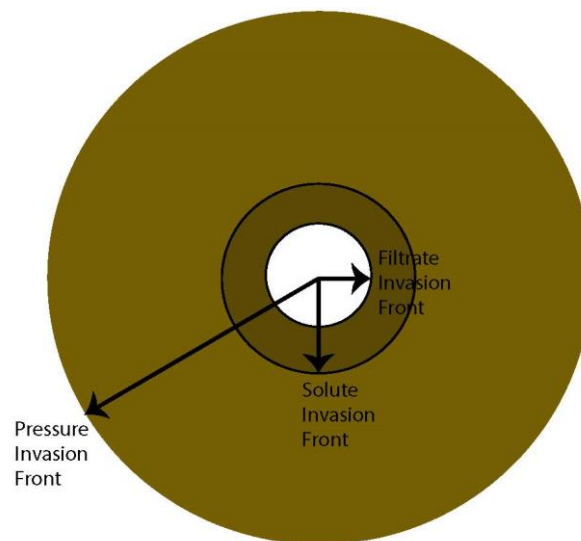


Figure 9. Simple diagram of the onset of several fronts around a borehole over a period.

The pore-pressure front is anticipated to travel faster than the solute diffusion front for low permeability-shales. Figure 9 explains this situation whereby the filtrate invasion front is led by a solute invasion front, which in turn is led by a pore-pressure invasion front. A general decree followed in the oil/gas industry is that "where bulk water invasion proceeds at millimeters a day, ion diffusion will diffuse over centimeters a day and pressure will diffuse over decimetres a day" [33].

2.2 Shale instability

Oil or Synthetic hydrocarbon-based muds (OBM) were embraced due to their superior shale inhibition properties and their ability to solve the wellbore instability problems. Unfortunately, high costs, challenges with disposing of the mud, safety and environmental restrictions have constrained the use and application of Oil-based muds. Consequently, Water-based muds (WBMs) that possess the ability to mitigate

shale instability challenges effectively have come into consideration worldwide to replace the OBMs but it should be noted that OBMs are still used worldwide, such as in the Bakken shale formation [36].

Shale instability leads to a multitude of different challenges: the wellbore might fail and break down through sloughing or caving, mud properties may become worse, pump pressure may increase, and torque and drag will increase. Figure 10 shows a simple scenario of how the problem of stuck pipe may arise due to shale instability. A few other factors that shale instability causes have been cited in the literature including shale formation's texture, structure, and fabric [24] and the distribution of stresses in situ [37].

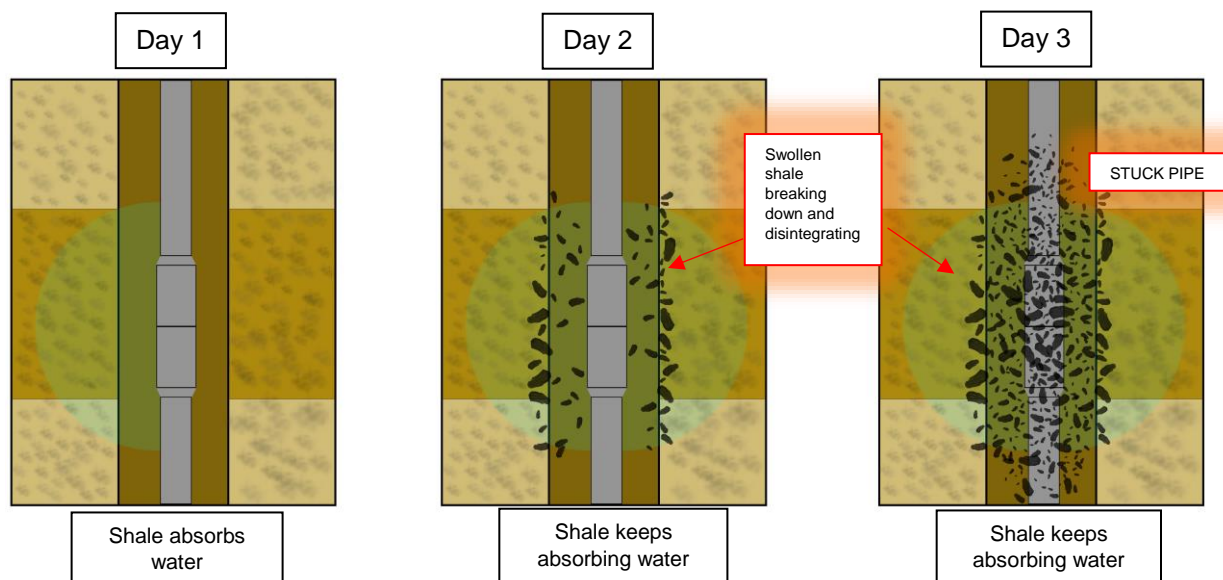


Figure 10. Shale Instability causing Stuck Pipe.

After the mud has circulated, it will usually contain drill cuttings. These range from coarse chips to the finest colloidal particles ($<1 \mu\text{m}$). One of the most critical parts of the mud equation is solids control: how efficiently the shakers, Hydrocyclones, and centrifuge remove cuttings. Cuttings are solid materials generated from the cutting action of a bit during the drilling activity. They are transported to the surface by the drilling mud and separated from the mud before the mud is re-injected down the borehole. Reduced efficiency of cuttings removal could lead to unwanted fine-grained cuttings to linger in the mud and drive viscosity above specification.

The role of solids control equipment is to discard the cuttings, retain as much barite as possible (as it is expensive) and keep enough colloidal matter to maintain

viscosity [38]. Numerous tools and equipment such as the Shale Shaker (Figure 11), Hydrocyclone, Mud cleaner, and Centrifuge are used in order to control the number of solids present in the drilling mud. Well site monitoring of the circulating mud is a crucial job that needs to be monitored continuously, usually by a team of drilling mud engineers. This is because reducing cost and protecting the environment require knowing the mud composition at every moment during drilling.

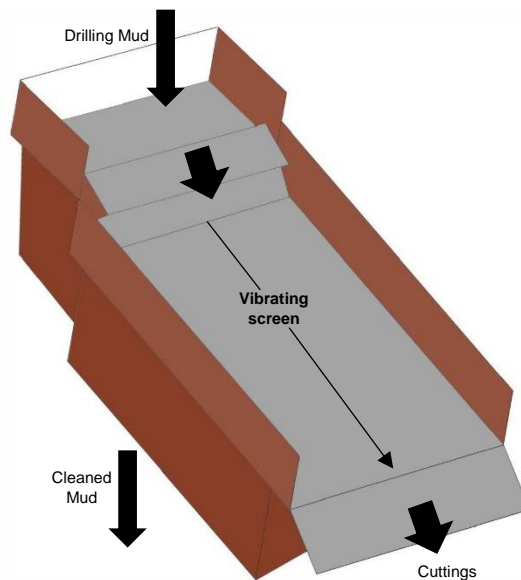


Figure 11. Schematic of a Shale Shaker.

Solid removal is a critical element in the overall success of the drilling operation. As the cuttings are transported to the surface by the drilling mud, they tend to degrade and break down into finer particles due to mechanical and chemical degradation. The Shale swelling described earlier, is a major contributing factor to subsequent breakdown. This is a challenge because if the particles are too fine, they cannot be separated by the solids control equipment such as the Hydrocyclone and they are then reinjected back down to the bottom hole with the drilling mud causing difficulties such as an increase in the wear rate of equipment and alterations to the mud viscosity. Figure 12 shows how the efficiency of the Hydrocyclone is determined by the size of the drill cuttings. Marthinussen's [39] experimental results have proven that Hydrocyclone efficiency increases with increasing cutting particle diameter. As can be seen, five different fluids with different viscosities were tested, and all the results confirm this statement. The larger the cuttings particle size, the more convenient it is for the solids control equipment to filter out the cuttings from the drilling fluid.

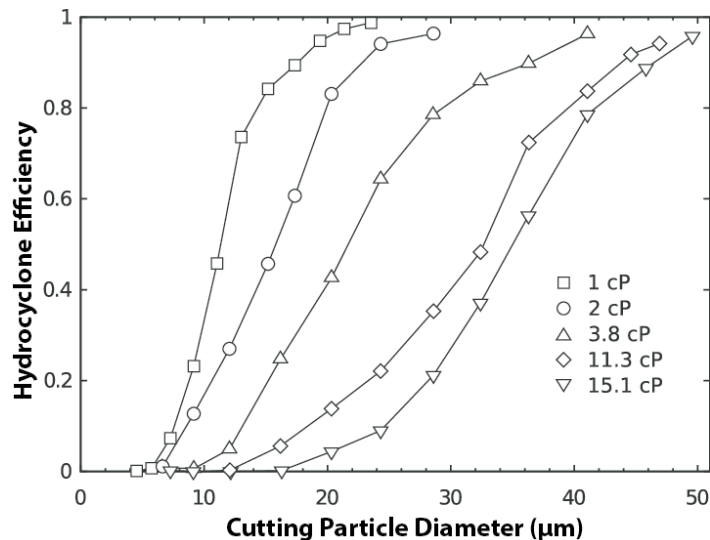


Figure 12. Hydrocyclone Efficiency increasing with increasing Cutting Particle Diameter [39].

Over the years, the quantity and quality of the chemical and solid additives have seen drastic improvements, but well site circulating mud monitoring has developed slowly. In the 60's and 70's, such mud circulation data used to be acquired with rudimentary and inaccurate tools with sampling being done only a few times a day. However, recent stringent environmental guidelines being enacted globally have changed this. Computerized reporting systems are now available in the industry that collect and analyze data in real time, every hour of operation but this area of drilling mud monitoring is still ripe for innovative research. Currently, mud engineering is enjoying a renaissance in which even small technical advances bring considerable savings. As mentioned earlier, most pressing in the present moment are improvements in well data acquisition – more reliable chemical measurements – and a method to detect polymer concentrations. A critical point that cannot be overlooked is that cost efficiency can be achieved if an independent operator controls all parts of the drilling mud operation.

It is critical to have a detailed understanding on the effects that drilling fluids may have on shale rock behavior as this will lead to a superior way in predicting and coping with borehole instabilities during a drilling operation. So far, numerous experimental tests and numerical models have been developed by researchers to describe the interaction between water-based drilling fluids and shale. It is important to note here that no one single test is the best for all cases and for all types of shale rock. Usually, a combination of tests are implemented to deduce qualitatively and quantitatively the reactivity of the sample with fluids. Chenevert et al. demonstrated a

few experimental devices that could be used to measure the swelling of shales as they come in contact with water-based muds [40]. Six tests were comparatively studied, and this is significant because it was the first time such tests were defined by their practicality in describing the rigorousness of the shale/mud chemical interaction. Amongst all the tests, the swelling and shale rolling test proved most valuable in the analysis of wellbore difficulties. The swelling test can be used to evaluate the shale's swelling tendencies under the exposure of various muds. In it, a "swelling indicator" displayed in Figure 13 is used, and the shale sample is fastened between the anvils of the core holder. Then the test fluid is poured into a plastic bag that surrounds the shale, and the resulting shale expansion is displayed on the digital displacement transducer and recorded. The shale rolling test works on the idea that more inhibitive muds reduce dispersion tendencies. In the test, cuttings are placed in a 400-mL aging cell that is partially filled with 350 mL of mud and allowed to roll at 50 revs/min for 16 hours at 65.6 °C. This mixture is then poured through a 200-mesh screen, and the amount of shale that passes through the screen is determined. This is compared to the initial total amount of shale that was tested. The swelling test categorizes shales based on their reaction rates while the rolling test provides useful information on the dispersion tendencies of a shale-cuttings/mud combination. Chenevert et al. descriptively explained all the tests with their advantages and disadvantages listed out. However, one major limitation of this work was that all tests were either time consuming or that they were laboratory-based with little direct application in the drilling field. For example, a simple rolling test usually takes 16 to 24 hours. As these experiments were designed in the very early phase of this field of work, these limitations can be overlooked as this work provides a solid foundation for future literature to build upon.

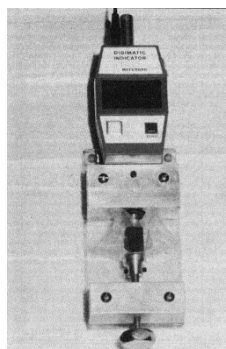


Figure 13. Shale Swelling Indicator.

Exposure on smectites-rich shales by various experimental techniques was investigated by Horsrud et al. [41]. Meanwhile, Molenaar et al. developed computational models to describe the interaction between the drilling fluid composition and the mechanical behavior of shale swelling based on transport equations for the fluids and ions [42]. The effect of physio-chemical shale-fluid interaction on shale formation pressure and swelling through numerical simulations and modelling was investigated by Huang et al. [43]. The implementation of modern sequential artificial neural networks for modelling the time-dependent swelling of expansive soils under various inputs was probed by Basma et al. [44]. It can be noted from the literature that the interest and awareness in studying shale swelling mechanisms rose in importance very late

Figure 14 shows photographic evidence of the disintegration of Shale. This image shows the results of a simple laboratory test whereby the deformation of different shales when they are submerged in fresh water for 24 hours can be observed. Shale is generally characterized by thin laminae or parallel layering or bedding less than one centimeter in thickness, and a major contributing factor is its composition of swelling clays, the majority of which is Smectite. The ratio of clay to other minerals fluctuates from one shale sample to another.

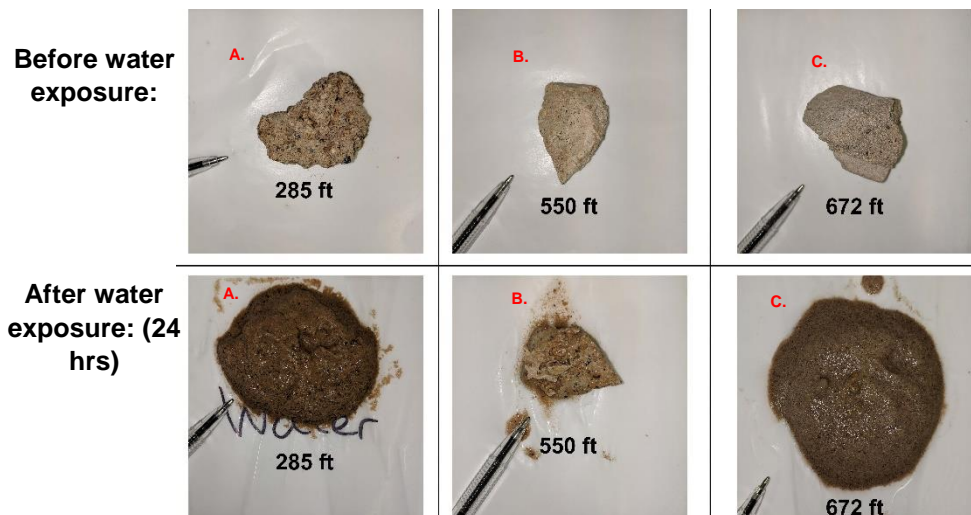


Figure 14. Shale Disintegration.

2.3 Shale inhibition

Inhibitors (chemical additives) are added to water-based drilling fluids to control and diminish the difficulties that arise due to clay swelling. They encapsulate the clay particles and act over the water-shale interface and maintain the strength of the formation. Organic and inorganic chemical inhibitors function by interjecting inside expandable clays and inhibit their hydration and swelling. Mostly, they hinder the entry of water molecules and efficiently reduce the hydration of the clay minerals. Cationic molecules containing quaternary ammonium groups (QAG) in their structure are the primary organic additives used as clay swelling inhibitors in many forms of industrial additives [45-48]. QAG are an ammonium group in which each hydrogen has been replaced by an alkyl or aryl group. Along with these organic inhibitors, inorganic salts of potassium and sodium are usually used. This is due to the simple reason that using a complete organic inhibitor mix is not considered cost-effective [49].

For many years, the wide-ranging answer to clay/shale challenges in the industry has been “inhibition”. In general, some additives, particularly salts, have been noted to inhibit the breakdown of bentonite in water and this is how the term inhibition arose. Inhibitors are essential additives that are formulated to reduce the swelling pressure. It is important to note that the swelling pressure cannot be brought down to zero by even the newest inhibitors available in the market [50, 51] as the remaining

repulsion between platelets will always be there due to hydration of the clay surfaces.

The reduction of swelling pressures in montmorillonite can be achieved through the use of K⁺ ions as additives, and this is well documented in the literature. This is believed to be caused by the low ion repulsion due to the small amount of hydration of these ions when in contact with water [52].

An excellent review of shale/clay inhibition has been completed by Van Oort [33], and in it, it was resolved that a strategy for shale stabilization exclusively based on the use of chemical inhibitors can never be entirely valid. Van Oort recommends that something more than just mere "inhibition" is required and that thermal conduction (Fourier's Law), i.e. flows in shale driven by gradients in hydraulic temperature need to be accounted for as they can affect the imbibition processes and that resulting thermal stability models are needed. This is an interrelated area of research as water based muds that allow for better control of thermal stabilities can further contribute to shale inhibition. This recommendation is important but is outside of the scope of this research thesis. This study will be based on novel ways of observing and studying cuttings disintegration and finding the optimum concentration of a particular additive based on the aforementioned cuttings analysis but it is important to note here that all tests in this study involved using isothermal conditions between the drilling fluid and cuttings. Thermal effects cannot be ignored as they are important but were not investigated at this point in time and this is an area of relevance for future research.

More recently, the advances in technology and invention of new apparatus and measurement techniques that allow for the understanding of drilling fluid/shale interactions under the close approximation of downhole conditions have been made. One of these approaches is through the use of advanced particle analyzers to gain information and appraise the shale inhibition performance of numerous chemical additives which will be detailed in the following chapter.

2.4 Analysing shale reactivity with laboratory methods

Due to the importance of the fluid and shale rock interaction, a multitude of laboratory test procedures were developed by the oil and gas industry to evaluate the compatibility of drilling fluid and formation shale. It is important to note again that no one single test is the best for all cases and for all types of shale rock. Usually, a

combination of tests are implemented to deduce qualitatively and quantitatively the reactivity of the sample with fluids.

Very often, researchers follow three steps to identify which test is best suited for the particular sample being investigated.

1. Preliminary sample analysis
2. Classifying the shale sample based on reactivity
3. Test selection

Figure 15, which was taken from the work of Stephens et al. [53], summarizes the test selection process based on standard features belonging to the select shale sample. Often, the common restrictions to each precise experimental plan are the quality and quantity of the sample. The type of sample (cuttings, cavings, and cores) or the quantity of sample needed can vary for each test. Table 1 gives the recommended quantities of the sample required to conduct the shale examination testing plan.

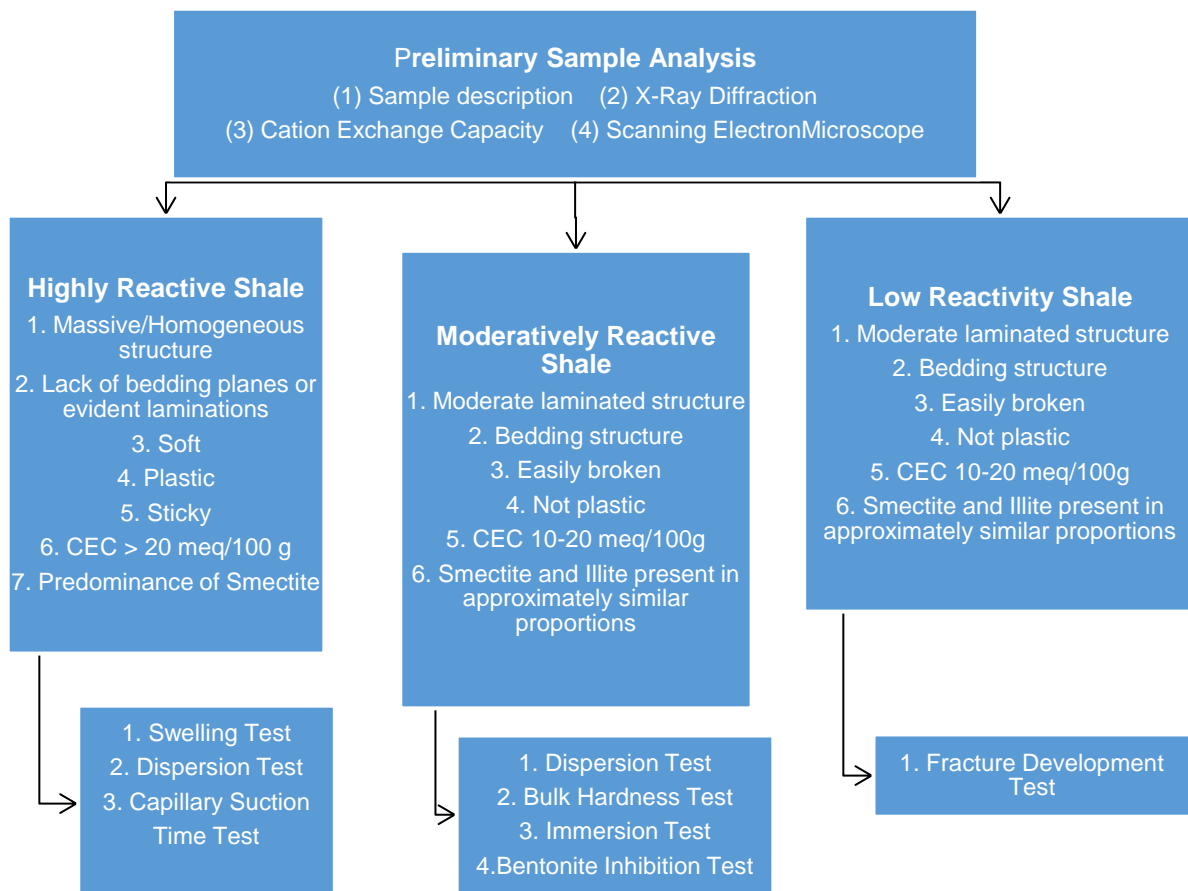


Figure 15. Process of test selection based on shared shale sample features [50].

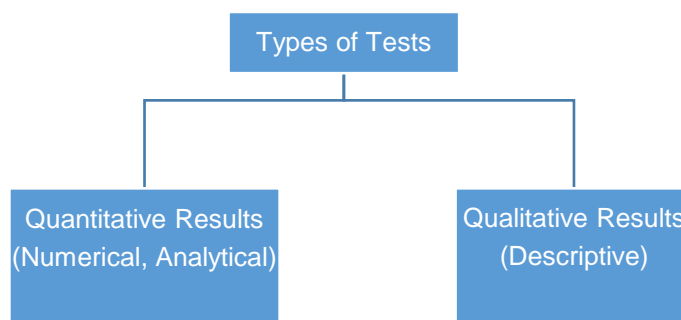


Figure 16. Types of testing.

Table 1. Recommended quantity of shale sample required for each type of test [53].

Test	Type of sample	Amount per Test
X-Ray Diffraction	Cutting, cavings, cores	5 grams of clean dry sample
Cation Exchange Capacity	Cuttings, cavings, cores	1 gram of clean, cry, ground powder
Scanning Electron Microscope	Cuttings, cavings, cores	1 gram
Water Activity	Cuttings, caving, core	100 grams
Thin Sections	Large cuttings, cavings and core material	Samples approximately 1 cm or larger
Swelling Test	Cuttings, cavings, core material	5 grams ground powder
Capillary Suction Time Test	Cuttings, cavings, core material	3 grams ground powder
Dispersion Test	Cuttings, cavings, core material	20 grams (-6 mesh and +20 mesh)
Bulk Hardness Test	Cuttings, cavings, core material	30 grams (-6mesh and +20 mesh)
Immersion Test	Cavings, core material	Similar sized pieces (cubic or cylindrical shape). Sample dimension (length or diameter) ~ 1-2 inches
Fracture Development Test	Core material	Similar sized pieces (cubic or cylindrical shape). Sample dimension (length or diameter) ~ 1-2 inches

The mineral content of the shale usually allows for the classification of the shale [54].

Types of shales include:

1. Calcareous Shale - Calcite or Dolomite
2. Limonitic or Hematitic Shale - Iron Minerals
3. Carbonaceous or Bituminous Shale – Carbon Compounds
4. Phosphatic Shale – Phosphate
5. Siliceous Shale - Silica

The composition of minerals present in the shale ends up controlling the colour of the shale as darker shales (black or grey) tend to have a higher organic carbon content. Red, purple or brown shale is a result of the presence of ferrous iron compounds and shales that are pale grey or yellow tend to contain a lot of calcite.

Other features such as the plasticity, hardness and permeability are controlled by the grain size and the composition of minerals in the shale. All shale's tend to be fissile by nature meaning that they can easily be split into layers parallel to the bedding plane. Geologically, shale is usually laminated, consisting of many thin layers that are composite. As a result of this, a number of tests are required for different types of shale and the outcrop or studies based on the physical sample descriptions are important and will be discussed in the next section.

Importance is given to proceed with an integrative approach when testing the shale samples. This includes using both quantitative and qualitative measures to evaluate the sensitiveness of shale to water-based drilling fluids. Characteristics of the shale formations can be observed and described through qualitative measures, and this will increase the understanding of the synergy between shale formations and fluids. The results from these tests can be used to give an overall cataloguing of the shale to sort the reactivity and forestall the potential instability they may cause when in contact with fluids. Preliminary sample analysis is essential because this process provides essential information about the sample before the testing.

A number of tests are described below and the type of responses measured between shales and drilling fluid are explicitly stated – physical, chemical or physiochemical.

2.4.1 Sample Description - Physical

This is a simple procedure which involves physical analysis of the sample identifying several key features. Usually, this descriptive information is qualitative, and the occurrence of characteristics such as natural fractures may point towards significant pieces of evidence on the source of shale instability. The strength of this technique is that sample description is possible with any size of the available sample. The equipment used is simple, mainly consisting of a hand lens and a simple stereomicroscope. Some of the critical geological features that may be identified include:

- Colour – Frequent shale colors – white, brown, grey, purple, green and black.
- Consolidation and state

- Hard
- Firm
- Friable
- Plastic and sticky
- Plastic and non-sticky
- Bedding structure
 - Massive – lack of bedding structure
 - Disturbed bedding
 - Sandstone or siltstone inner beds
 - Graded bedding
 - Laminations
 - Current deposited – wavy bedding, flaser bedding, cross-bedding, starved ripples, ripples [55]
- Sedimentary structures
 - Burrows
 - Sole marks
 - Load casts
 - Mud cracks
- Fractures - Figure 17 shows a photograph of fracture propagation.
 - Parallel to bedding or laminations
 - Shear fractures
 - Cracks

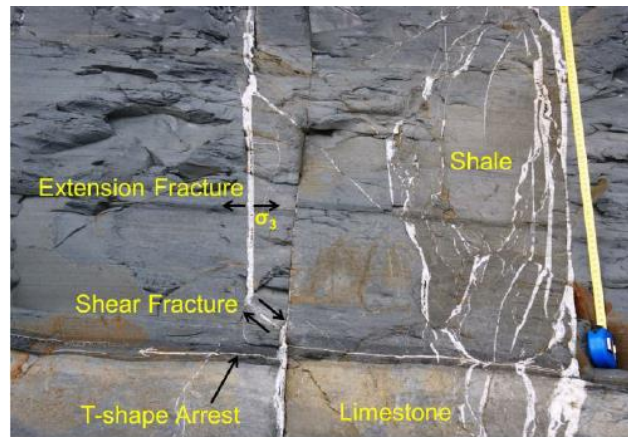


Figure 17. Fracture propagation from shale to limestone [56].

2.4.2 X-ray Diffraction - Physiochemical

Historically, X-ray Diffraction (XRD) methods have been used to classify different varieties of minerals existing in a sample [57-59], and sample results can be seen in Figure 18 and Figure 19. As a sample is rotated and illuminated with the X-ray beam inside an XRD apparatus, the crystalline arrangements of the specific minerals existing diffract the X-ray beam resulting in an X-ray diffracting outline that is distinctive for every individual mineral in the sample [60]. The accompanying software then recognizes the occurring minerals and defines the semi-quantitative measurements of each. Ideally, the samples ought to be cleaned and dried to remove drilling fluids and other contaminants before testing.

This technique is used in a wide range of industries from research to production and engineering as it is one of the essential forms of non-destructive testing. One of the strengths of this technique is that XRD on a wide variety of samples: cuttings, cavings or cores. The main disadvantage of this technique is that the XRD analysis requires expensive equipment and a knowledgeable analyst to study and interpret the data.

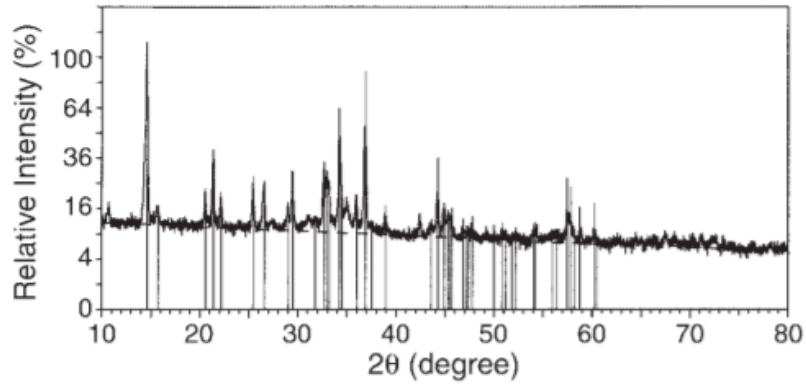


Figure 18. Sample diffraction powder patterns - vertical lines represent $Cu_2Br(OH)_3$ [61].

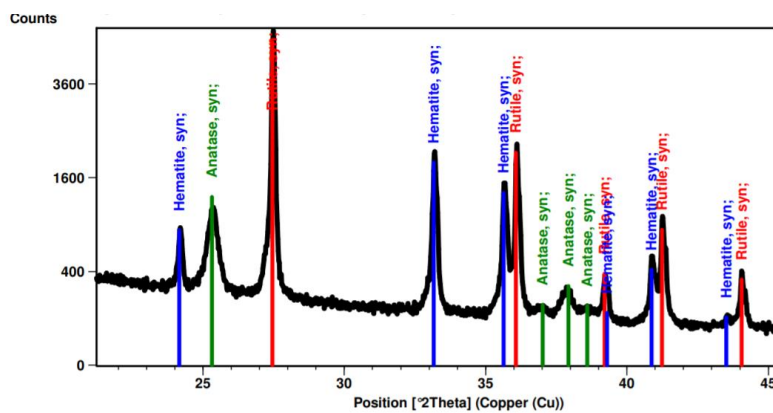


Figure 19. Sample XRD test result showing how each different phase produces a different combination of peaks [56].

2.4.3 Cation Exchange Capacity - Chemical

The Cation Exchange Capacity (CEC) is a reading of the transferrable cations existing on the clays in a shale sample. The clay particles are negatively charged, and the exchangeable positively charged ions neutralize these. Usual exchange ions are iron, potassium, magnesium, calcium, and sodium. Bentonite and montmorillonite clays contain the majority of the exchangeable negative ions in the shale samples. The higher the CEC is, the more reactive the shale is. However, it is important to note that a low CEC can still be an issue if the minor amount of clays present swell and lead the shale to disintegrate. A higher CEC shale usually is denoted as "gumbo shale" which is a generic term for soft, sticky, swelling clay formations.

The API recommended methylene blue test measures the CEC and sample results are shown in Figure 20. One of the advantages of this test is that it can be completed in the laboratory or in the field with simple tools and equipment.

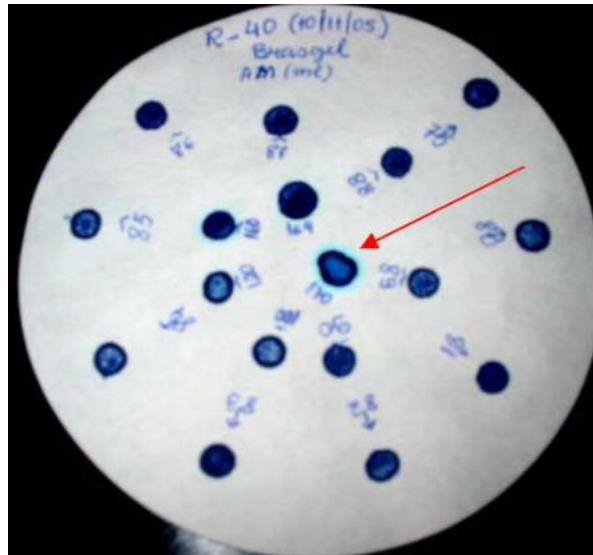


Figure 20. Filter paper showing the end point in CEC determination by titration with methylene blue: a light blue halo around the drop [62].

Table 2 and Figure 21 give the common CEC values for clays that are commonly found in shale samples [53].

Table 2. Common CEC values for various clays found in shale.

Smectite	80 to 120 meq/100 g
Illite	10 to 40 meq/100 g
Kaolinite	3 to 15 meq/100 g
Chlorite	10 to 40 meq/100 g
Sand	<0.5 meq/100 g

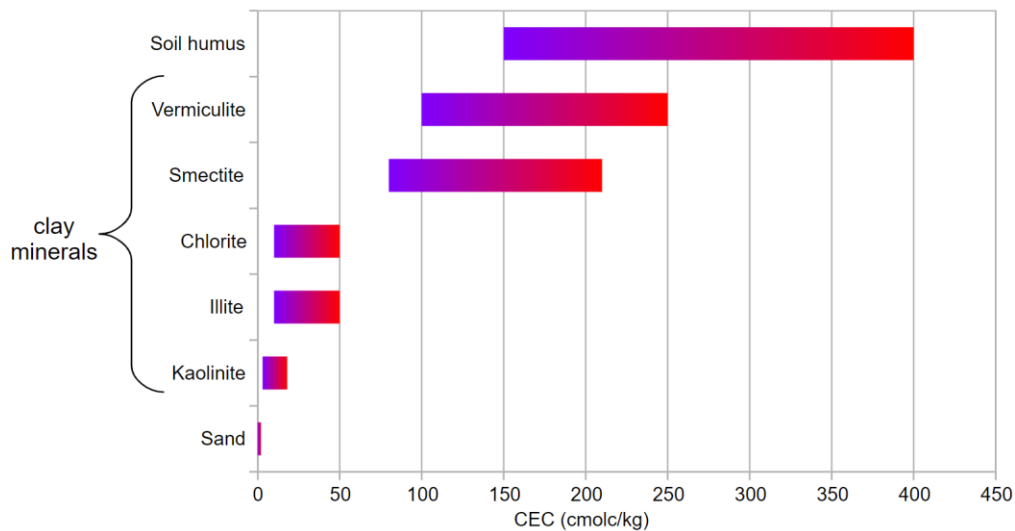


Figure 21. Typical results for CEC ranges of soil materials [63].

2.4.4 Scanning Electron Microscopy - Physical

Scanning Electron Microscopy (SEM) is a procedure that is used for obtaining high magnification analyses of shale. Cracks, openings, and micro-fractures that are not straightforwardly observed through transmitted light techniques are easily observed using the SEM. A significant advantage of using this method is that the foray of drilling fluid over the pores of the sample is observed through the use of SEM. This type of testing can be completed on caving, cores, or larger sized cuttings.

Learning to use and eventually using the SEM instruments can be quite a time consuming and requires relatively expensive equipment that is not common in most laboratories. SEM photographs are essentially a qualitative method used to study the general nature of the shale, and a sample photograph can be seen in Figure 22.

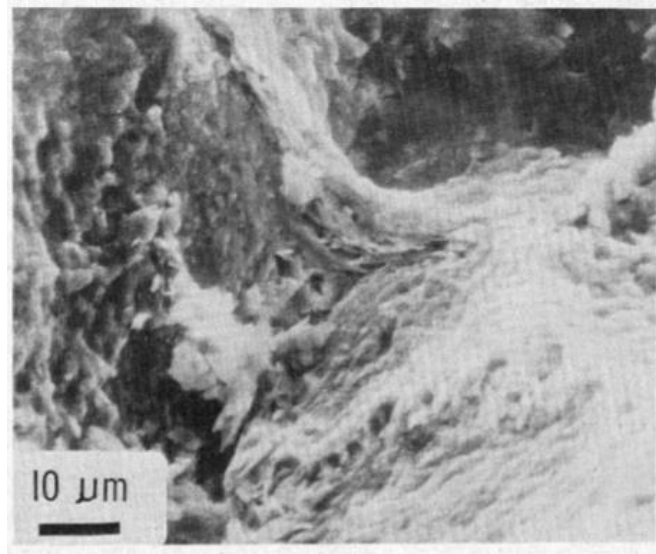


Figure 22. SEM photograph of a Kaolinite sample [64].

2.4.5 Swelling Test – Physiochemical

A linear swelling tester is a device that is used in conducting the swelling test. It measures the swelling of a reconstructed shale capsule once the shale has been submerged in the drilling fluid. The reactivity of the shale to the drilling fluid is linked to the degree of swelling the shale undergoes after it comes into contact with the fluid.

The shale capsules are created by adding ground-up shale with water and then pressing them in a compaction cell for a long duration of time. Figure 23 provides a schematic of the swelling test apparatus, and Cuttings can also be used. The swelling of the shale causes the linear variable differential transformer (LVDT) sensor to increase, changing the inductance of the transformer and producing a current variation which is sensed by the A/D converter. This is examined by the computer software at small intermissions over a long period for a few hours and the results provided are in the form of percent volume expansion of the shale throughout testing time.

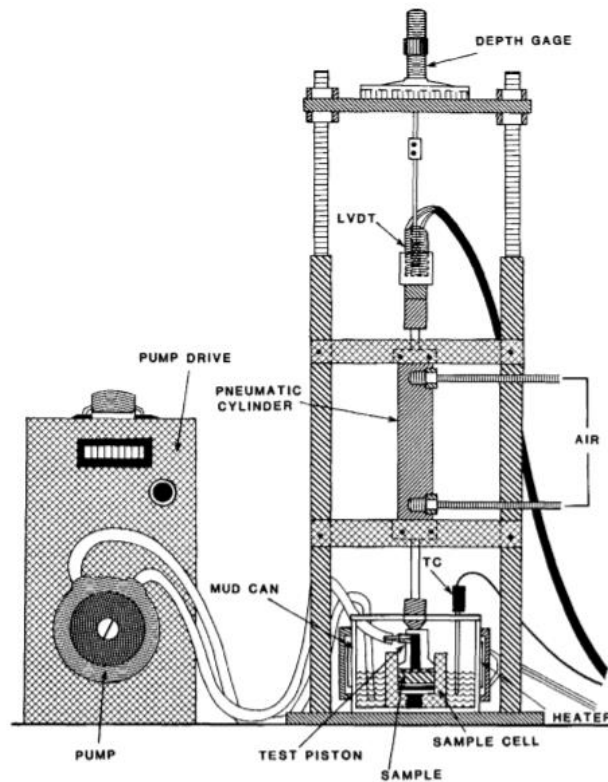


Figure 23. Swelling test apparatus [65].

Figure 24 shows an example result obtained from the swelling of identical shale capsules in different brine concentrations, after equilibration and at different humidities. As can be seen, the results are quantitative, and this test is an excellent indication of the reactivity of the shale sample in the fluids that are experimented on. A key point to note is that the formulation of the shale capsule requires heavy compaction which implies disintegration. This could affect the end result, so these results are related mainly with chemical interaction and less on physical properties [66].

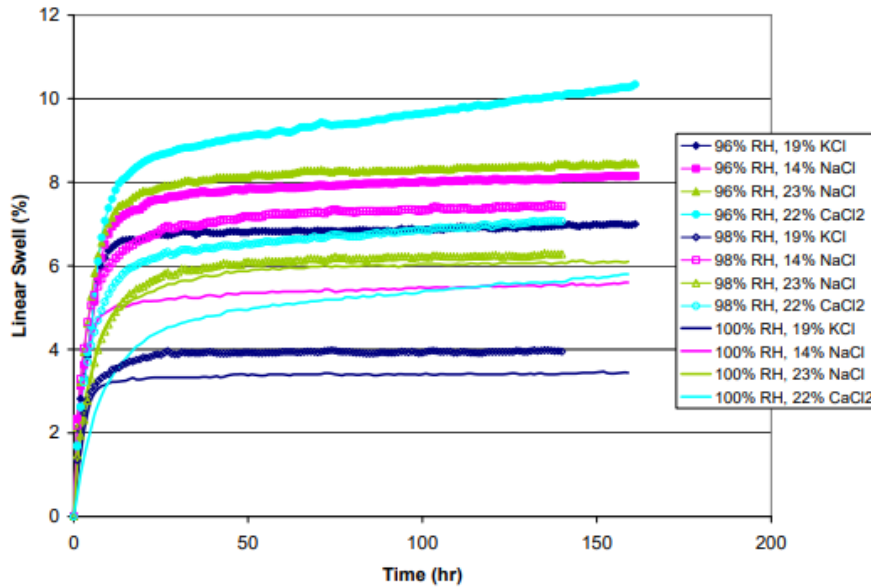


Figure 24. Sample swelling test results of shale capsules in different brines [66].

2.4.6 Dispersion Test - Physical

This test screens the integrity of the cuttings by observing the change in weight of submersed cutting fragments before and after mild agitation and is used to design inhibitor additives. Sample results are shown in Figure 25, and the test procedure involves providing mild agitation over a long period to a shale sample immersed in a fluid solution in a conventional roller-oven cell [67]. As a result of this action, the shale will disperse into the fluid. The level of dispersion will depend on the clay content of the shale and the inhibitive capabilities of the fluid. The test is run for 16 hours at 150 °F. Subsequent to cooling, the retained shale fragments are removed through the use of a 50-mesh sieve, cleaned, weighed and dried for 12 hours at 210 °F. These fragments are then re-weighed to find the recovery percentage which is provided by the equation:

$$\text{Percent Recovery} = \frac{\text{Final Weight}}{\text{Original Weight}} \times 100$$

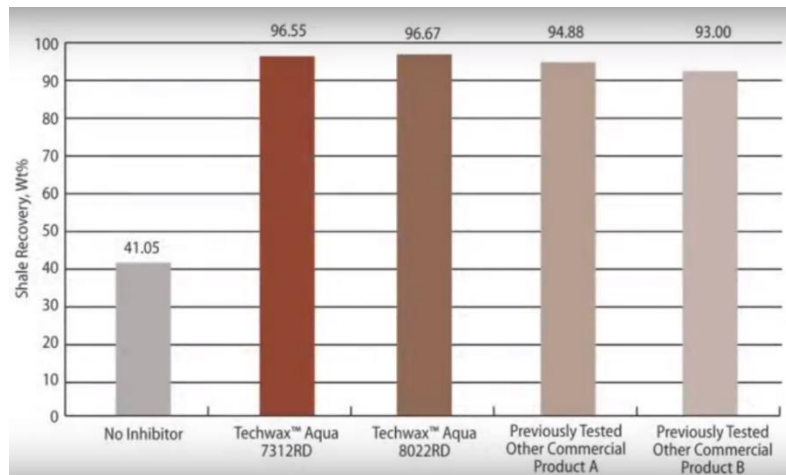


Figure 25. Sample dispersion test results involving industrial additives [68].

Suitable for this test are shales with large quantities of Smectite and a reasonable amount of Illite. Cuttings are often used although cuttings recuperated from water-based fluids are not advisable due to the fact that the cuttings would have reacted and broken down before the Dispersion Test.

2.4.7 Capillary Suction Time Test - Physical

The Capillary Suction Time (CST) apparatus was initially used to record the amount of time that a slurry filtrate would take to move a certain amount of distance on a dense porous filter paper [69]. The CST apparatus now tests relative fluid interactivity with ground material. It records the CST of clay and shale slurry which is a thin mixture of shale and usually water. CST can be used to study the filtration capabilities of aqueous systems by using the capillary suction pressure of a porous paper to affect filtration. It is a simple test where a small amount of shale (minimum of 3g of either dry cuttings, cavings or core material) is mixed with brine, water, or mud filter in the sample cylinder and the filtrate is drawn out due to the suction pressure of the filter paper beneath the sample. This filtrate then flows radially, and the timer is started when it reaches the first pair of electrodes. The timing stops, and a signal is sounded when the filtrate reaches the third electrode. Different salt concentrations are chosen, and multiple experiments are conducted at these concentrations. If the shale is more reactive, this will lead to a larger CST value and also to a higher Smectite clay content. Sample results can be seen in

Figure 26 [70]. The CST test is highly affected by operator and unit operations (same grind size, fill method, operator manual operations) thus making measurements by varying labs difficult to directly compare [71]. It also produces an integrated result of several processes and cannot be scaled back to one specific process [72].

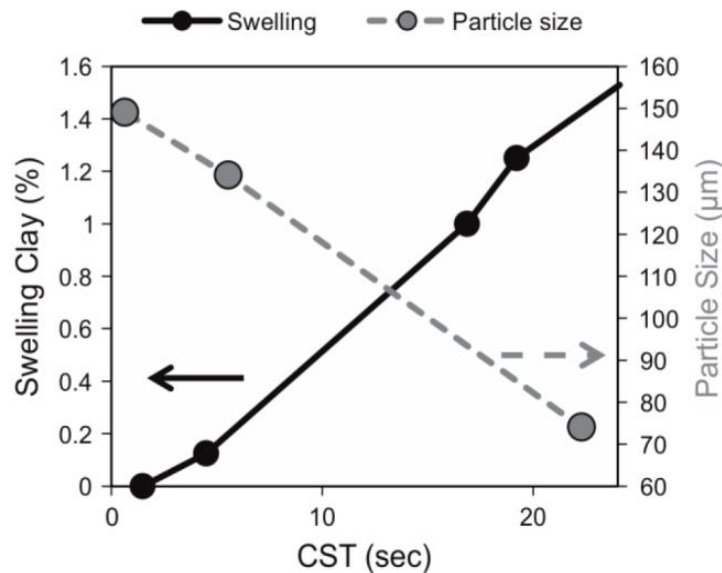


Figure 26. Sample CST results of how increasing the swelling clay percentage or decreasing the average particle size of a sample will result in increased CST times [70].

2.4.8 Bulk Hardness Test - Physical

As the name suggests, this test gauges the hardness of the shale after they come in contact with different fluids. This test is similar to the dispersion test in that the shale fragments are hot rolled in the test fluid for 16 hours at 150 °F. Then they are recuperated on a 50-mesh sieve and transferred into the bulk hardness tester - Figure 27. The operator then uses a torque wrench to extrude the sample through a perforated plate. The metric that is recorded is the torque required for each turn. Harder samples will require more torque while softer samples will require less torque.

The inhibitive properties of the drilling mud being investigated can be linked to the hardness of the shale as shale that interacts with water and becomes weaker owing to the adsorption of water, swelling and the consequent scattering of small particles. This can then lead to the compressive strength of the shale to reduce which then leads to severe wellbore stability problems. Soft and sticky cuttings can cause additional problems such as mud rings, bit balling and sticking problems.

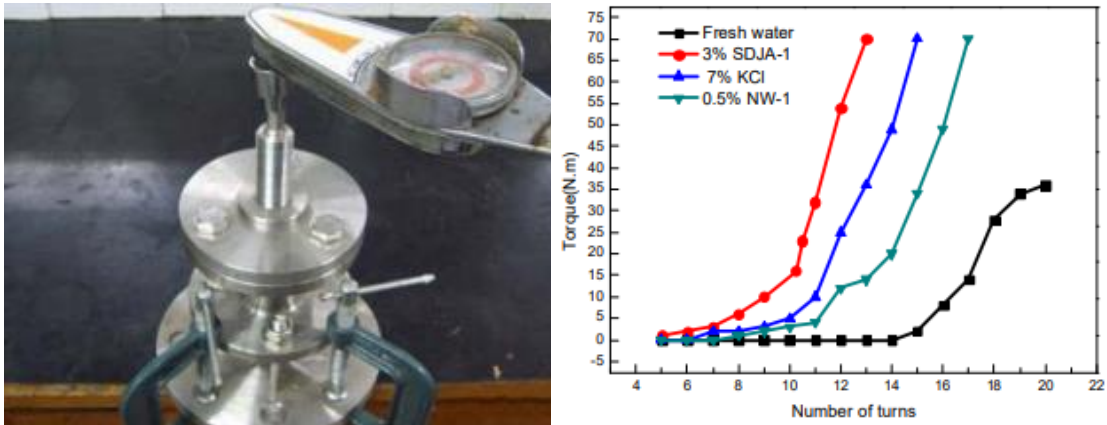


Figure 27. (Left) Bulk hardness tester; (Right) sample results using shale cuttings with additives [60].

2.4.9 Bentonite Inhibition test – Physio-chemical

This is a screening test used to find out the ability of a product to avert the bentonite from swelling and preserve a low rheological profile [73]. This test measures how effective a single treatment of shale inhibitor can inhibit the maximum amount of API bentonite. In short, 400 mL of water containing different concentrations of inhibitors are treated with 20 g of sodium bentonite each day after hot rolling at 150 °F for 16 hours. The rheological characteristics are recorded after each cycle. The procedure is repeated until the fluid is too viscous to be measured.

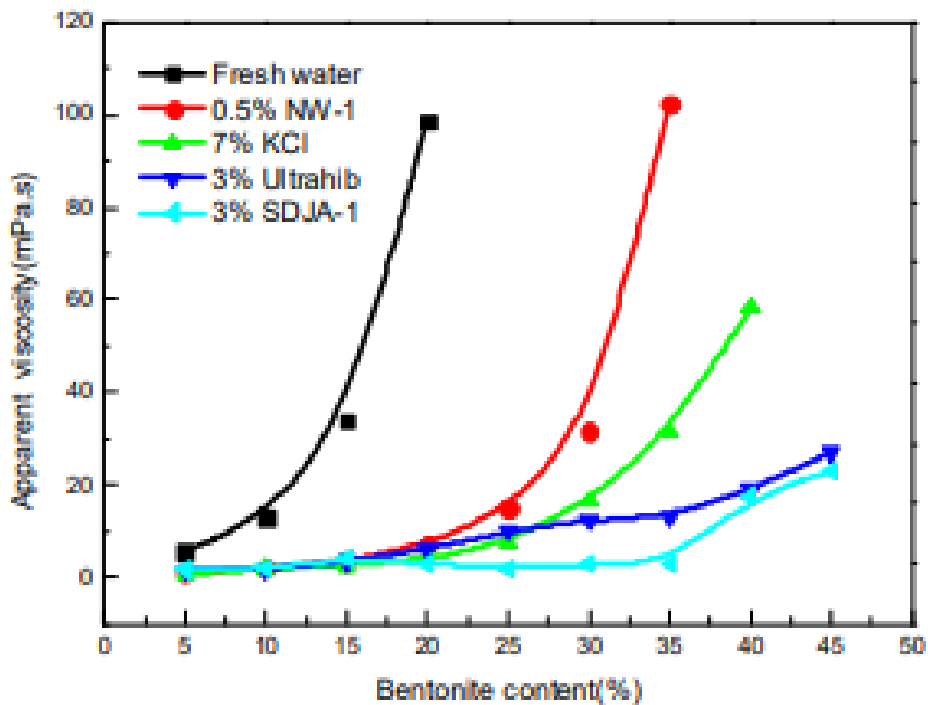


Figure 28. Sample bentonite inhibition test results with apparent viscosity variation vs bentonite content [73].

As can be seen in Figure 28, the apparent viscosity and yield value of the fresh water increase significantly at increasing bentonite content due to clay hydration and dispersion. For the different additives, the apparent viscosities increased at a lower rate depending on the bentonite content.

2.4.10 Fracture Development Test and Immersion Test - Physical

The Fracture development test is a qualitative method that uses Time-Lapse Photographs (TLP) to identify and track the expansion of fractures in shale formations as they come into contact with drilling fluids [74]. TLP is a method whereby the frequency at which the frame rate captured is much lower than that which will be used to play the sequence back, and a sample result is shown Figure 29.

One severe limitation of this technique is that the fluids being used must be clear in order for photographic analysis as the fracture development cannot be documented otherwise. Quantitative measurements can also be made such as the amount of fractures present, peak fracture width, and average fracture width.

The Immersion test primarily uses TLP to classify, track and define by qualitative means the source of instability occurring in shale samples when submerged in various liquids.

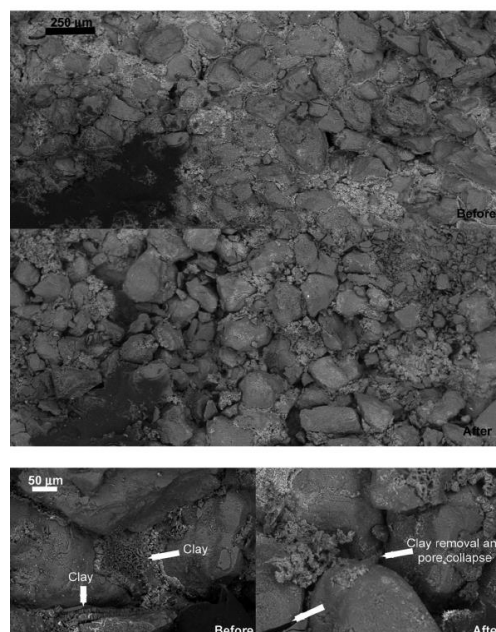


Figure 29. Time-lapse images showing changes in the microstructure of sandstones before and after injection of CO_2 aqueous solution ($\text{pH}=2.8$) [75].

Review of laboratory tests

There is no single standardized test for all types of shales and additives as each test could measure different variables that cannot essentially be directly compared. This, in fact, could be an advantage as different tests produce different metrics which can then be used for a better understanding of the shale/fluid dynamic. As mentioned before, some tests are difficult to repeat as the end result can be dependent on the operator running the test such as the Capillary Suction Time Test. The industry is continually evolving and developing new methods specific to the shale interval that is of interest to them. Even more tests exist such as the Bentonite sedimentation test, Dynamic linear swelling test (DLST), Wettability alteration test, Zeta potential measurement test [76] but these are less preferred and also fall outside the scope of this work.

The three most popular methods used to gauge inhibitor performance are the Bentonite inhibition test, Bulk-hardness test, and the Hot-rolling Cuttings dispersion test. Although all these tests are useful, each describes the interactions differently and do not always show the same trend. For example, Bentonite inhibition tests and Hot-rolling Cuttings Dispersion tests have shown unlike outcomes and results when the same fluid systems were used [77]. It can be summarized that the currently available inhibition tests are yet to deliver coherent and thorough data on the causes of the inhibitory action and mainly focus on comparing results between varying additives at different concentrations.

2.5 Particle analysis

Real-time analysis of a process stream, tracking the grain size distribution, enables accurate observation of the changes that happen during shale particles-water interaction. Particle size analysis is the standard terminology of the methodical procedures that identify the size range of the particles in a liquid or powder sample. In this research project, two specific properties of particles are focussed on, namely the particle size distribution and the particle count. The particle size distribution (PSD) can be measured through several methods, but in all methods, the size is an indirect measure where a shape hypothesis is obtained by a model that transforms the real particle shape into a standardized shape like a sphere or cuboid [78]. In many cases, knowing just the particle size is not sufficient, so a particle count was

also tracked to enable a better understanding of the material and processes. Particle count tracking can be done through several methods too, and in all these methods, a high-intensity light source is used to illuminate the particles as it passes through a detection chamber [78]. Figure 30 shows sample results, obtained from the literature [79, 80], of Malvern Mastersizer testing and FBRM testing.

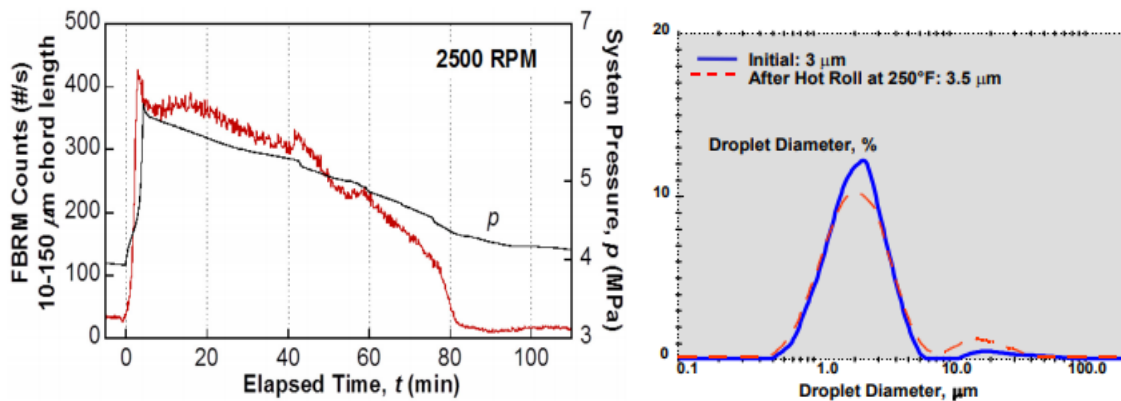


Figure 30. (Left) Sample particle count result from FBRM [72]; (Right) Sample particle size distribution result from Mastersizer [73].

It is important to reiterate that observing the effect and resulting magnitude of the interactions between water and shales is one of the primary goals of this research project. Developing a new way of testing involving these new tools was much of an iterative process as such procedures are not widely cited in the literature. There was, however, research work by Ronaes et al. [81] that provided some inspiration. In their paper, they described the successful use of the FBRM in the North Sea for remote real-time monitoring of drilling fluid particle size distributions. The live and real-time PSD recordings were employed to study the effect of the supplementary particulate material on the drilling fluid and whether the full effect of formation strength could be achieved. Figure 31 shows examples of how FBRM is being used to gather data through real-time measurement.



Figure 31. (Left) FRM electronics box and purge unit; (Right) FBRM apparatus and pipe-mounting adapter [75].

As it will be made evident at the end of the following chapter, the proposed experimental program leads to the successful extracting of quantitative data from the clay particles being tested.

2.6 Clay/Shale particle inhibition test

A primary goal of this thesis was to find a novel way to quantify the disintegration of clay cuttings after their exposure to fresh water. Of the earlier described tests, few of them give quantitative results and often require complicated equipment that need specialized knowledge. In general, the shale hydration-disintegration in aqueous mediums has rarely been studied using in-situ particle analyzers according to literature and is an area of research that has only recently been gaining traction. At present, there is only one research article by Kartnaller et al. [82] published in 2017 that recommends the use of laser backscattering (FBRM technology) to gauge the shale inhibition process. Although this paper reveals exceptional novel results, just one particle analysis tool is applied to shale inhibition, namely the FBRM, and the Malvern Mastersizer or any laser diffraction tool to obtain particle size distributions is not researched. Particle analysis, especially particle size analysis, is of significance since particles affect fundamental colloid properties such as rheology, surface area, and packing density.

As described earlier, the interlamellar swelling of clay minerals in shale formations is most often acknowledged as one of the leading causes of failure in wellbore stability [26, 33, 83]. This could be because of their laminated sequencing and composite makeup. A vast number of additive inhibitors are applied to function inside the

passageways of the water-sensitive clays. In this thesis, firstly the shale/clay water interaction is studied using a new methodological procedure and this same methodology is used to study this phenomenon to validate inhibitor performance and characterize the breakdown of cuttings. A robust laboratory process was developed where advanced particle analyzers were implemented in process streams to give data that can be used to make quantifiable comparisons of the results.

To characterize the variation of clay particle sizes and count, three methods of particle analysis were implemented: particle tracking, particle size distribution, and rheology measurement.

i. Particle Tracking

Focused Beam Reflectance Measurement (FBRM M500) system was used as a tool to track the particle count of clay after it was submerged in an aqueous solution. The FBRM, often denoted as scanning laser microscopy (SLM) [84], was an approach developed in the 1990s with the aim of observing particle and aggregate properties with prospects to be drilled applied to suspensions across of a full concentration range

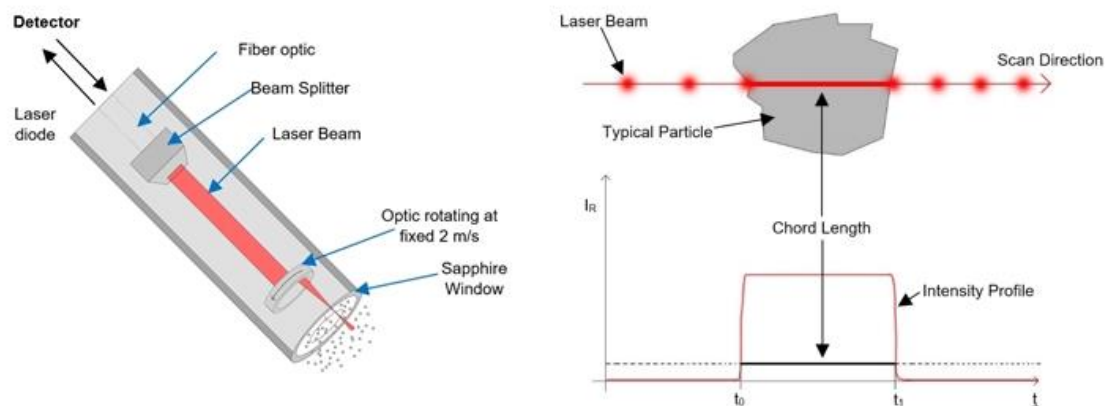


Figure 32. (Left) FBRM Probe Schematic; (Right) Chord Length of particle schematic.

In order to take measurements, the FBRM M500 probe is injected directly into the target solution, at an angle, and the particles that flow across the probe window are tracked in-situ. A laser beam is directed across the sapphire window of the probe, rotating at a speed of 2 m/s and as this laser beam scans through the particles arrangement, discrete particles of the sample will backscatter the laser light to the detector as shown in Figure 32. The chord length, which is defined across each

particle, is then calculated by counting backscatter pulses and the multiplying the scan speed by the duration of each pulse.

The chord length is an essential dimension of the particle directly linked to the particle size. As the test is run (Figure 33), many thousands of particles are tracked per second. From the start the final moments of the tests, the chord length distribution tracks how the particle count changes and produces real-time tracking of particle size, population, and events.



Figure 33. (Left) Schematic drawing of probe position relative to the overhead stirrer; (Right) Sample photo.

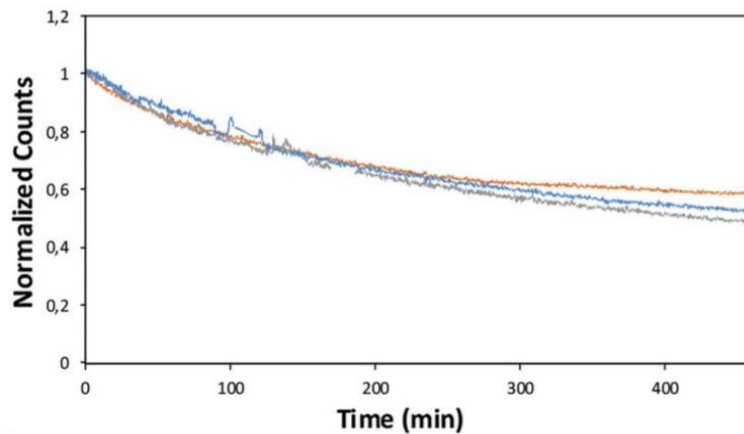


Figure 34. Results of the use of FBRM as a tool for real-time measurement of solid particles [82].

Figure 34 shows a sample result obtained by Kartnaller et al. [82] showing the normalized counts over time for a triplicate of experiments using a shale sample in a fluid system. Normalization was performed by Kartnaller et al. to allow for reproducibility, as reproducibility can be adversely affected by small differences in mass, the height of FBRM probe in dispersion and angle of the probe's fiber optics.

In this case, by dividing the measured values at time $t(C_{range})$ by the original amount ($C_{range}(0)$):

$$C_{range}^{norm}(t) = C_{range}(t) \div C_{range}(0)$$

Allowing this change makes it easier to observe the changes in the curve relative to its original value. The value would be higher than one if the signal is increased and similarly the value would be higher than 0 and lower than one if the signal is decreased.

Observing the particle count gives a qualitative explanation of what impact the additives have on the clay/water interaction. In theory, it is agreed that an increasing or increased particle count indicates that the particles are disintegrating and breaking down into finer particles thus increasing the total particle count in the fluid. A decreasing or decreased particle count indicates that the additive is having an inhibitive effect on the clay cuttings and preventing it from breaking down into a finer size. As the consequence of continuous shale hydration and as the fluid is stimulated in water, the quantity of coarse particles decreases whereas the quantity of smaller particles increases. These outcomes are caused by clay packets breaking and discharging a substantial amount of small tactoids [84].

ii. Particle size distribution

The particle size distributions for each sample were generated using the Malvern Mastersizer 3000. The Mastersizer is a compact optical structure that uses the technique of laser diffraction to quantify particle size distribution for both dry and wet dispersions. As the name infers, the dry dispersion unit is where dry (usually powdered) samples can be sampled, and the wet dispersion unit is where wet samples can be sampled. In summary, a scattering pattern (Figure 35) is obtained from a target sample by passing a laser beam through the cell. The dispersed particles in the cell disseminate the light thus generating a scattering pattern. The optics in the Mastersizer measure the angles of scattering and the intensity of the scattered light from which the Mie theory is applied to calculate the particle size distribution [85]. In summary, smaller particles scatter light at greater angles, and

larger particles scatter light at lesser angles. The particle size is then reported as a volume equivalent sphere diameter [85].

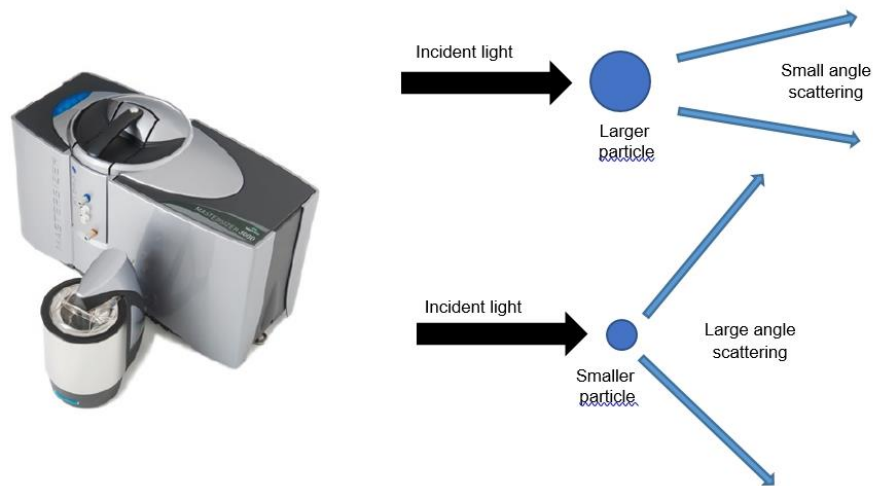


Figure 35. (Left) Malvern Mastersizer 3000; (Right) Laser Diffraction Schematic.

iii. Rheology measurements

This final method of particle analysis is not as pertinent as the earlier two mentioned topics, but it is important to note some key definitions.

Rheology is the study of the flow of matter, mainly in a liquid state. Three dynamics impact the rheology of any suspension.

1. Particle size
2. Particle size distribution
3. Percentage of solids present

Viscosity is defined as the resistance of a fluid to flow or change in shape and is commonly known as "thickness". Liquids that possess a high viscosity are relatively motionless when shear is exerted on them while low-viscosity fluids flow much more easily.

The speed with which a material is being deformed is known as Shear rate. If the viscosity of a fluid stays the same while shear rate rises, then a fluid is described as Newtonian. Non-Newtonian fluids do not display this response, and they either fall into the shear thinning or the shear thickening category. With shear thickening, the

fluid displays increased viscosities at increasing shear rates. Shear thinning fluids have their viscosity decrease with increasing shear rate. Most fluids and semisolids fall into this category, and Figure 36 [86] shows the relationship between Newtonian and Non-Newtonian fluids. The flow behavior of some mud systems is illustrated in Figure 37 as an example [4].

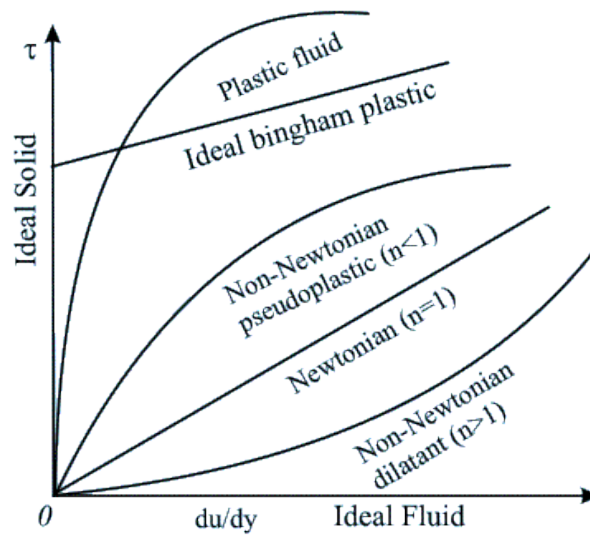


Figure 36. Shear stress and deformation rate relationship of different fluids [86].

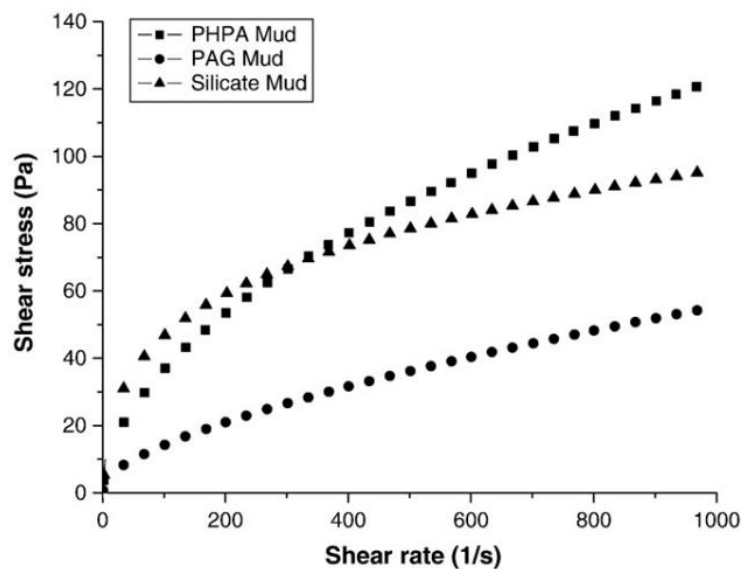


Figure 37. Shear stress vs. shear rate of whole mud systems [4].

Chapter 3

Research Methodology

3.1 Introduction

In this Chapter, the experimental program employed to characterize the breakdown of drill cuttings is detailed. In this procedure, a known size distribution of cuttings are introduced to a background solution, and the variation in the size distribution of the particles is quantified with the use of particle analyzers. In addition to this, to avert the accumulation of fine particles into much larger, unwanted units, steps need to be implemented to prevent particles from aggregating due to inter-particle collisions in the fluid medium. To achieve this, an overhead stirrer attached with an impeller is used in the experimentation.

A customized experimental program was developed to study the clay-water interaction and how numerous chemical additives impact this interaction. Modern laser particle analyzers were employed to perform a benchmark of the tested additives and these tools have successfully been applied to various other industries such as the pharmaceutical & paper industries [87] but have only recently been applied to the domain of drilling fluids. A vital goal of this research project has been to provide an extensive experimental program that can characterize the breakdown of clay cuttings over time, and this chapter will detail this aspect.

It is very important to note here that there are limitations to this experimental method when compared to a real borehole drilling environment. The developed method only focuses on the fluid interaction between the shale through the study of particle count and particle size with isothermal test conditions and also does not encompass structural effects, geo-mechanical effects and the impact of bottom-hole pressure.

3.2 Experimental Program

The literature has limited information available on the use of particle analyzers in drilling fluid environments and thus designing an experimental program was much of an iterative process. An all-encompassing, sequential experimentation program was developed, with the aim of benchmarking the performance of various additives at inhibiting the clay particles and minimizing formation of smaller cuttings.

Criteria for designing the experimental program:

There was one fundamental criteria that this program had to adhere to –

Application-based research – The experimentation must involve copious amounts of testing that produces quantitative results and it would be ideal to have an experimental approach where identical tests are conducted on a range of additives. This will allow future testing to be continued on numerous additives and a standard benchmark to be available on all tested additives.

As the procedure was thought out and designed, there arose five specific variables for the testing. The first is the type of equipment used to extract different forms of data. FBRM was used to obtain particle count, Mastersizer was used to obtain particle size distributions, and a Viscometer was used to obtain rheology. Next, the type of clay samples being tested were limited to two – Sodium Montmorillonite and a Shale core sample which will be detailed in the further pages. Thirdly, the type of additives used was varied. Potassium chloride is used, and then various industrial additives are tested. The fourth variable was the concentration of the additive tested – it varied depending on the additive. And finally, the fifth variable was the duration of testing – either for 2 hours (regular test) or 47 hours (long duration test).

The management of pH to a constant level is also important as the pH can have a large effect on dispersion and agglomeration. The pH was not measured during tests but all tests were conducted using hard water obtained from the same source.

Summary of procedure:

1. 75 μm Sodium montmorillonite clay is gathered through sieving. This size is used as the initial size distribution of the dry clay. The criteria for selecting this

size is because this size lies within the range of very fine to very coarse size range and represents the cuttings produced from percussive and rotary drilling.

2. The probe, overhead shearer, baffle bucket (with one ltr of fresh water) are all arranged as shown in Figure 39. A baffle is used to allow for optimum mixing.
3. Overhead Shearer set to rotate at 900 RPM.
4. The FBRM Probe is set to record the clay count. A laptop having "FBRM Data Acquisition" software installed is connected to the FBRM and records the data.
5. At the one-minute mark, the selected additive is gently added to the fresh water in the bucket. This time period was chosen as a constant for all tests.
6. At the three-minute mark, 5% Sodium montmorillonite particles ($75 \mu m$) are added into the bucket/fresh water. This time period was chosen as a constant for all tests.
7. This solution continues to be mixed, and Particle count data is recorded using the FBRM for a total of 2 hours. Attached computer with FBRM software records data.

The experiments were performed at different background concentrations of the select additive with a dynamic condition provided by an overhead mixer. The shear rate, the volume of water, duration of testing were all kept constant to some degree. Every attempt was made to ensure reproducibility of sampling methods but it should be noted that there could be a minimal percentage error arising due to human error or equipment malfunction

8. Immediately after the FBRM tests, the fluid sample is collected and split equally into four plastic containers as described in Figure 38. This is so that Particle Size distributions (PSD) can be obtained with the aid of the Malvern Mastersizer 3000.
9. Each container fluid is sampled three times to obtain a total of twelve PSD's. These results are averaged to obtain one final representative PSD. This

averaged PSD is used as the final PSD result of that sample. Figure 39 provides an overview of the entire experimental setup.

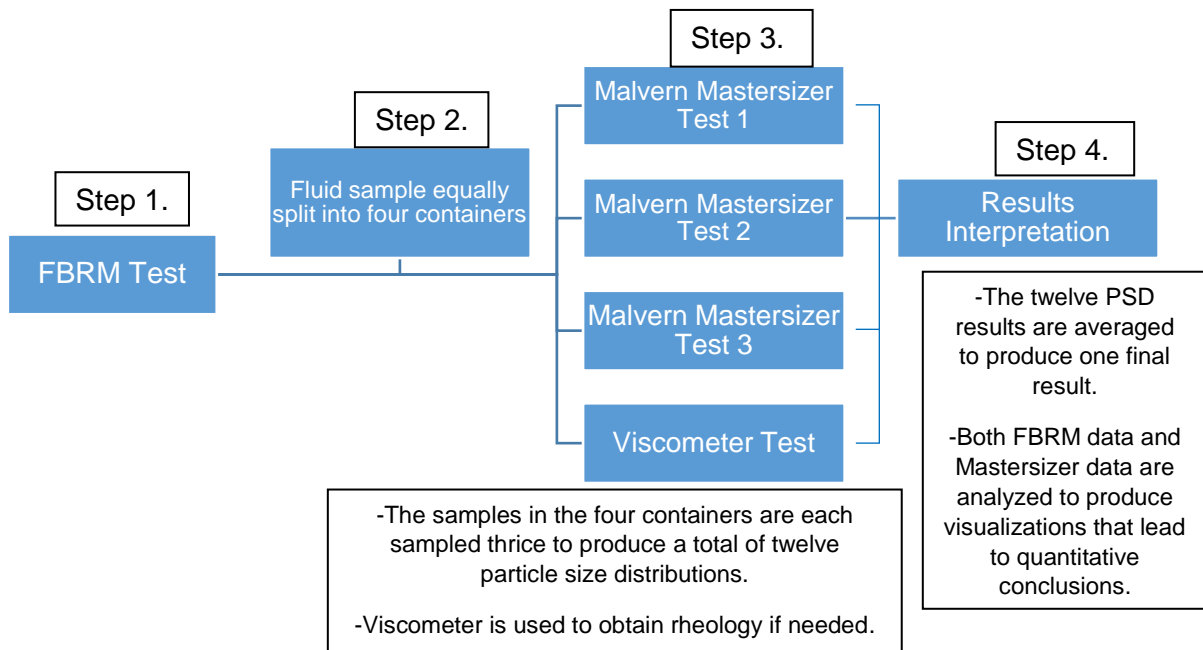


Figure 38. General procedure chart.

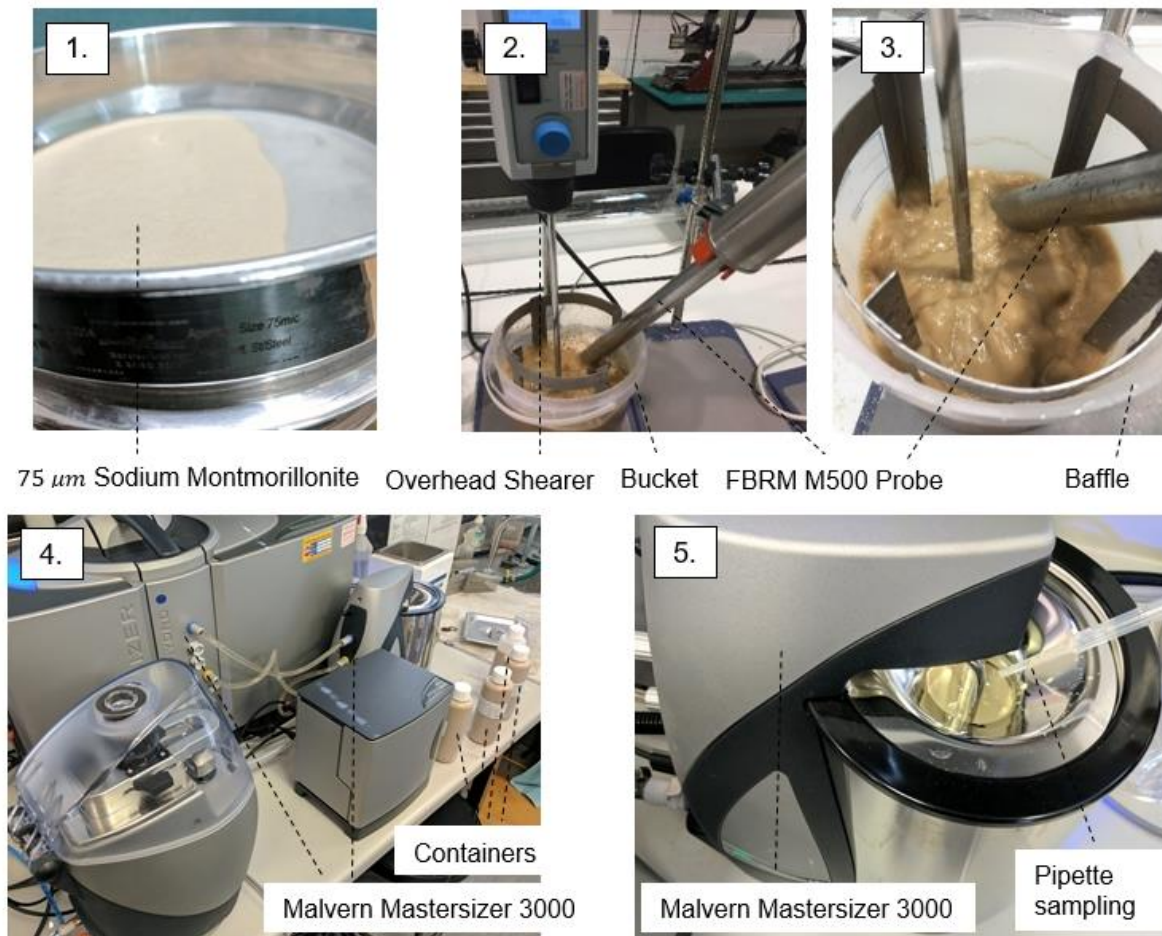


Figure 39. Experimental setup.

Sample results obtained from FBRM are illustrated in Figure 40 , and these are the results of a triplicate of experiments conducted under identical conditions to prove that the FBRM experiment results are reproducible. This repeatability is a control step and a pre-step to testing the formation samples to assure compatibility of additive with representative mud additives to be used on the well. In short, this is an effective way of assuring or testing variable additives in the mud to assure a stable system before testing with shale samples as mud systems can include a number of additives. The varying particle counts are shown over 3,500 seconds. The three results are not identical but border on a similar range of ~19,000 particles for each test. This verifies that the test is indeed repeatable and the procedure can be followed and similar results replicated.

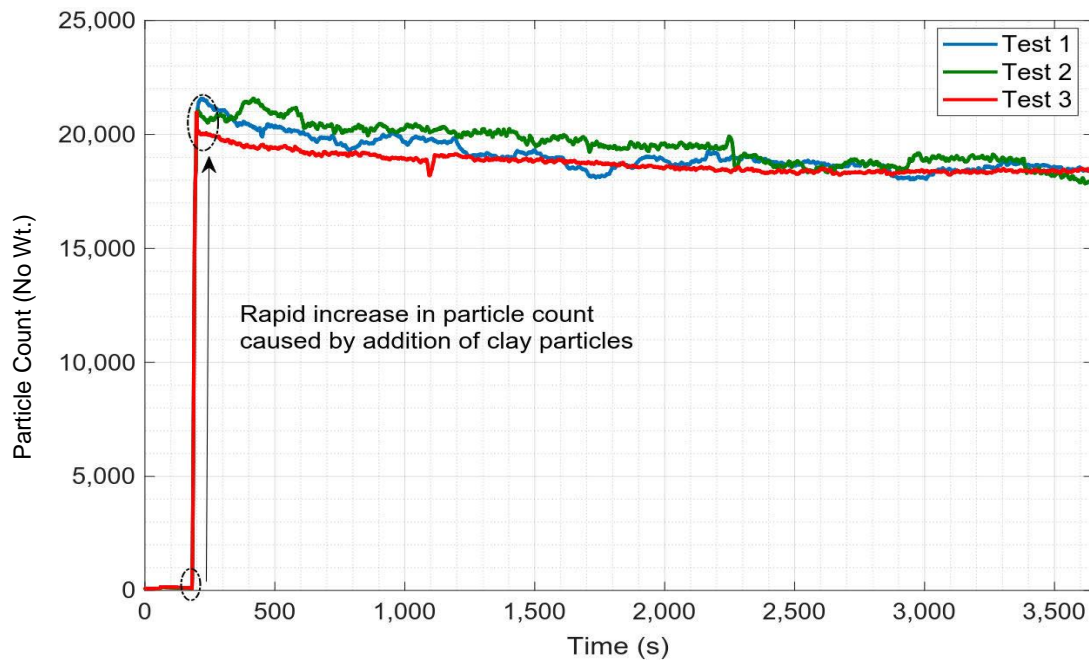


Figure 40. Sample FBRM results of a triplicate of tests

If testing parameters are identical, analogous results are expected to be generated by the FBRM. Results cannot be precisely replicated as the FBRM records data rapidly every second and small discrepancies are bound to happen. As a result, to rule out the possibility that the FBRM particle count data was not reproducible, each FBRM test in the procedure was repeated three times. A single result out of the three was selected based on how well it aligned and represented all three results. It must be noted that for all tests, the three results had a similar particle count range albeit them not being the same.

Figure 41 shows example results that were obtained using the Malvern Mastersizer 3000. These are twelve identical test results and all results resemble each other and follow a similar trend. The average is obtained from the twelve results and used as the final PSD result of the sample.

After careful observation of Figure 41, it can be observed that for all twelve test results, there is a significant portion of particles with sizes larger than 100 microns. This is an unusual result as the original particle size for the clay particles is mostly all smaller than 100 microns (see Figure 47). These spikes can be attributed to erroneous measurement as distributions with distinctly different modes of occurrence i.e disconnected peaks can be caused by errors such as bubble peaks. In essence what occurred was that during the testing, bubbles were formed during the measurement of the PSD of the samples and these bubbles were then detected by

the machine as solid particles of a size range larger than 100 microns. In general, most particle size measurement devices cannot differentiate between species present in the distribution [88]. If size distributions are collected from both samples and bubbles, the device being used for measurement will report both in a random manner. This error is in fact a common error associated with the Mastersizer laser diffraction measurement technique. There is a clear distinction between the clay particle peaks and the bubble peaks. What is important to note is that the bubble peaks do not overlap with the clay particle peaks but they will undoubtedly impact the cumulative size of each plot and will render any related data invalid.

Figure 42 shows an example of a sample result that includes a bubble peak, found in the literature [88]. In contrast, this issue of erroneous measurements of PSD has been addressed by other measurement techniques such as the JM Canty particle analysis system [89]. However, the Canty instrument was not available at the time of conducting these experiments. This knowledge of bubble peaks was also confirmed after consulting with multiple researchers who had experienced this problem arising through the use of the identical Mastersizer 3000 device. There was no other solution available at that particular point in time so it was assumed to best to ignore all the particles greater than 100 microns.

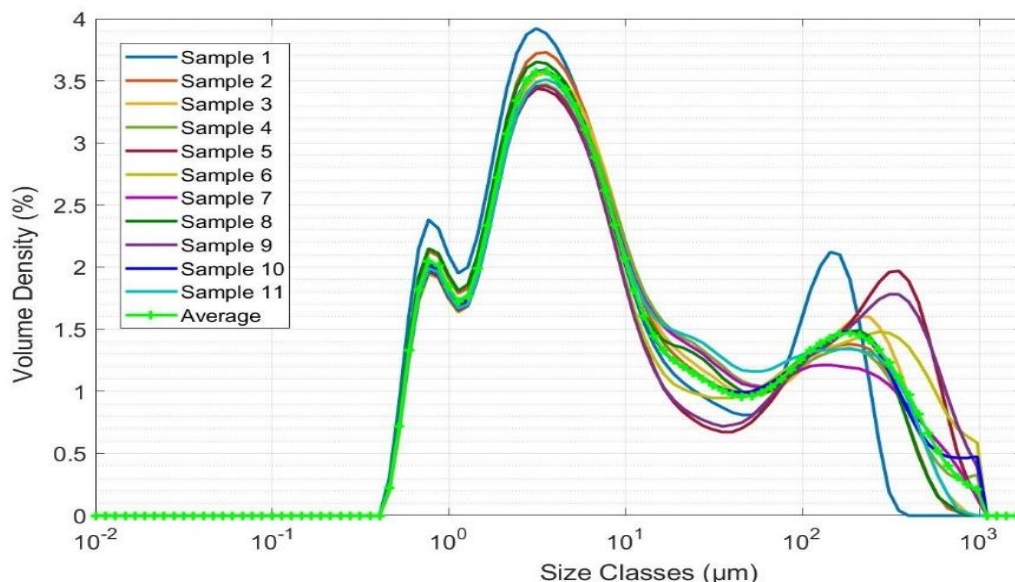


Figure 41. Sample result showing how the average is obtained from 12 tests.

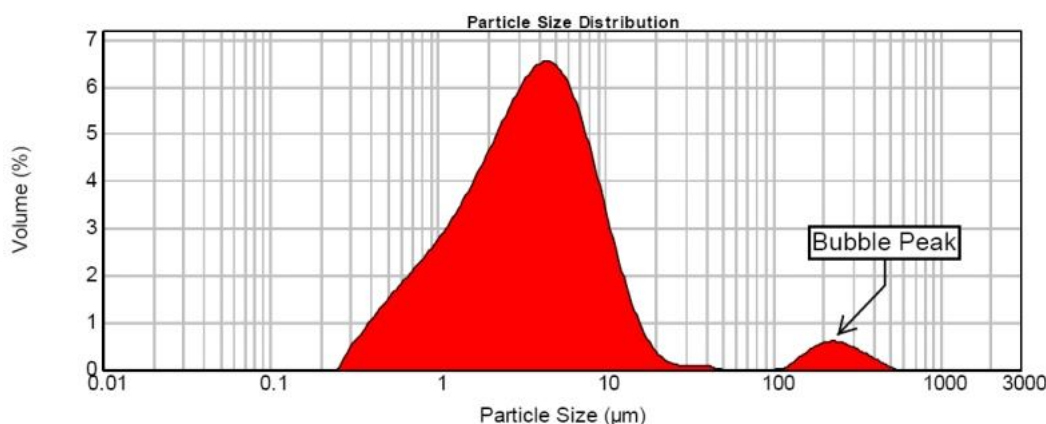


Figure 42. Sample bubble peak in an aqueous dispersion [88].

3.2.1 Testing with shale rock

Here, a shale rock obtained from half-core samples was used instead of sodium montmorillonite particles. Identical steps are followed as outlined earlier except for one fundamental difference:

The shale rock sample used for the testing was obtained from a field trial near Port Augusta, South Australia (Figure 43). A few trial pictures are shown in Figure 44 and Figure 48. As can be seen from Table 3 the drilling operation intersected weathered Quaternary conglomerate and variably weathered Neoproterozoic shale, sandstone, dolomite and basalt. The specific shale sample was obtained from a depth of ~40 m and was identified as Tregolana Shale. The average specific gravity for the Tregolana Shale is 2.57 g/cc [90].

Table 3. Summary Geology log for Port Augusta drill hole [90].

From	To	Lithology (Major)	Lithology (Minor)	Stratigraphic unit	Description
0	6.25	Conglomerate	Sand	Unnamed Cenozoic sediments	Light grey, coarse-grained to cobble, poorly sorted, sub-angular to sub-rounded, clast-quartzite, highly weathered.
6.25	136.58	Shale	Sandstone	Tregolana Shale Member	Dark reddish brown to greyish brown, laminations, fine-grained, very well sorted, interbedded shale and sandstone.
136.58	146.89	Sandstone	Dolomite	Nuccaleena Formation	Greyish brown, fine- to medium-grained, well sorted, sandstone interbedded with dolomitic shale.
146.89	164.95	Sandstone	Shale	Yerelina Subgroup	Pale reddish brown to greyish brown, fine- to medium-grained, moderately to well sorted, convolute bedding, flaser bedding, laminations, interbedded shale and sandstone.
164.95	223.15	Sandstone	Conglomerate	Yerelina Subgroup	Moderate brown, fine-grained to pebble, poorly sorted, sub-angular to sub-rounded, clast-volcanics, slump structures.
223.15	224.5	Sandstone	Mudstone	Upalina Subgroup	Moderate brown, fine-grained to gravel, poorly sorted, sub-angular to sub-rounded, clast-volcanics, ?slump structures.
224.5	397.95	Shale	Dolomite	Tapley Hill Formation	Dark grey, very fine-grained, very well sorted, sub-rounded, shale interbedded with dolomitic rock.
397.95	564.5	Basalt		Beda Basalt	Greenish grey to pale reddish brown, amygdaloidal, fine- to medium-grained.

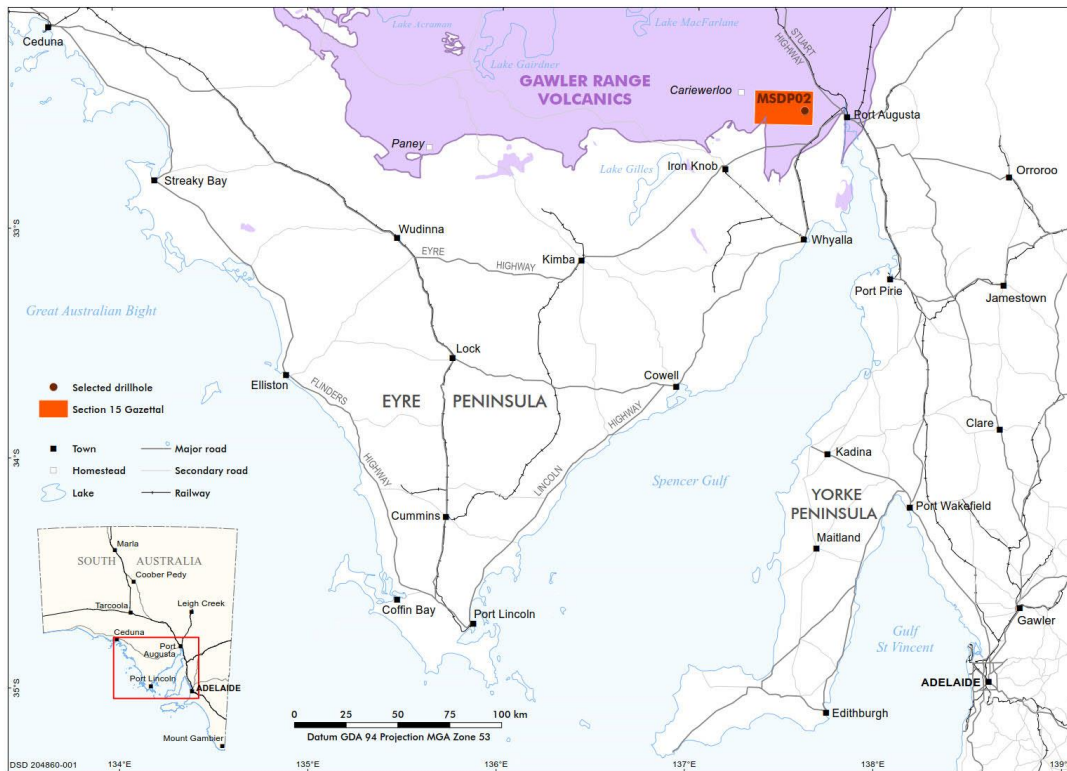


Figure 43. Exact location of drill hole (MSDP02), ~52 km west of Port Augusta [90].

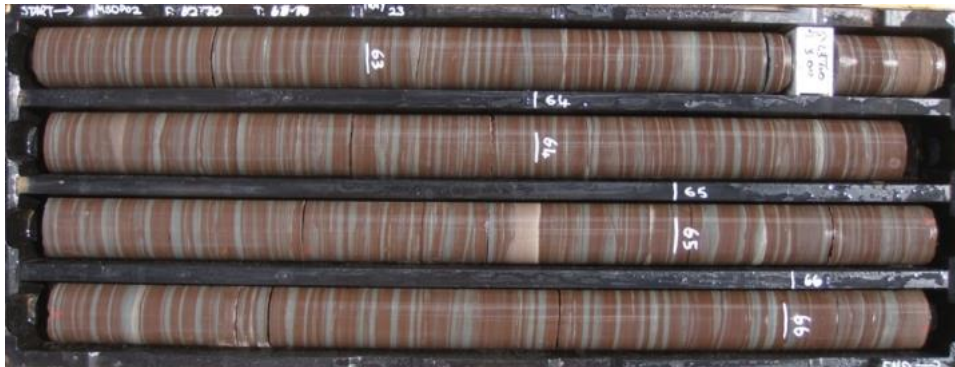


Figure 44. Red and green, finely laminated shale with minor sandstone, Tregolana Shale Member (~64m) [90].

Real time XRF Geochemistry and XRD Mineralogy on drill cuttings was provided by the Lab-at-Rig technology and its results are shown in Figure 45. It is again important to note that the selected shale sample was from a depth of ~40m.

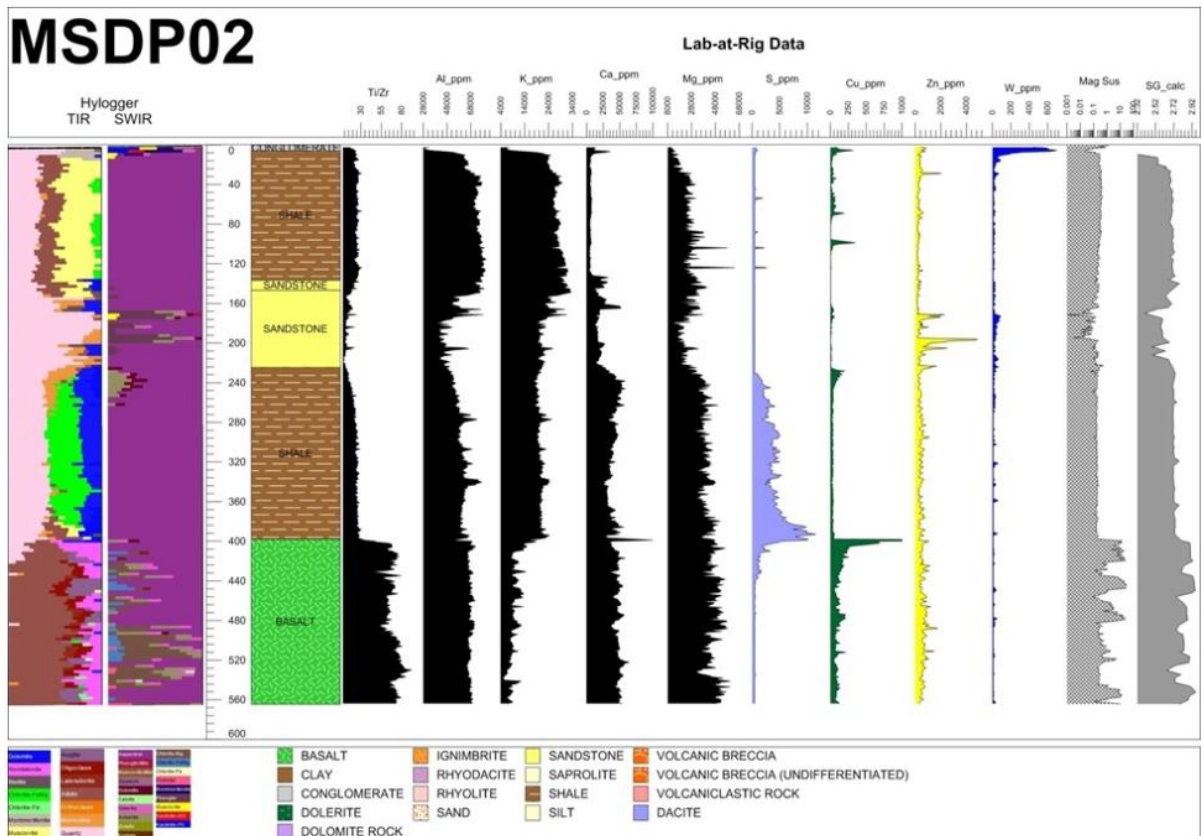


Figure 45. Real-time XRF geochemistry and XRD mineralogy on drill cuttings [90].

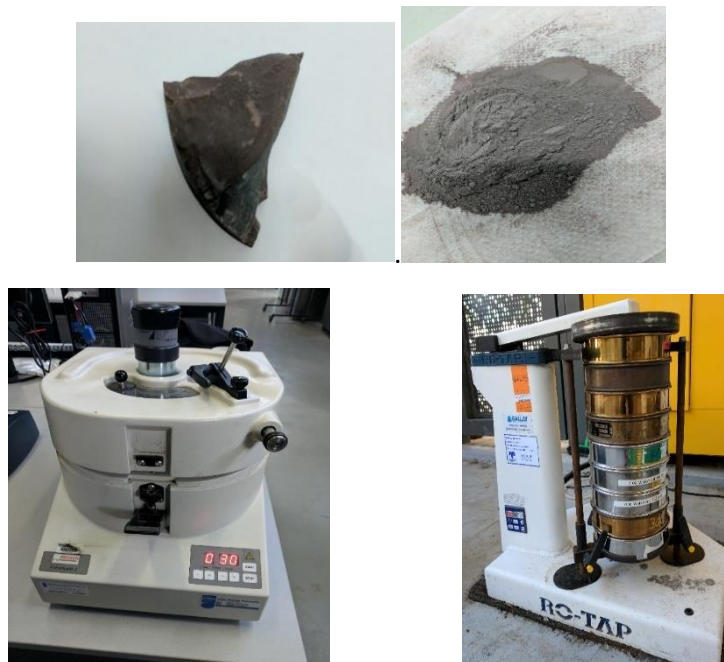


Figure 46. (Top) Port Augusta shale rock sample; pulverized shale; (Bottom) Pulverizer/Grinder; Motorized sieve shaker

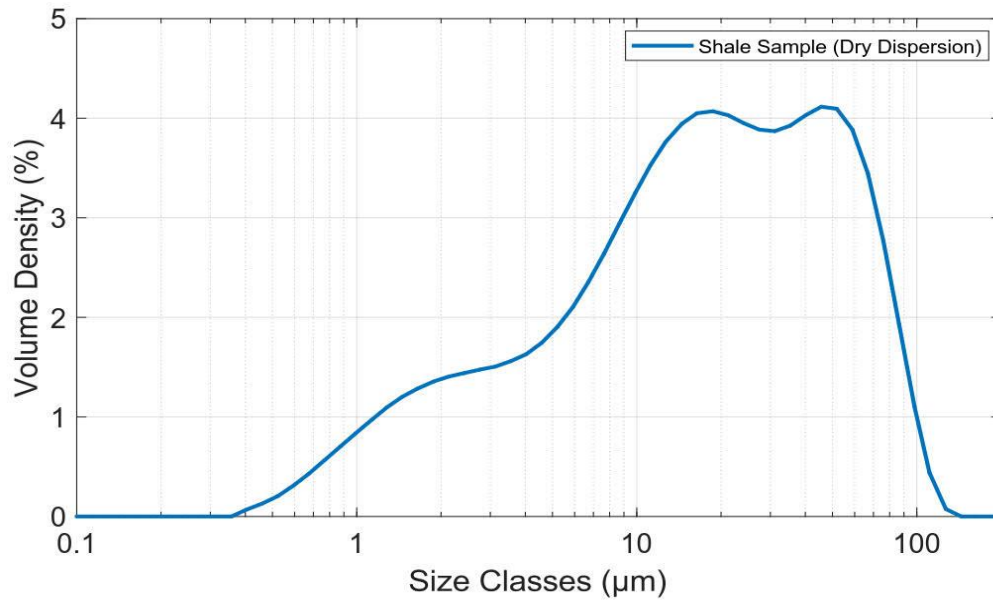


Figure 47. PSD of dry shale sample.



Figure 48. Field trial of RoXplorer Coiled Tubing rig at Port Augusta - Photo courtesy of DET CRC.

3.2.2 Extended test

An extended test was conducted to find the relationship between particle size distribution, viscosity and time. The hypothesis at the time of experimentation was that the particles would disintegrate further and further with time due to clay hydration leading to the particle size distribution to become increasingly concentrated in smaller particles.

For this test, the same procedure was followed as before with three differences: the FBRM was not used – particle count was not tracked, no additives were added, and the mixing (using overhead shearer) was done for a total of 47 hours at a stretch. At time intervals of 10 minutes, 1 hour, 2 hours, 6 hours, 24 hours, 30 hours and 47 hours, samples were obtained from the baffle bucket using a pipette and a single PSD was obtained using the Mastersizer. Along with PSD, rheology measurements were obtained using a viscometer.

At various phases of the experimentation, the rheological properties of the fluid were quantified using an Ofite Model 900 Viscometer (Figure 49).

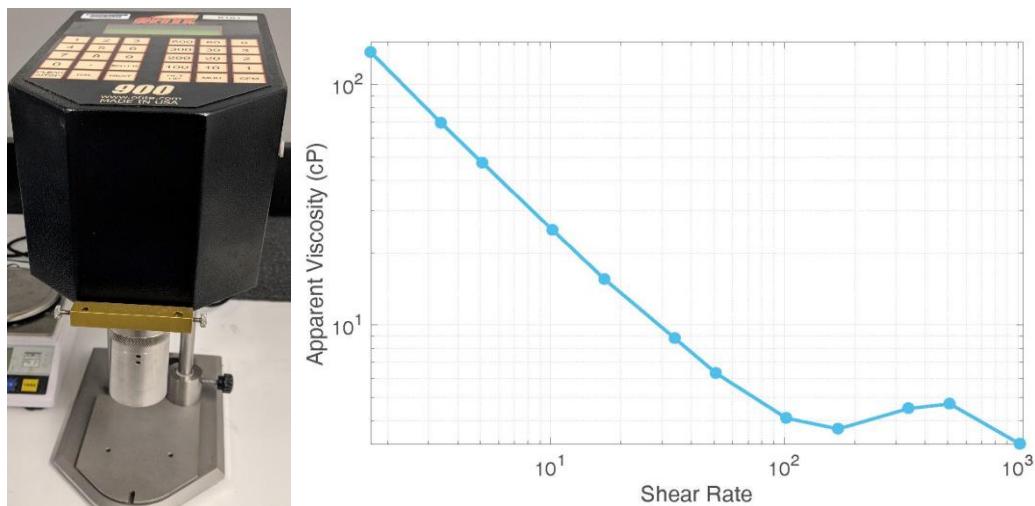


Figure 49. (Left) Ofite Model 900 Viscometer; (Right) Sample Viscometer results of a simple additive solution.

3.2.3 Materials used in testing

a) Clay Sample:

API grade Bentonite (Sodium Montmorillonite Clay) was used as the clay sample. Bentonite is very commonly used in drilling operations primarily as a viscosifier, for filter cake building and filtration control. It hydrates more than other types of clays, has a small particle size and a unique flat shape, which all make it ideal for particle analysis through the FBRM and Mastersizer. Rheoben NT is a naturally occurring clay mineral in Australia and its composition is summarized in Table 4 and its dry particle size distribution (in its raw state) is shown in Figure 50.

Table 4. Rheoben NT composition.

Ingredient	Content
Quartz	2 to 10%
Bentonite	90 to 98%
Soda Ash	2 to 4%

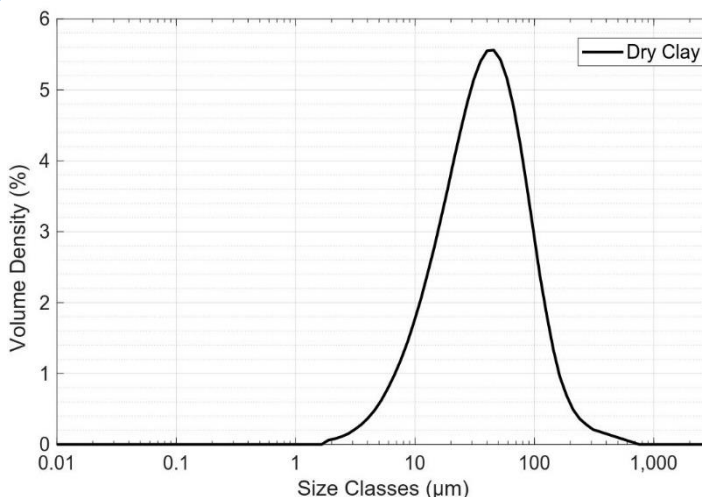


Figure 50. (Left) Sack of API Bentonite used for testing; (Right) PSD of dry Sodium Montmorillonite sample.

b) Additives:

Potassium Chloride (KCl) was used as the inhibiting additive for all the tests for the preliminary stage of experimentation. This is because the inhibiting effects of potassium based drilling fluids on shale instability are widely discussed in the literature [24]. K-based fluids have been observed to affect the swelling and dispersion behavior of problem shales dramatically.

After the testing of a vast concentration of KCl was completed, industrial additives were then tested. The goal here was to incorporate industrial additives and test their inhibition capabilities. An identical procedure as described earlier was followed, but instead of KCl, the additives detailed Table 5 were incorporated in the testing.

A series of clay inhibitive additives were tested using the earlier described procedure. The additives along with the concentrations used are summarized in Table 5. These additives were selected due to their full usage in the drilling industry. All five of these additives are widely used throughout Australia and worldwide. In the next chapter, the effectiveness of these additives in controlling cutting degradation is detailed and benchmarked.

Table 5. Additive Information.

Additive Name	Concentration	Description
i. AMC Xtrahib	a. 3%	An amine based product that has minimal chloride content, making it more environmentally friendly than Potassium Chloride as an additive.
	b. 5%	
	c. 7%	
ii. Low Molecular Weight PHPA	a. 0.02%	A Water-soluble polymer that is commonly used as a drilling fluid viscosifier. Known to inhibit cuttings dispersion to make solids removal easy and efficient.
	b. 0.05%	
	c. 0.1%	
iii. High Molecular Weight PHPA	a. 0.02%	A Water-soluble polymer that is commonly used as a drilling fluid viscosifier. Known to inhibit cuttings dispersion to make solids removal easy and efficient.
	b. 0.05%	
	c. 0.1%	
iv. Kla-stop	a. 0.05%	Liquid polyamine shale inhibitor used in polymer-based drilling and drill-in fluids.
	b. 0.1%	
	c. 0.2%	
v. Xanthan Gum	a. 0.2%	A polysaccharide with a wide variety of uses. Commonly used as a food additive. Used in the oil industry to thicken drilling mud and to provide great low-end rheology

The Safety Data Sheets (SDS) of these additives are included in the appendix.

Chapter 4

Results and Discussion

4.1 Introduction

The results of the experiments and their interpretations will be presented in this chapter. The inhibition potential that several inhibitors had on shale-water interactions will be discussed, and a benchmark of the tested inhibitors will be provided. The results and discussion section will follow the same order of the experimental program as detailed earlier:

- Effect of potassium chloride on
 - a) Particle count
 - b) Particle size distribution
- Field Application Studies
 - a) Effect of using shale core rock on Particle size distribution
- Effect of time on
 - a) Particle count
 - b) Particle size distribution
 - c) Rheology
- Effect of industrial additives on Particle count and Particle size distribution
 - i. Xtrahib
 - ii. Low Molecular Weight PHPA (LMwPHPA)
 - iii. High Molecular Weight PHPA (HMwPHPA)
 - iv. Kla-stop
 - v. Xanthan Gum

As mentioned earlier, the goal was to find the best additive which controls the particle count to a minimum and increases the average particle size distribution thus inhibiting the clay particles/shale rock. A larger particle size will allow for easier

separation of cuttings from the drilling mud thus allowing for efficient recycling of the mud. As the Shale-water interaction is complex and there are no standardized testing procedures available in the literature, the best additives will be listed and ranked on the basis on their effect on Particle size and count.

4.2 Experimental results

The forthcoming results will be presented in sections so as to describe the results systematically.

4.2.1 Effect of potassium chloride on particle count and particle size distribution

Particle count

In this section, the process of variation of clay particle count distribution with time is described. This variation is then quantified in the precedence of the concentration variation of potassium chloride.

Figure 51 shows the variation of particle counts measured by the FBRM probe. It is important to note that just the first hour of the two-hour test is shown for all results as the data suggests that the one hour result is representative of the two-hour trend.

The procedure included the addition of KCl at the 1-minute mark, and then the clay particles were added at the 3-minute mark. The KCl was added first and allowed to mix into the solution for ~2 minutes.

The results in Figure 51 show a spike around 180 seconds, and this is the period of time when the clay particles were added to the water solution for each test.

Reviewing the results, it can be clearly seen that there is a definite impact made by the addition of KCl on the particle count. Amongst all the tests, the 0% KCl plot has the highest particle count average with time, but this same particle count steadily decreases over time which was unexpected and unusual. A possible reason for this could be that the FBRM M500 could not detect the correct particle count due to the condition of the probe as the probe was manufactured in 1999. A decline in performance could have ensued over time, or the technology is merely inadequate to give accurate particle count readings under all conditions. This result gave the initial idea that this technique of measurement and the FBRM M500 are not sufficiently

reliable for all conditions. The general trend observed is that with increasing KCl concentration, the particle count decreases, thus indicating that KCl inhibits the breakdown of clay particles.

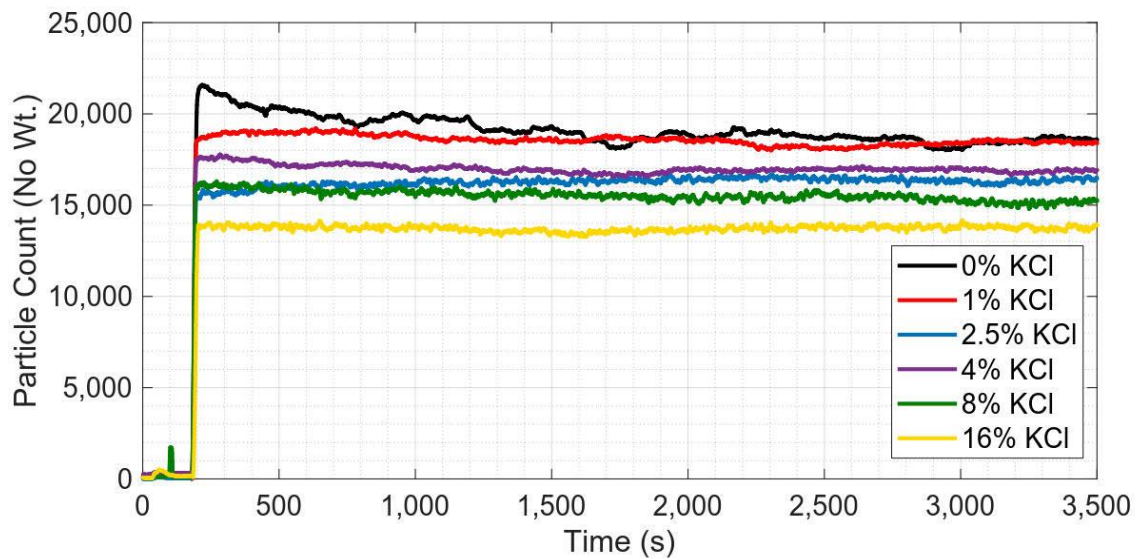


Figure 51. The variation of particle count during 2hr degradation experiments performed at various concentrations of KCl.

The benchmark of KCl concentrations based on observation is listed in Table 6. The ranking is based on the simple premise that the concentration giving the lowest count is most effecting while the concentration giving the highest counts is least effective.

Table 6. Qualitative benchmark of KCl concentrations.

Rank #	Additive Concentration
1	16% KCl
2	8% KCl
3	2.5% KCl
4	4% KCl
5	1% KCl
6	0% KCl

Although this ranking is qualitative and based on observation, it gives quite a good depiction of how the addition of KCl and increasing the concentration has what effect on the particle count of the clay particles. The most effective additive tested was the highest concentration, 16% KCl. Comparing this plot along with the plot of 0% KCl,

we can observe an average difference of around ~6,000 particles. Although this number is drawn upon pure observation, it should be noted that each test was repeated thrice and a final representative test (which matched the results of the other two tests) was chosen, and this is what was described earlier in Figure 40.

Although the relationship is not linear, it can be presumed from the FBRM results that increasing the KCl concentration is generally beneficial in maintaining the clay particle count lower.

Particle size distribution

The experimental results show that the degradation of clay particles can be controlled by the background concentration of potassium chloride (KCl).

Figure 52 shows the distributions of two different tests conducted after 60 minutes of mixing and the size distribution of the dry powder clay. The dry powder clay has a larger size distribution compared to the two solutions. The size distribution of the particles at 0% KCl solution is distributed across a wider range of particles, whereas the 2.5% KCl plot is more concentrated in the range of 1 to 100 μm . The results show that the background KCl initiates particle aggregations, which results in a larger mode of particles.

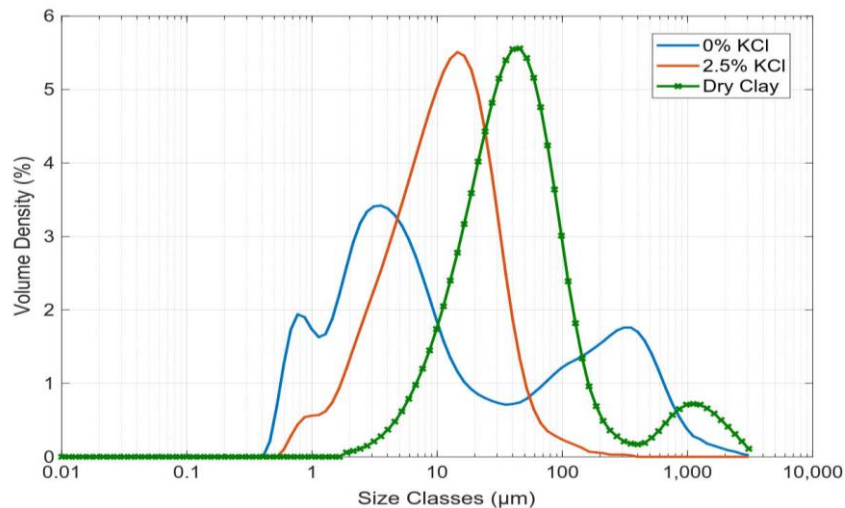


Figure 52. The effect of KCl on the size distribution of clay particles.

Another significant distinction between the 0% KCl and the other two plots is that the 0% KCl plot is not symmetrical whereas the other two plots are symmetrical. This indicates that not all the particles that were mixed into the solution had the same level of disintegration although they followed the same procedure and constraints as the other tests.

The mode is the highest point of the frequency distribution – in this case the Volume Density. The mode defines the particle size range most commonly found in the distribution and can be used to compare data points for particle size analysis. As can be seen, the plot with the mode being farthest to the right, and thus larger in size, is the dry clay. This is expected the clay has not come into contact with the fresh water. However, when the clay does come in contact with water the mode shifts way further to the left, thus indicating a smaller size range. This result is seen in the 0% KCl. This plot is of interest because not only has the mode moved farther to the left but also there are now three peaks in the plot instead of just one.

As can be observed in Figure 53, the mode of the graph moves towards the right due to the increase in concentration of KCl again. The result with the highest volume of small size classes ($<0.1 \mu\text{m}$) is the 0% KCl concentration, and the concentrations with the highest volume of large size classes ($>0.1 \mu\text{m}$) is the 16% KCl plot. The results shown in this figure again prove the effect KCl on maintaining the particle size distribution of clay thus inhibiting it from breakdown.

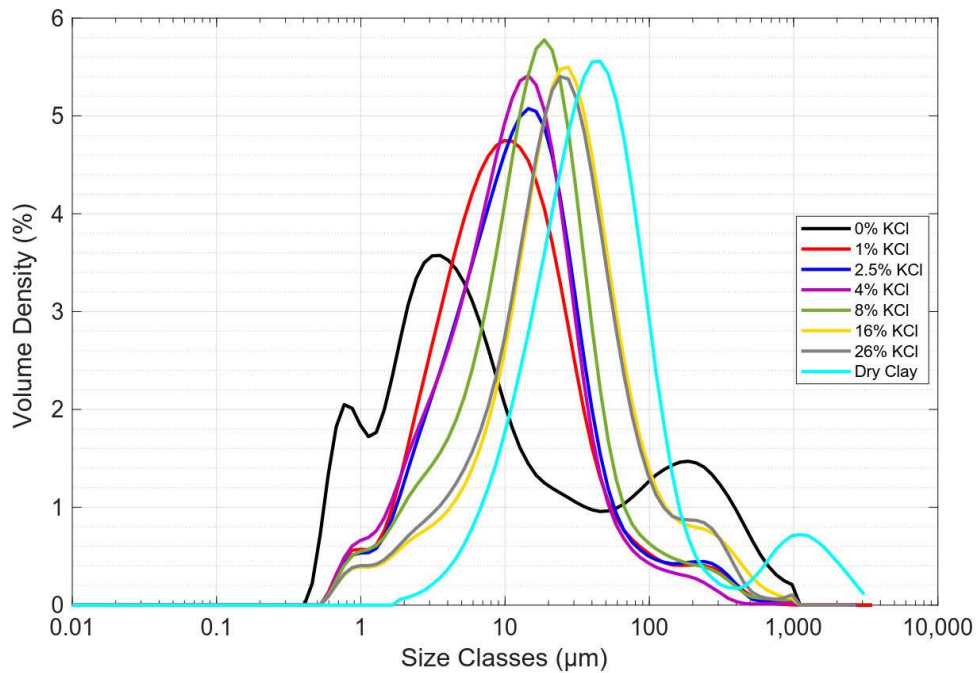


Figure 53. The variation of particle size distribution of clay particles after 2 hours of mixing at various KCl concentrations.

From the earlier described results, it can be deduced that the KCl has an aggregating effect on the clay particles causing the particle size distribution to be symmetrical with only one peak. Particle aggregation is also known as particle agglomeration, and throughout this process, particles disseminated in the liquid phase stick to each other and instantly form different particle groups, flocs, or aggregates. It is well known that particle aggregation can be brought about by adding salts or any other chemical referred to as coagulant or flocculant [91]. Once particle aggregates have formed, it is not easy to unsettle them, and this is usually an irreversible process. In time, the aggregates will grow in dimension, and as a result, they may settle to the lowermost part of the container, which is denoted to as sedimentation.

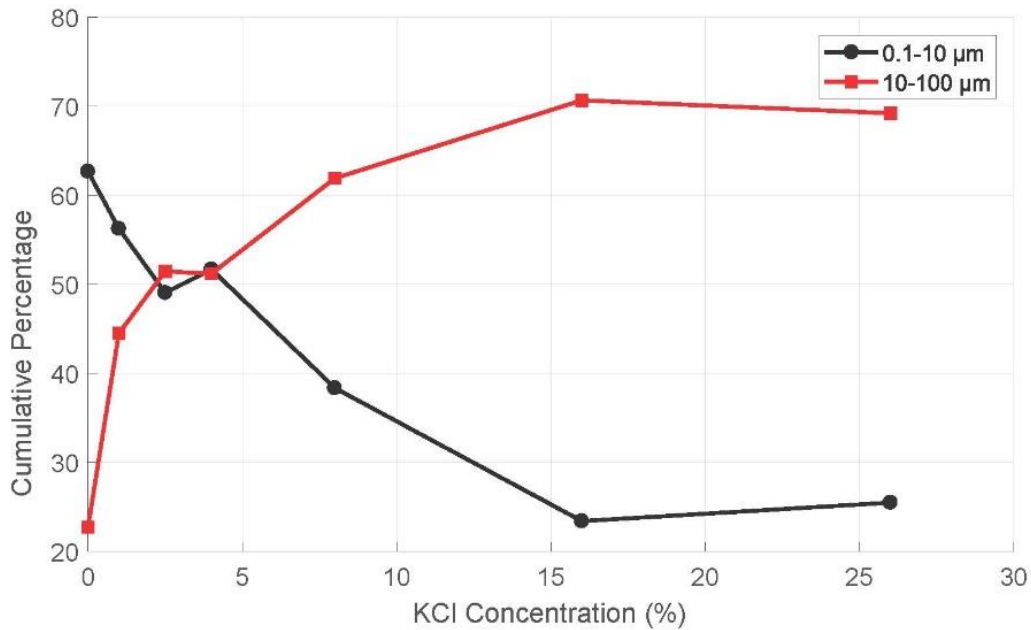


Figure 54. Variation of two group sizes of clay particles at different KCl concentrations after two hours of mixing.

The effect of increasing potassium chloride concentration on particle size can be easily observed from Figure 54 which was plotted with the same data that produced the plot in Figure 53. For the smaller particle size range of 0.1-10 µm, the total percentage of particles decreases with the increase of KCl concentration. For the larger particle size range of 10-100 µm, the total percentage of particles increases with the increase of KCl concentration. This, indeed, proves that KCl has a beneficial effect of preventing the breakdown of larger particles to finer particles.

4.2.2 Field application studies

Effect of using shale core rock on particle size distribution

A similar test procedure was applied to core samples obtained from a shale formation in South Australia in order to optimize the concentration of KCl in the drilling fluid design of a drilling trial. Photos taken at the drilling trial can be seen in Figure 55.

In this coiled tube drilling trial, the downhole motors, made of a positive displacement motor and a downhole hammer, were connected to 500 m of coiled tube. The downhole motors received hydraulic energy from the drilling fluid to deliver the rotary and reciprocating movements to the percussive bit. Two solid removal units made of two shale shakers and two centrifuge decanters were used to separate the cuttings from the drilling fluid. The drilling fluid was solid free, and it was imperative to reduce

the solid particles produced from the drilling process to less than $40\ \mu\text{m}$ due to the sensitivity of the downhole motors to solid particles.



Figure 55. Coiled tube drilling system, RoXplorer, used in the drilling trials in South Australia - courtesy DET CRC.

To achieve the required target of solid removal, it was required to adjust the fluid property to minimize size degradation of clay cuttings. Therefore, samples from the clay formation were received and were crushed and grinded to form a fine powder. The crushed cuttings were tested using the same methodology described earlier to optimize the concentration of KCl in the drilling fluid. The experiments were performed using four concentrations of 0%, 1%, 2% and 3% KCl. The results of the experiments along with the particle size distribution of the dry crushed cuttings obtained using the dry dispersion unit of the Malvern Mastersizer are shown in Figure 56. Pertaining to the earlier results, it can be seen that the mode of the graph shifts to the right with the addition of KCl. It is interesting to note that there is a clear trend being followed, reinforced by the fact that the dry sample (Initial) shows to have the mode farthest to the right thus proving that the particle size is increased or maintained due to an aggregating effect caused by the KCl. Figure 57 illustrates how the percentage of shale cuttings in size groups of $0.1\text{-}1\ \mu\text{m}$, $1\text{-}10\ \mu\text{m}$ and $10\text{-}100\ \mu\text{m}$

is affected by KCl background concentration. Just by looking at the 10-100 μm size range is enough to get a clear ranking of the best concentration at maintaining particle size. Naturally, the fraction with the highest volume in the 10-100 μm size range is the Dry shale powder. The next is 3% KCl concentration followed by 2% which is then followed by 1%, and finally the last is 0% KCl.

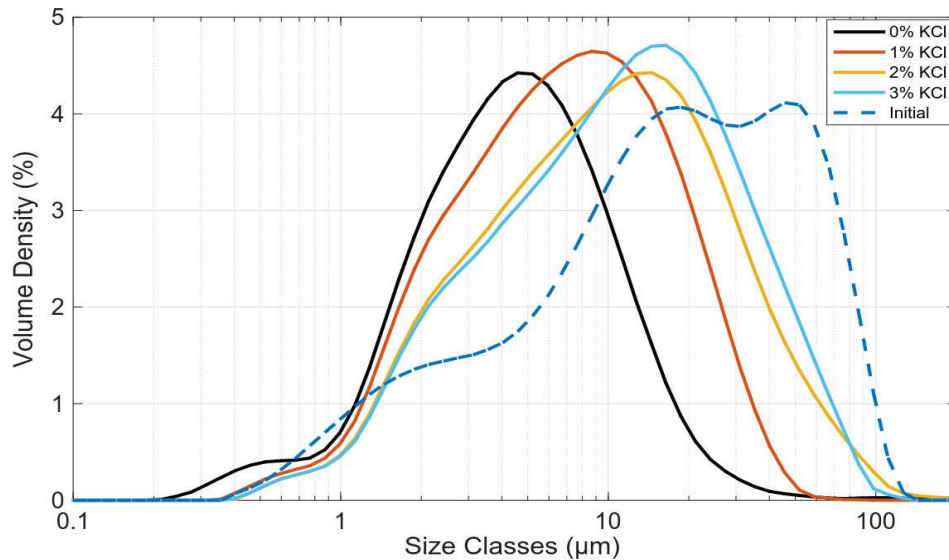


Figure 56. Variation of size distribution of shale formation at different KCl concentrations.

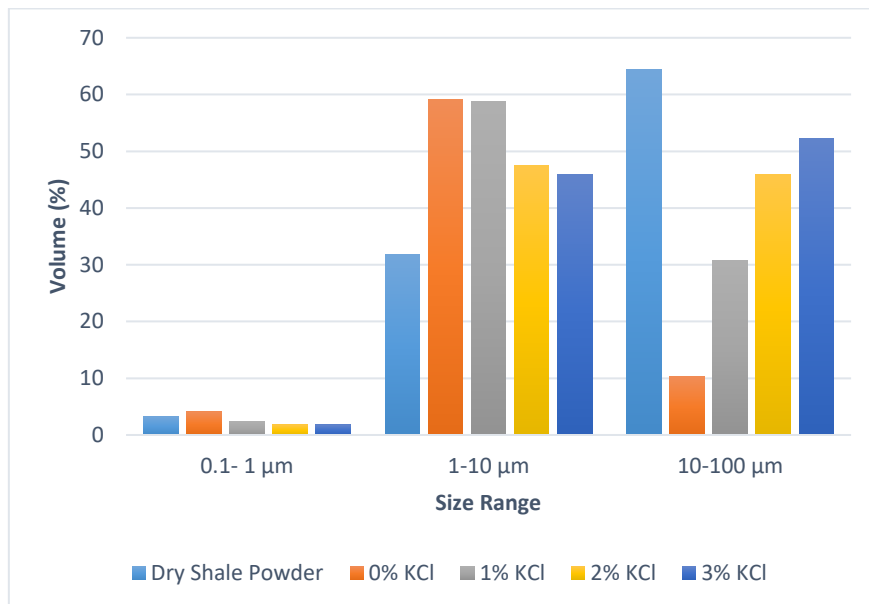


Figure 57. The effect of KCl concentration on the particles in the range of 0.1-1 μm , 1-10 μm and 10-100 μm .

Based on the results, it can be argued that the solutions with 2% and 3% KCl concentration tend to exhibit a similar size distribution, and therefore, the concentration of KCl was set at 2% in the drilling fluid system. The concentration of

KCl was consistently kept in the range of 1.8 to 3% during the operation, and the targeted cleaning level of $40\mu m$ was achieved.

4.2.3 Effect of time on

Particle count

Figure 58 is again used to show how there is no linear increase in particle count over time. The trend is unexpected as it is expected to show an increase in particle count over time and plateau after a period of time— since the clay particles are disintegrating over time. A possible explanation for this could be that the FBRM is not appropriately recording the particle breakdown. As mentioned earlier, the FBRM is not a particle counter but more of a tracker. As there are many different methods used for the determination of particle count and these different methods are not expected to give identical results: the count depends on the method used for its measurement. For this study, as there was just the FBRM used for tracking particle count, it was assumed that the line gives a fair indication of the number of particles that were being tracked in that system since every test had every other variable being kept constant with proper controls.

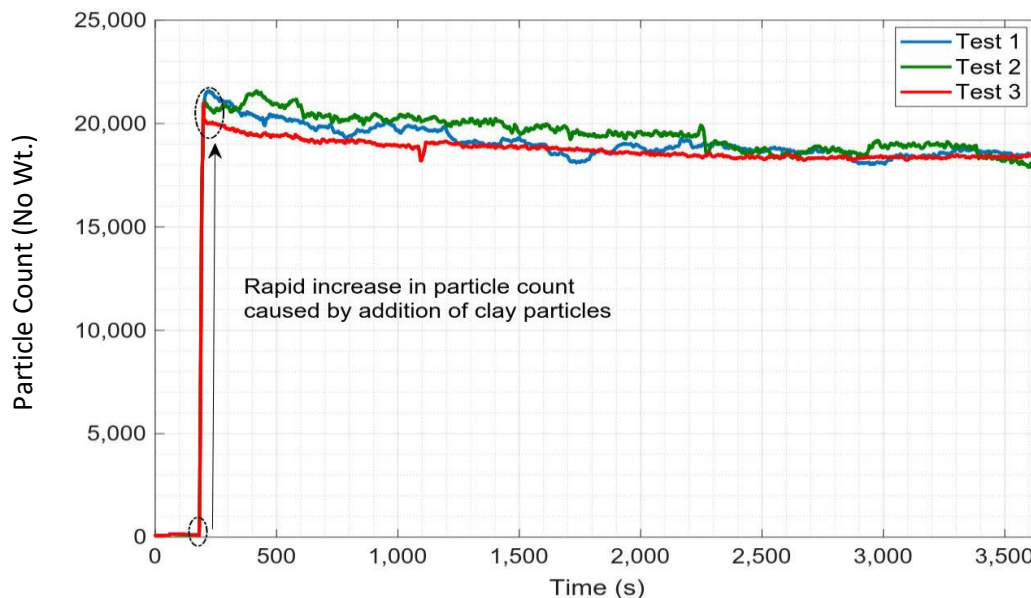


Figure 58. Sample FBRM test results.

Particle size distribution

As described in the methodology section, in order to characterize the process of change in size distribution of clay particles, a 47 hr test was performed, where size distributions of the solution and viscosity measurements were manually obtained at intervals of 10 minutes, 1 hr, 2 hrs, 6 hrs, 24 hrs, 30 hrs, and 47 hrs. The size distribution of the final results corresponding to time is shown in Figure 59. It is evident that the shape of each is quite similar with each plot having two peaks: one major peak and another minor peak. The shortest time, i.e., the distribution at 10-min is the most to the right indicating that this result has a larger size class. The size distribution tends to shift towards left with the increase in mixing time suggesting that particles decrease in size and increase in numbers. The clay particles are reacting with the fresh water, swelling and breaking down into finer smaller particles and the overhead shearer's action further facilitates this break down process due to its mechanical action.

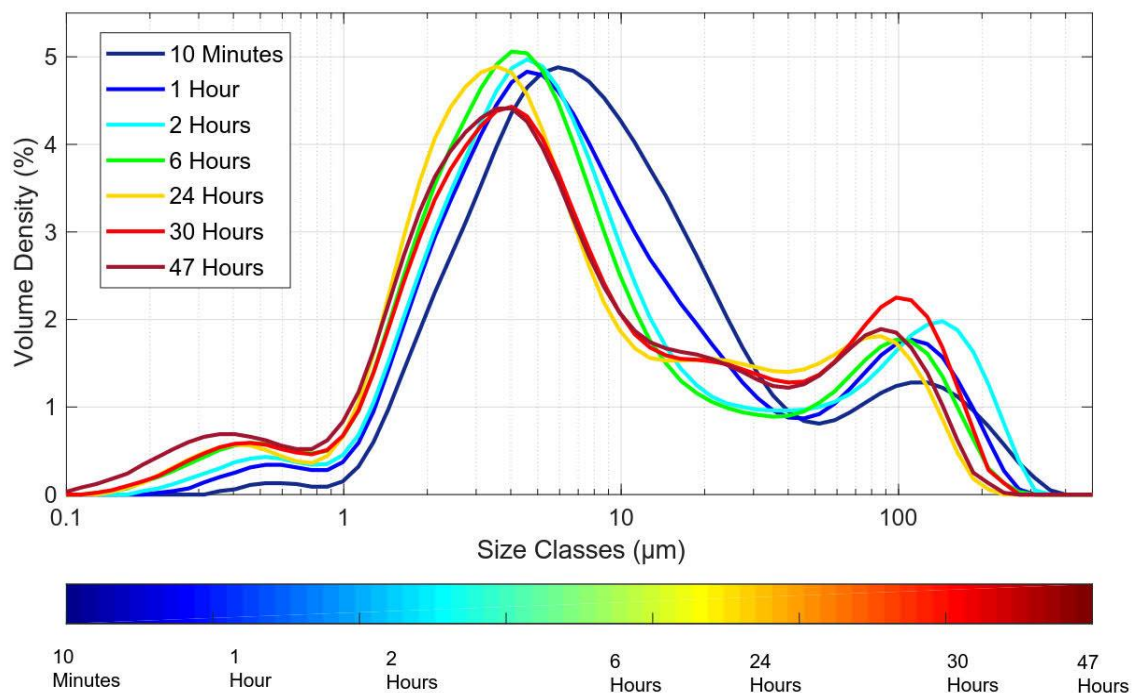


Figure 59. Variation of clay particle distribution in water during a 47 hr experiment.

In order to adequately characterize the size distributions shown in Figure 59, the volumetric frequency of particles in ranges of 0.1 – 1 µm, 1-10 µm and 10-100 µm are calculated and shown in Figure 60 at different intervals. It is evident from the graph that the volumetric percentage of particles in the group of 0.1-1µm increases as time increases, while it is not such a linear relationship for 1-10 µm and 10-100

μm . The most substantial proportion of particles lie in the 1-10 μm profile, so it is worth studying this region. The volume of particles steadily increases up until 6 hours, and then it suddenly drops for 24 hours and 47 hours. A possible reason for this anomaly could be the fact that the overhead shearer could have gotten heated due to continuous use and this temperature translated to the fluid thus making it even quicker for the particles to break down to a finer size.

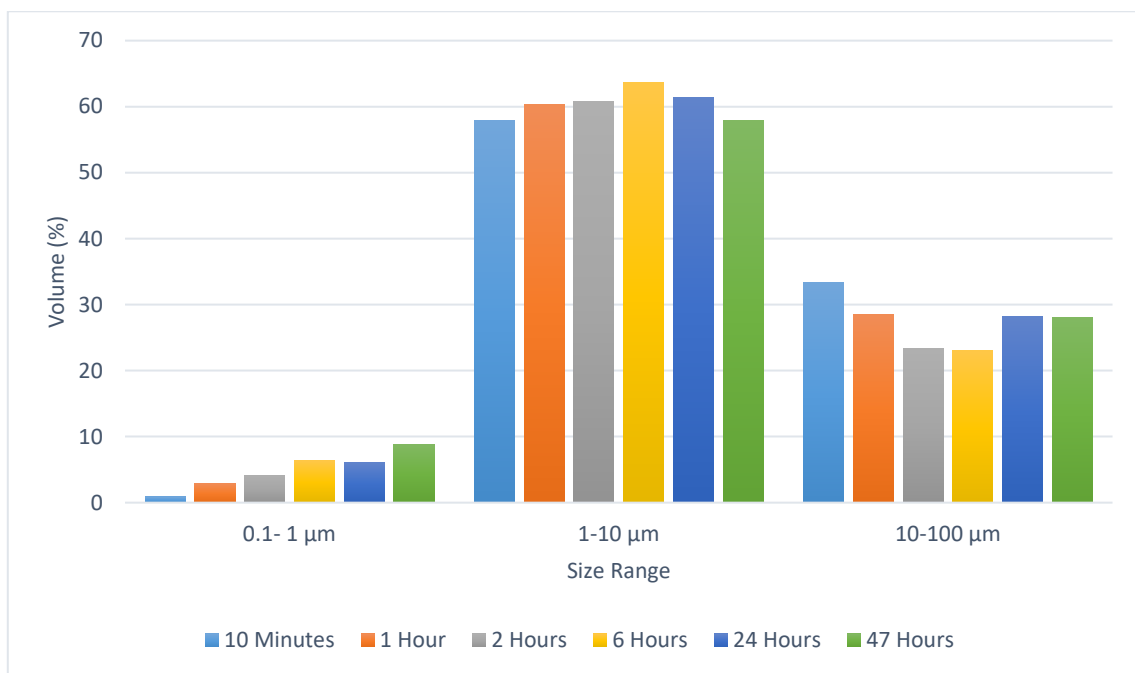


Figure 60. Variation of volumetric percentage of particles in groups of 0.1-1 μm , 1-10 μm and 10-100 μm at different times.

Rheology

The results of the viscosity measurement of the solutions show that the viscosity increases with time. The variation of viscosity at different shear rates is shown in Figure 61 and the variation of viscosity with time is shown in Figure 62. This result illustrates the viscosity at a shear rate of 1020 1/s. It is evident that the apparent viscosity at a shear rate of 1020 1/s increases from 1.5 cP to about 3.2 cP during the experiment. This trend can be explained by the breakdown of clay particles, also known as clay hydration in drilling fluid preparation, which is related to the dispersing of clay particles and therefore, increasing the viscosity over time.

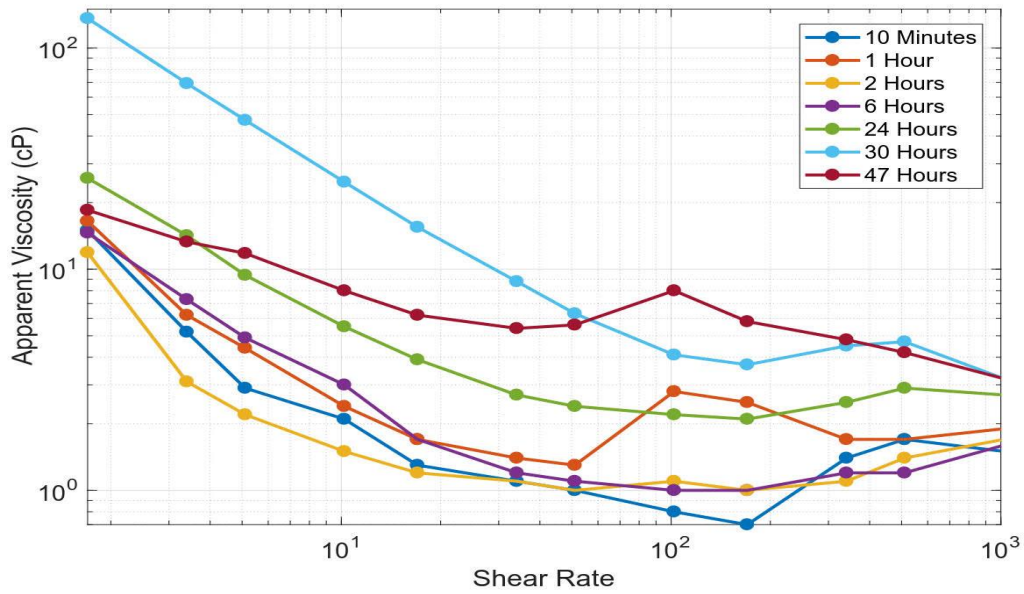


Figure 61. Variation of apparent viscosity during the 47 hr test.

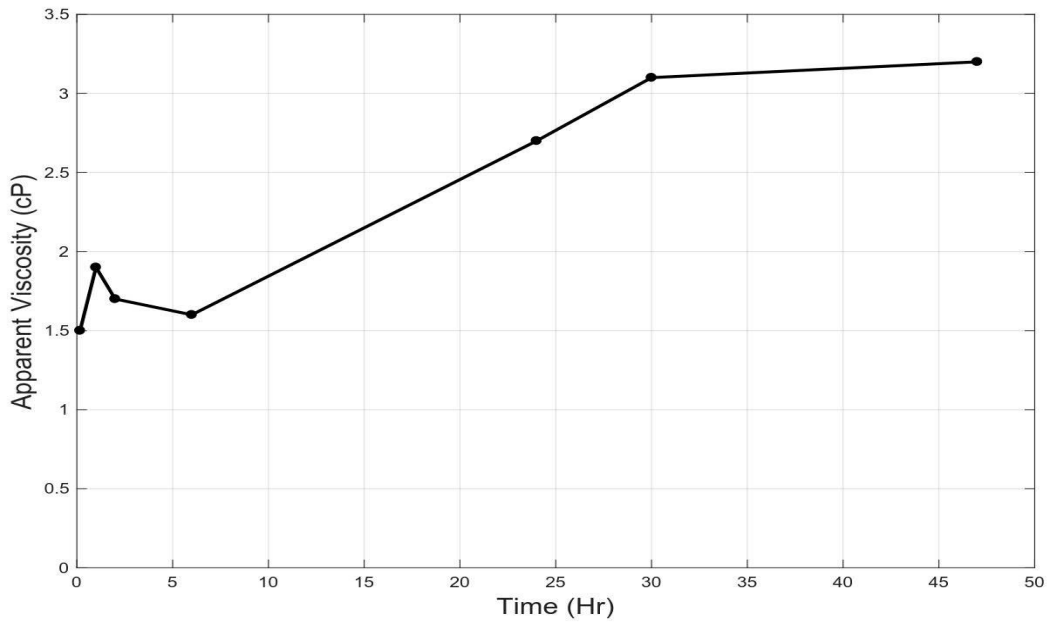


Figure 62. Variation of apparent viscosity at shear rate of 1020 1/s during the 47 hr test.

4.2.4 Industrial additives

As mentioned in the methodology, the effect of various industrial additives on the particle counts and particle size distributions of clay were studied using the additives and concentrations listed in Table 7. It should be noted here that all these tests were conducted using only API Bentonite (Rheoben NT) and not the shale core rock samples obtained from Port Augusta, South Australia.

Table 7. Additive names and concentrations tested.

Additive Name	Concentration
i. AMC Xtrahib	a. 3%
	b. 5%
	c. 7%
ii. Low Molecular Weight PHPA	a. 0.02%
	b. 0.05%
	c. 0.1%
iii. High Molecular Weight PHPA	a. 0.02%
	b. 0.05%
	c. 0.1%
iv. Kla-stop	a. 0.05%
	b. 0.1%
	c. 0.2%
v. Xanthan Gum	a. 0.2%

The results presented from now on will be specific to the additive. The results of each additive are plotted together with the results of the plain clay and fresh water interaction test, i.e. no additive. There are four graphs for each additive - Particle count results will be followed normalized count results which will then be followed by particle size distribution results and the fourth final plot will be of the percentage of particles falling within the following size ranges: 0 - 1 μm ; 1 - 10 μm ; 10 - 100 μm ; 100 - 3500 μm . This will allow for a quantitative comparison of the results along with a qualitative comparison of the graph. A color scheme is followed with each concentration range of additive being of the same color:

Table 8. Colour scheme of results.

Plain clay + fresh water (No Additive)	Black
Low concentration of the additive	Red
A moderate concentration of the additive	Orange
High concentration of the additive	Green

In several instances of the results discussed, the term "mode" will be repeated to judge, compare and conclude on results. This term is specific to the Malvern Mastersizer results, i.e. particle size distributions. By statistical definition, the mode is defined as the value that occurs most frequently in a given set of data. In terms of particle size distributions, the mode is the tallest point of the particular plot.

i. AMC Xtrahib

While observing the results of the particle counts obtained from the FBRM, it became clear that the results would show a distinct outcome from early on in the experimentation. As can be seen from Figure 63, the particle count jump is present for each of the four tests. After the particle count jump, the particle count tends to be constant around a baseline for each result. This is observed for the entire duration of the experimentation. There can either be a gradual increase or a small gradual decrease in particle count over time. A drastic increase or decrease in particle count is rarely seen. This can be attributed to the fact that for all the tests, the additive/inhibitor was added to the fresh water base before the clay/shale particles. This was done to allow for the additive to properly mix and hydrate also to simulate the drilling condition: exposing cuttings to an inhibited drilling fluid. If the clay/shale were added before the additive, then this would not have allowed for the additive to mix and hydrate and thus impede its inhibitive action properly. This is particularly important for polymer solutions that require up to 30 minutes of hydration.

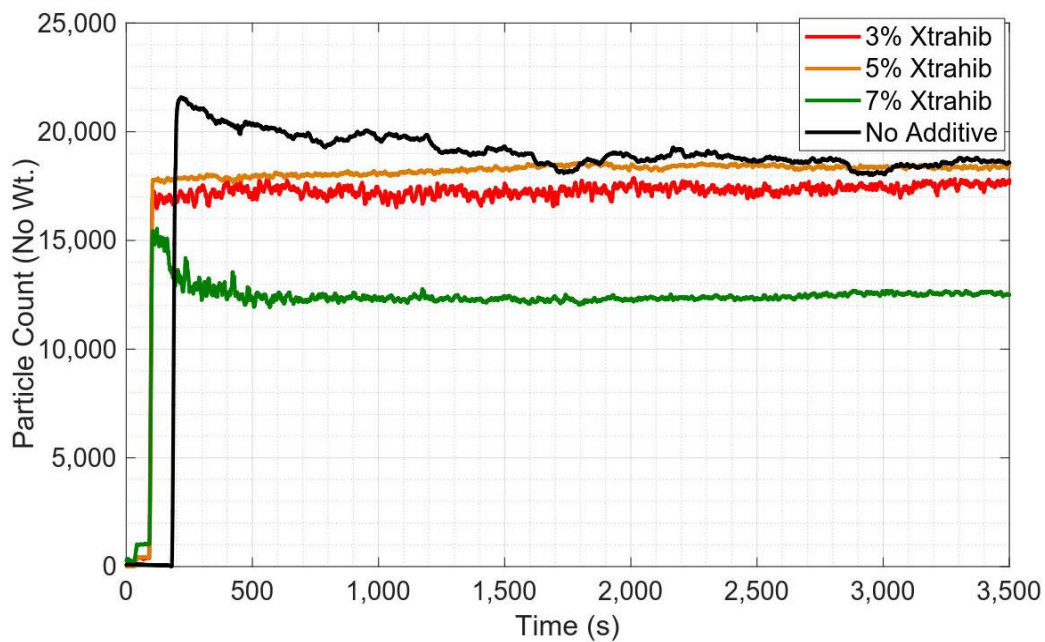


Figure 63. AMC Xtrahib particle count results.

As can be seen in Figure 64, all three concentrations of Xtrahib exhibit a lower particle count than the no additive plot. The no additive plot is around the 18,000 particle count mark while 3% and 5% Xtrahib concentrations are verging on a close particle count range of ~ 17,500. The 7% Xtrahib concentration has significantly

reduced this particle count to around 12,000. It can be concluded from this plot that increasing the concentration of Xtrahib has a significant positive influence on inhibiting the clay cuttings and preventing the particle count from increasing.

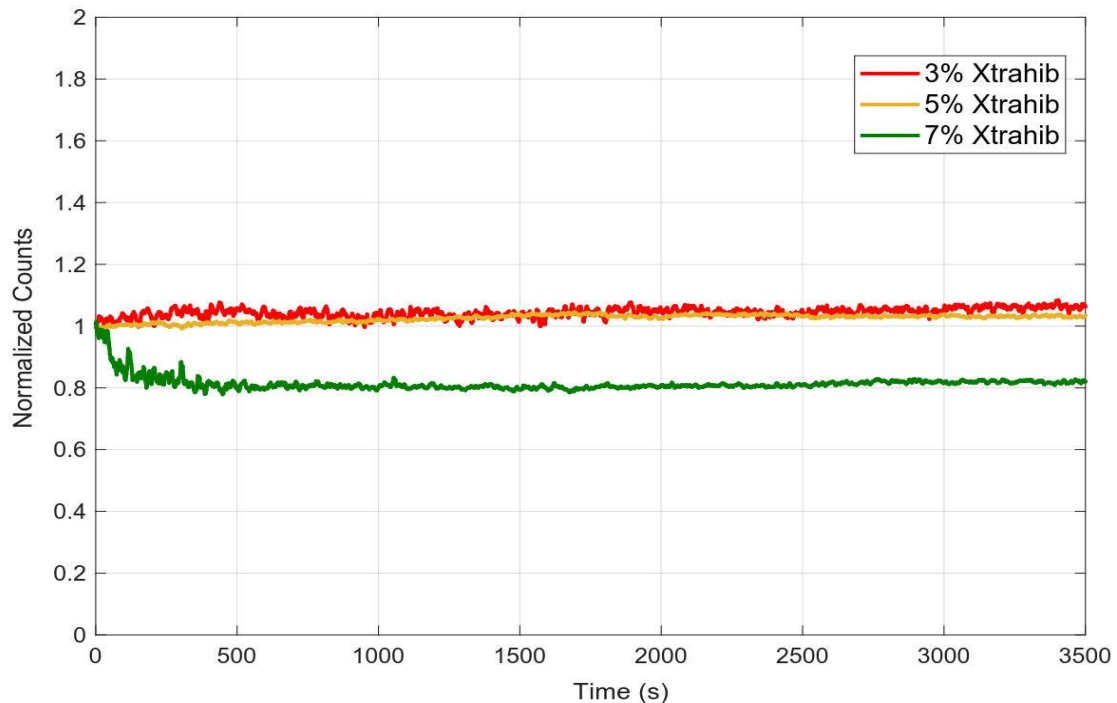


Figure 64. AMC Xtrahib normalized count results.

Figure 65 shows the no additive plot that has a distinct shape with a much wider particle size distribution range. It has three peaks at approximately 0.3 μm , 4 μm and 200 μm . In contrast, the three plots for Xtrahib have a much narrower particle size distribution range. All three concentrations are very similar with the 7% Xtrahib having the tallest peak, ~6.6% of all particles are around 30 μm . Directly contrasting the shapes gives a clear and succinct idea of the effect of using additives on the particle size distribution. The results show that Xtrahib does indeed help in inhibiting the clay breakdown as the mode (or peak) of the 3%, 5% and 7% KCl concentrations is more to the right (of a larger size class) than the mode of the no additive plot. In regards to Xtrahib concentration, it can be asserted that the optimum concentration is 3% Xtrahib as this provides almost as good as inhibition properties as the 7% Xtrahib concentration while being less than half the dosage. Another observation is that Xtrahib has an aggregative effect on the clay as the size distribution is more of a cluster or group compared to the widely distributed no additive plot that has multiple peaks. A question may arise that if the particle size increases due to aggregative effects, then why is it that the particle count (Figure 64) decreases. This can be

explained by linking the FBRM and Mastersizer results. The Mastersizer shows a higher concentration of larger particles, which then means that there is a smaller volume of smaller particles. This then is in agreement with the FBRM results. Overall, it can be concluded from these results that the Xtrahib has a profound positive impact in maintaining the size of the clay particles above a threshold which confirms that Xtrahib is indeed an excellent additive for shale/clay inhibition.

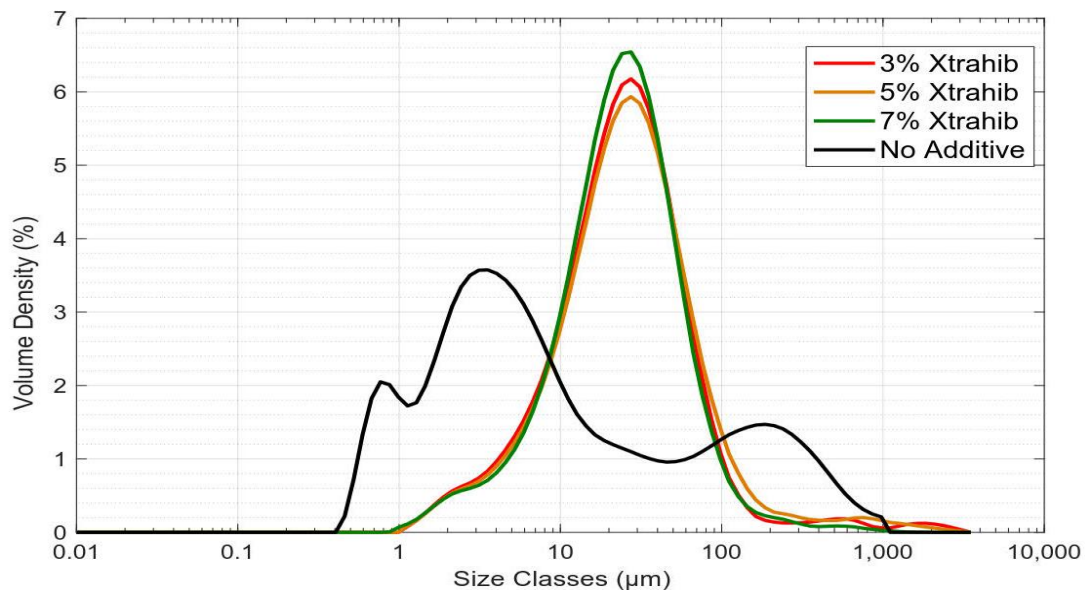


Figure 65. AMC Xtrahib particle size results

Figure 66 allows for a quantitative study of the particle size distribution compared to Figure 65. This plot again shows how the no additive test produced results that are more widely distributed along the size range. It is important to note that 50.9% of particles for the no additive test lie in the 1-10 µm range. This size range is where the majority of the no additive clay particles are distributed. However, in sharp contrast, it can be seen that the vast majority of particles for Xtrahib, for all three concentrations, lie in the 10 -100 µm size range. This proves that Xtrahib is effective in maintaining a larger particle size distribution. 79% of all particles lie in the 10-100 µm size range for 7% Xtrahib which is a significant increase compared to the no additive range of which there are only 21.4% belonging to the same size range.

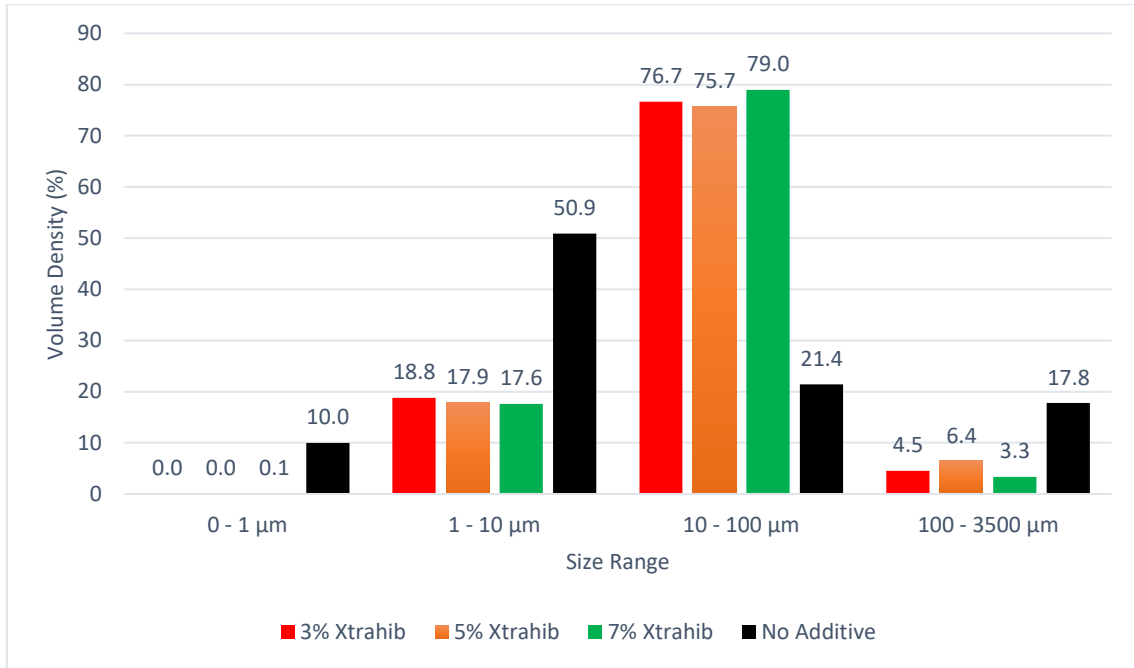


Figure 66. AMC Xtrahib particle size distribution.

ii. Low Molecular Weight PHPA

Figure 67 shows that the No Additive plot has a lower particle count than all three Low Molecular Weight PHPA results. This result however is not unexpected as it is known that PHPA is added to the fluid system to better disperse the clays and lower the filter cake. In low-solids muds, PHPA interacts with minimal concentrations of bentonite to link particles together and improve rheology without increased colloidal solids loading [92, 93].

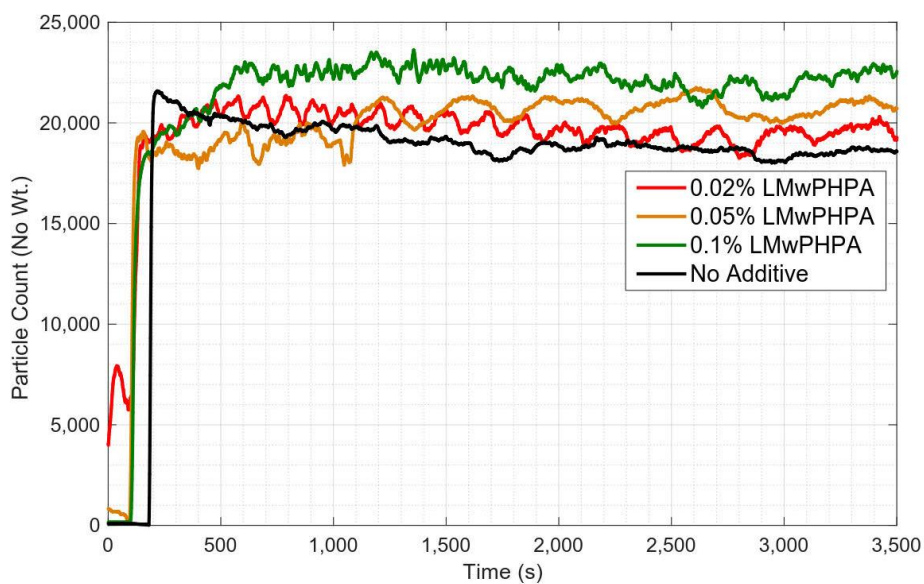


Figure 67. LMwPHPA particle count results.

Figure 68 shows this same result.

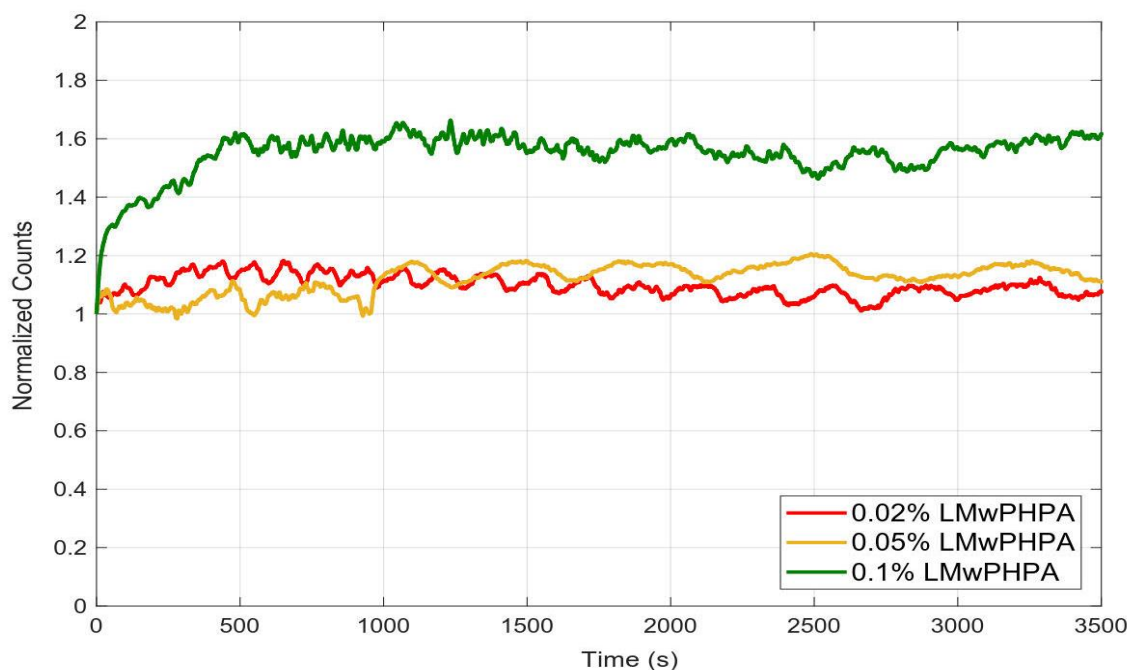


Figure 68. LMwPHPA normalized count results.

As can be seen from Figure 69, all concentrations of the LMwPHPA have a broad particle size distribution range. These results are similar to the no additive plot. The LMwPHPA does have an aggregating effect like Xtrahib but there are multiple peaks. However, there is a significant proportion of particles above the 100 μm size range which gives evidence that LMwPHPA could be effective at maintaining a larger particle size. This could also be caused by the bubble formation discrepancy caused by the Mastersizer 3000 equipment that was being used.

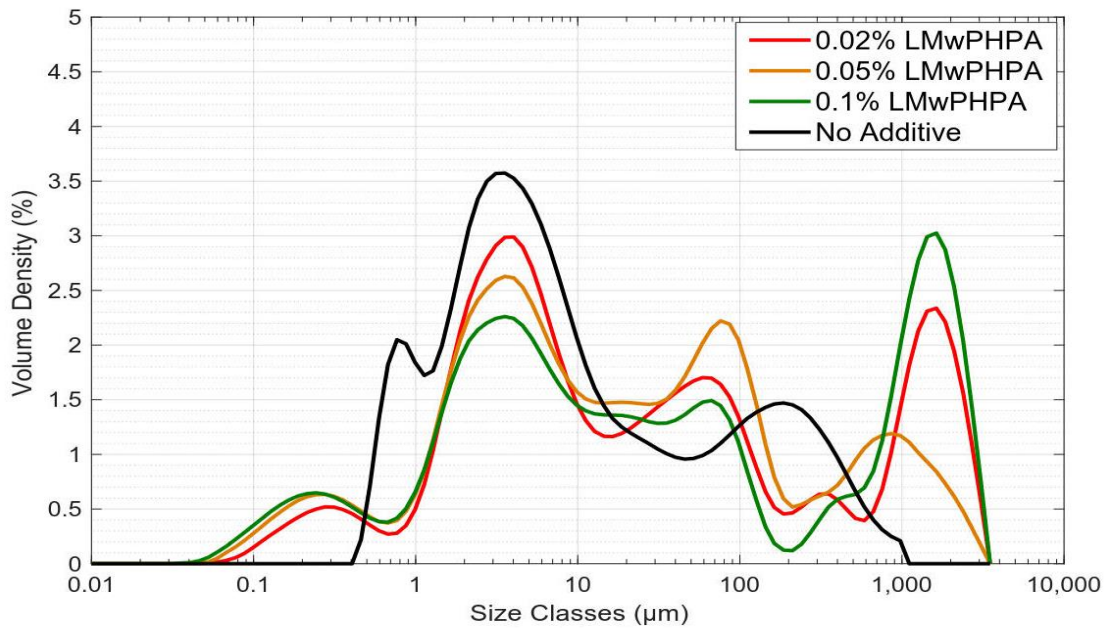


Figure 69. LMwPHPA particle size results.

From Figure 70, it can be observed that both the no additive and LMwPHPA results have the highest Volume Density (%) in the 1-10 µm size range. The results conclude that the LMwPHPA does not assist in preventing the breakdown of the clay particles as well as the Xtrahib. It should be noted that the 0.1% LMwPHPA has a noteworthy proportion of particles in the largest particle size range of 100-3500 µm which is at 32.4% but this volume is not high enough to conclude that the LMwPHPA is effective at maintaining a larger particle size distribution. This distribution is quite erratic and it is difficult to make conclusions as for all three concentrations, there is a large proportion in the 1-10 µm size range, a small proportion in the 10-100 µm size range and then a large proportion again in the 100-3500 µm size range. This wider distribution range is not desirable and it can be concluded that Xtrahib is superior to LMwPHPA at maintaining a uniform and larger size range based on the PSD's.

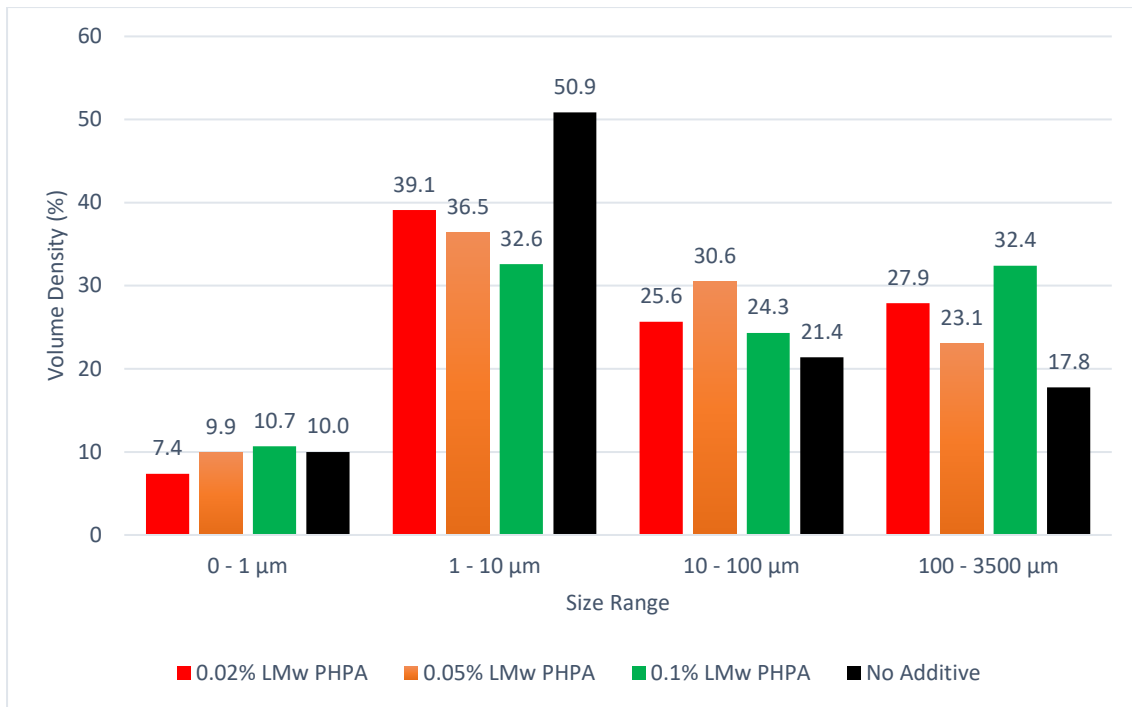


Figure 70. LMwPHPA particle size distribution.

iii. High Molecular Weight PHPA

The results from Figure 71 and Figure 72 show very different results compared to the LMwPHPA results. High Molecular weight PHPA is commonly used in the industry as a shale-stabilizing polymer in PHPA mud systems while Low Molecular weight PHPA is a known clay deflocculate [94].

The results show that lower concentrations of HMwPHPA, i.e., 0.02% and 0.05% have results that range within the same particle count of the No additive which is around 18,000 particles. These results effectively indicate that these two concentrations have no effect in reducing the particle count of the clay particles. The 0.1% HMwPHPA concentration is shown to have the best inhibitive results with the particle count peaking at 13,000 particles. This is around a 27.8% decrease in particle count compared to the No Additive results. It is however clear that although the particle count is lower, it is increasing steadily over time. It was noted during the testing that the 0.1% HMwPHPA was significantly more viscous than the other two smaller concentrations. The solution possessed a thickness and the overhead shearer was having difficulty properly mixing the solution in the first 35 seconds of the testing. Gradually, as the clay particles were added, the solution was getting a

better mix with time and this could cause the increase in detection of particles thus leading to a larger particle count.

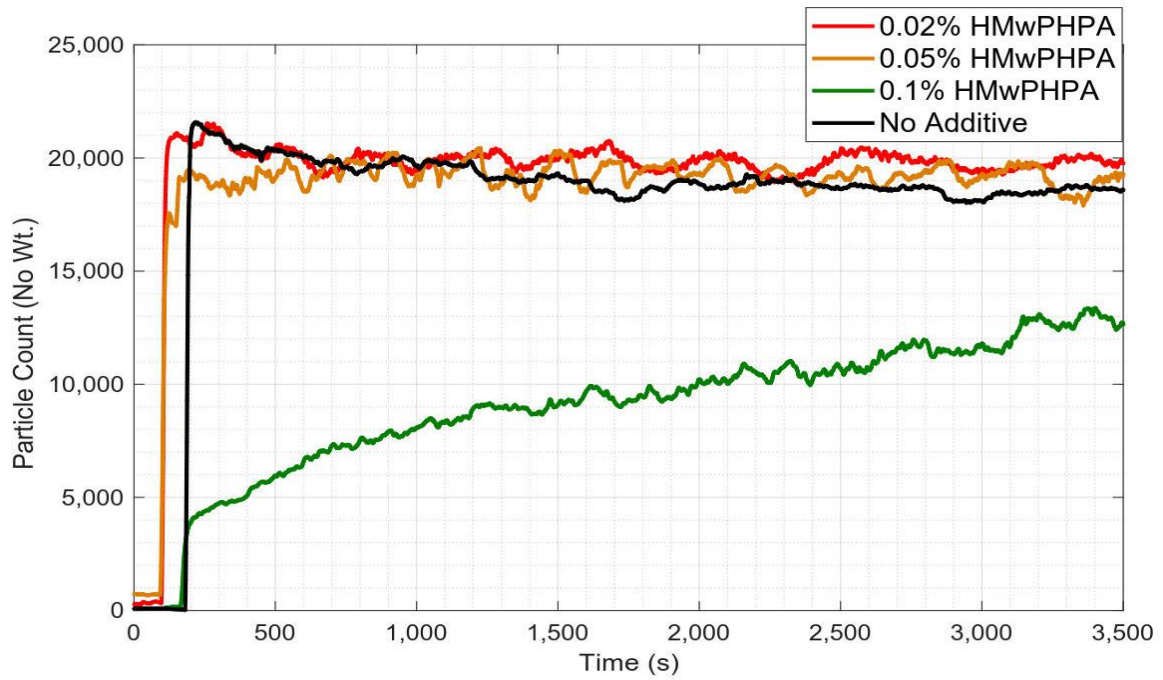


Figure 71. HMwPPHA particle count results.

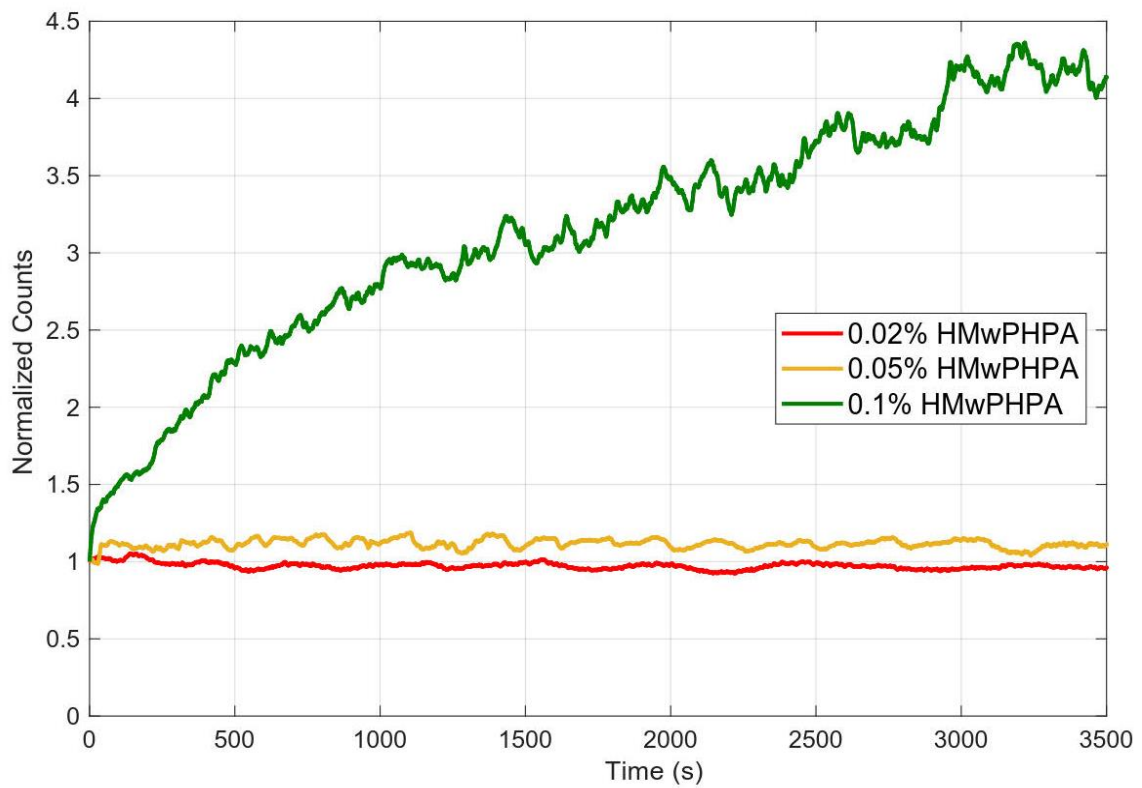


Figure 72. HMwPPHA normalized count results.

The results for the size distribution tests shown in Figure 73 correspond to the FBRM results. Both the 0.02% and 0.05% HMwPHPA have a similar distribution which is quite wide. They have a similar shape except with different peaks at four distinct size classes: $\sim 0.2 \mu\text{m}$, $\sim 2 \mu\text{m}$, $\sim 70 \mu\text{m}$, $\sim 1000 \mu\text{m}$. The No additive plot follows a similar shape except it has three specific peaks at the size classes of $\sim 0.8 \mu\text{m}$, $3 \mu\text{m}$, $200 \mu\text{m}$. Amongst all the results, the plot that is most distinct is the 0.1% HMwPHPA. It has two peaks at $\sim 4 \mu\text{m}$ and $\sim 150 \mu\text{m}$ and this plot has the mode farthest to the right compared to the other plots at around $150 \mu\text{m}$. It can be observed that there is a significant amount of particles >1000 micron size and this is a result of the bubbles arising in the Mastersizer tubing system. Any result above 1000 micron is ignored. Further analysis of results will be provided after studying the results shown in Figure 74.

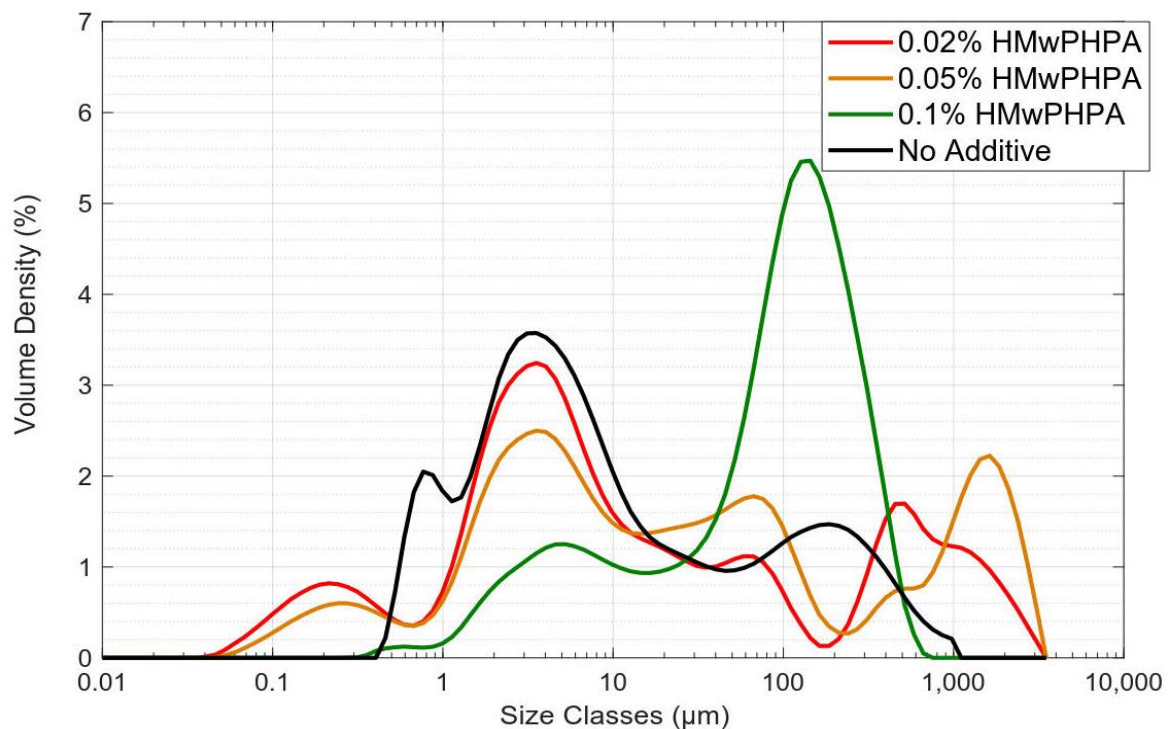


Figure 73. HMwPHPA particle size results.

Observing Figure 74 shows that this is the first series of experiments amongst all particle size distribution tests that produced vastly differing results for each concentration of the same additive – in this case, the HMwPHPA. The No Additive results have the most significant volume density percentage in the 1-10 μm range, and this is the same for both 0.02% and 0.05% HMwPHPA. It can be seen that with increasing HMwPHPA concentration, the volume density of particles shifts to a larger

size range. This result is particularly evident in the shift from the 10-10 μm to 10-100 μm size range where the results switch and reverse. This trend is continued in the 100-3500 μm size range where the highest concentration of 0.1% HMwPHPA is dominant with a very high 47.7% of particles in that test lying in this size range. This result provides concluding evidence that HMwPHPA is superior to both Xtrahib and LMwPHPA and is indeed an excellent shale stabilizer that prevents the breakdown of clay particles. The optimum concentration of the HMwPHPA amongst the tested samples is 0.1%.

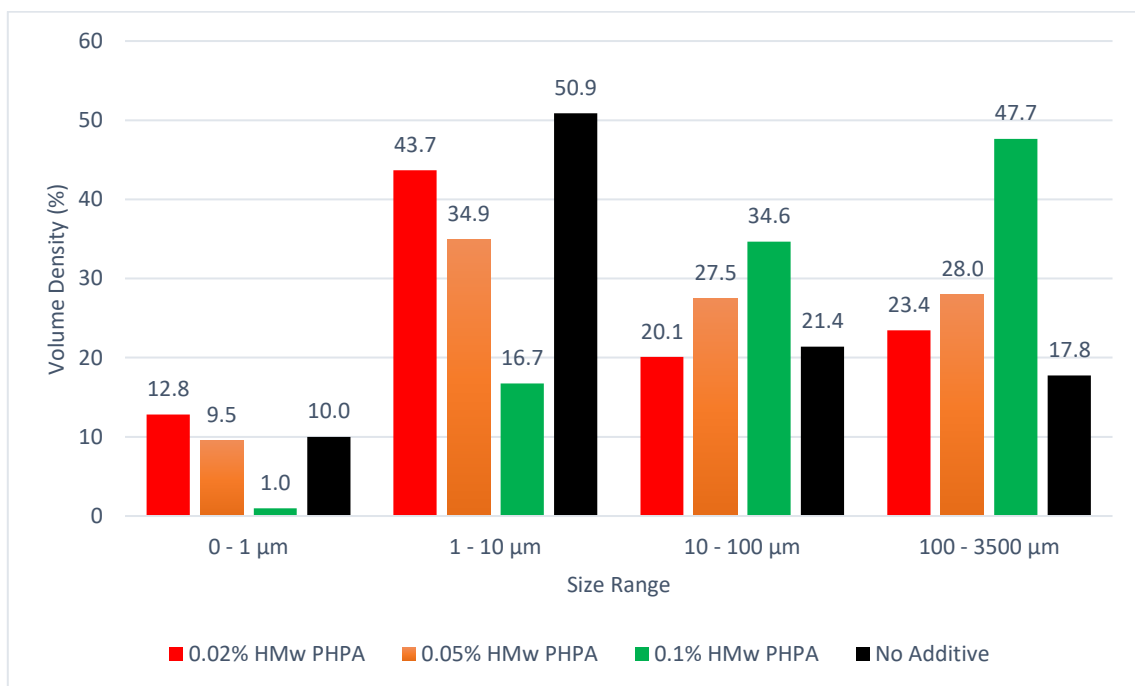


Figure 74. HMwPHPA particle size distribution.

iv. *Kla-stop*

The results shown in Figure 75 and Figure 76 show that the particle count for all three concentrations of *Kla-stop* is higher than the No additive test. The 0.05% and 0.1% *Kla-stop* start with the highest initial particle count at ~22,000 particles and gradually decline with time and end at ~ 20,000. This 9.1% decrease is not observed in the 0.2% *Kla-stop* concentration test where the opposite trend is observed. The particle count starts at around 19,000 particles and increases steadily before ending at ~21,000. A possible cause for this 10.52% increase in particle count could be improper mixing as the solution could have been marginally too viscous thus preventing the proper hydration of the clay particles initially. With time exposure, the

clay particles would hydrate, react, swell and disintegrate thus increasing the particle count. Another cause for this could be the effect of pH on this test. Kla-stop buffers the sample pH at 9-10. KCl would buffer at a slightly higher than neutral pH and PHPA are generally non-ionic. The pH is a variable for these tests and does control results but this variable was not measured and this is a shortcoming that has to be addressed in future testing.

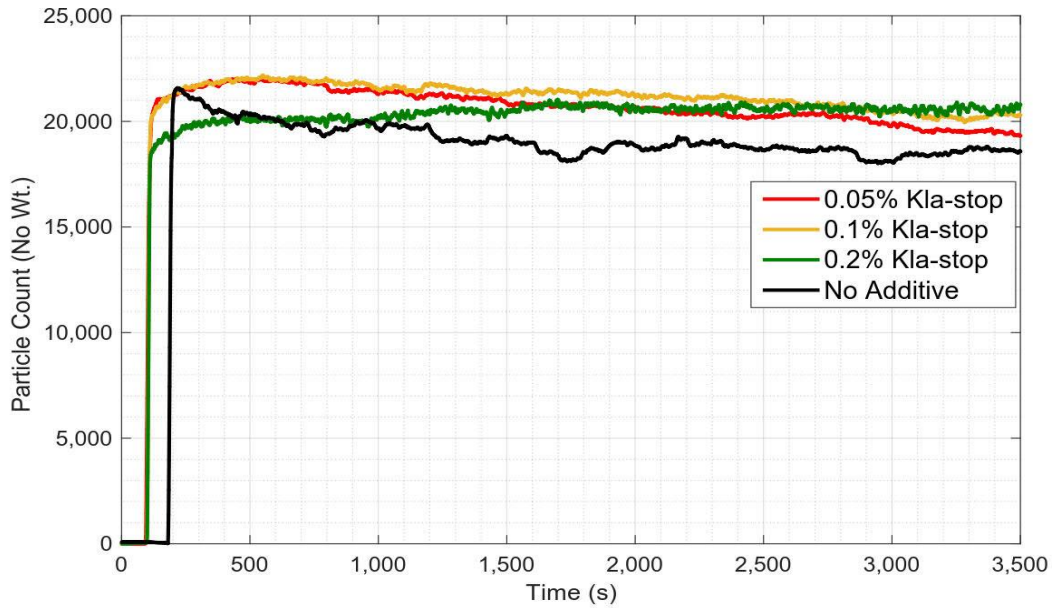


Figure 75. Kla-stop particle count results.

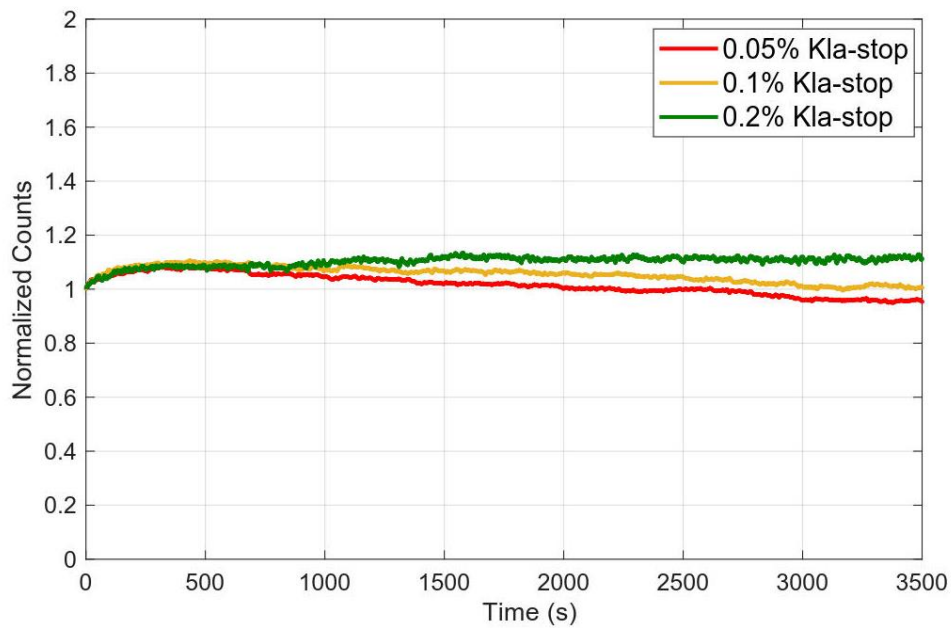


Figure 76. Kla-stop normalized count results.

For PSD results, all three Kla-stop concentrations show similar results as seen in Figure 77. However, carefully observing the peaks reveals a different outlook. 0.05% Kla-stop has one peak at $\sim 5 \mu\text{m}$ at which 5% of the volume density is in this size range. 0.1% Kla-stop, meanwhile, has two peaks at $\sim 5 \mu\text{m}$ and $\sim 1500 \mu\text{m}$ and finally, 0.2% Kla-stop has two peaks too, although these peaks are at a slightly larger size class at $\sim 8 \mu\text{m}$ and $\sim 1500 \mu\text{m}$. These results indicate clearly that increasing concentrations of the Kla-stop have a positive influence on maintaining shale stability and preventing particle break down as the size classes are shifting to larger size classes. Further support to this conclusion is the fact that the No additive plot covers a smaller range of size classes with all three of its peaks shifting to the left compared to the Kla-stop plots.

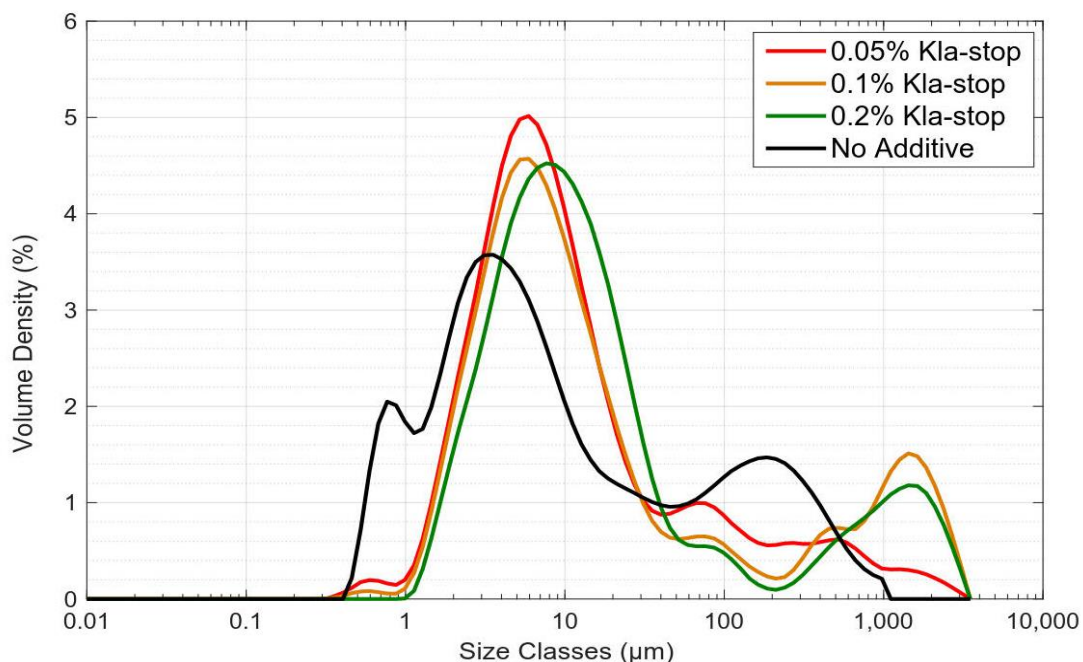


Figure 77. Kla-stop particle size results.

Figure 78 shows that the majority of the particles for all three concentrations of Kla-stop lie in the 1-10 μm size range which is undesirable. 58.6% of particles tested from the 0.05% Kla-stop test lie within this size range while this reduces to 49.4% for an increased concentration of 0.02% Kla-stop. There is a more significant proportion of particles from the 0.2% Kla-stop test in the 10-100 μm range than the other two concentrations.

The results from this plot show that Kla-stop is the least effective additive tested so far as the mode of each plot is farthest to the left compared to the previous three

additives. This indicates that the clay particles reacted and disintegrated and the Kla-stop did not provide efficient inhibition. The 0.05% and 0.1% concentrations produced results that are uniform to the no additive results and thus are not recommended for field application.

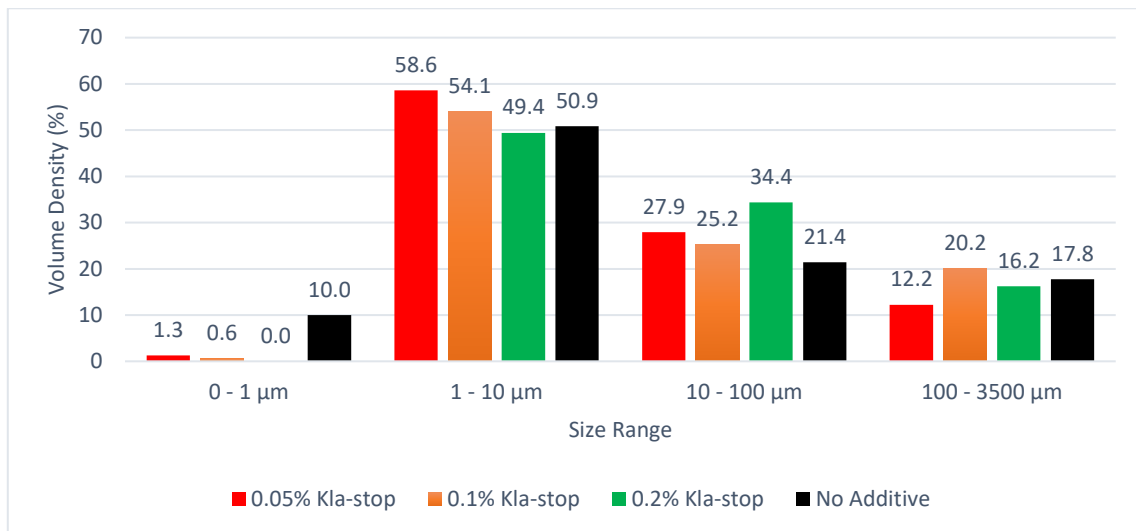


Figure 78. Kla-stop particle size distribution.

v. Xanthan Gum

For Xanthan Gum (XG), only one concentration was tested as it is a difficult polymer to mix. Often, additives are added to commercial XG products to aid hydration by independently adjusting the pH of the solution to aid dispersion and Hydration. As a result, additives are often added to commercial XG products to aid hydration by independently adjusting the pH of the solution to aid dispersion and hydration. However, this would not be applicable here though as it will evidently affect the overall shale inhibition capabilities of the XG solution. XG is soluble in cold water and is highly pseudoplastic – when shear stress is increased, viscosity is reduced. The XG used for these experiments was a commercial AMC Xanthan Gum and the pH was unavailable. Results from Kla-stop tests are shown together with XG to provide a comparison. As can be seen from Figure 79 and Figure 80, the particle count of XG is above the No additive test. This result is similar to the Kla-stop tests. A possible reason for this could be the viscosity of the 0.2% XG being high during the earlier stages of the experiment leading to improper mixing. Based on the particle count results, the evidence points to the fact that 0.2% XG should not be recommended as it does not effectively stabilize the clay-water interaction.

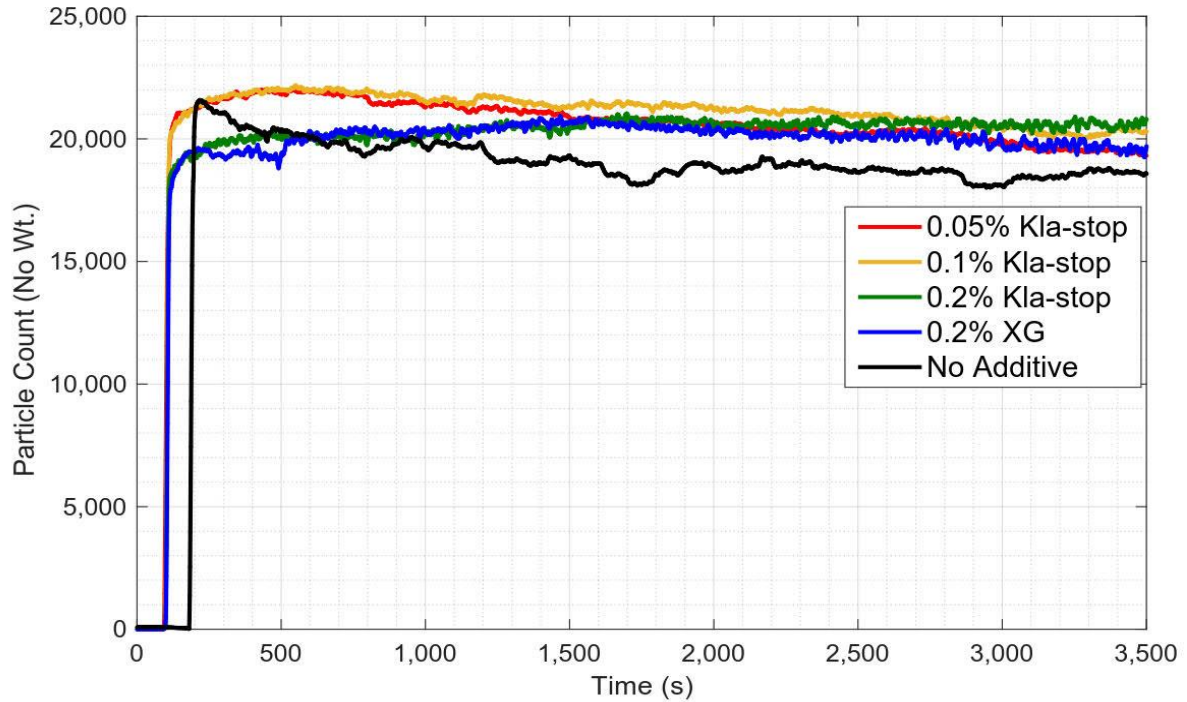


Figure 79. Xanthan Gum particle count results.

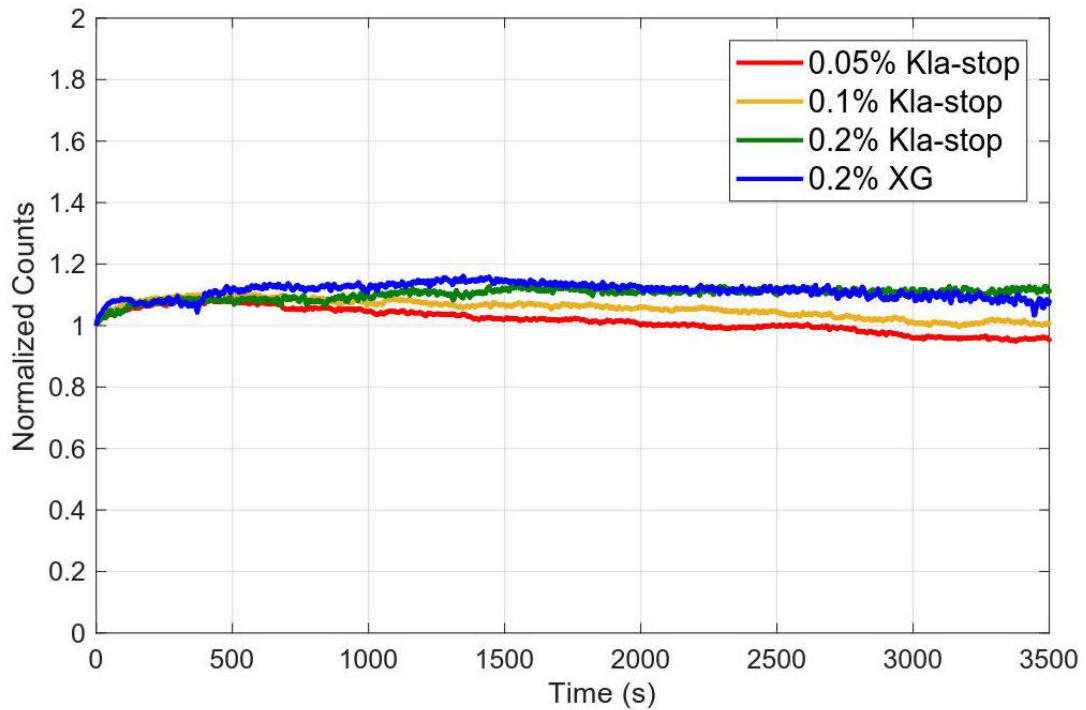


Figure 80. Xanthan Gum normalized count results.

Coming to the PSD results, the 0.2% XG plot shown in Figure 81 is quite distinct but more similar to the No additive plot than any of the Kla-stop results. The mode of the plot is quite near the mode of the No additive plot at around 3 μm which indicates that although the Xanthan Gum does have inhibitive properties, it is not that great of

an option. An ideal plot would have seen the mode of the XG plot farther to the right indicating a larger volume density percentage at larger size classes.

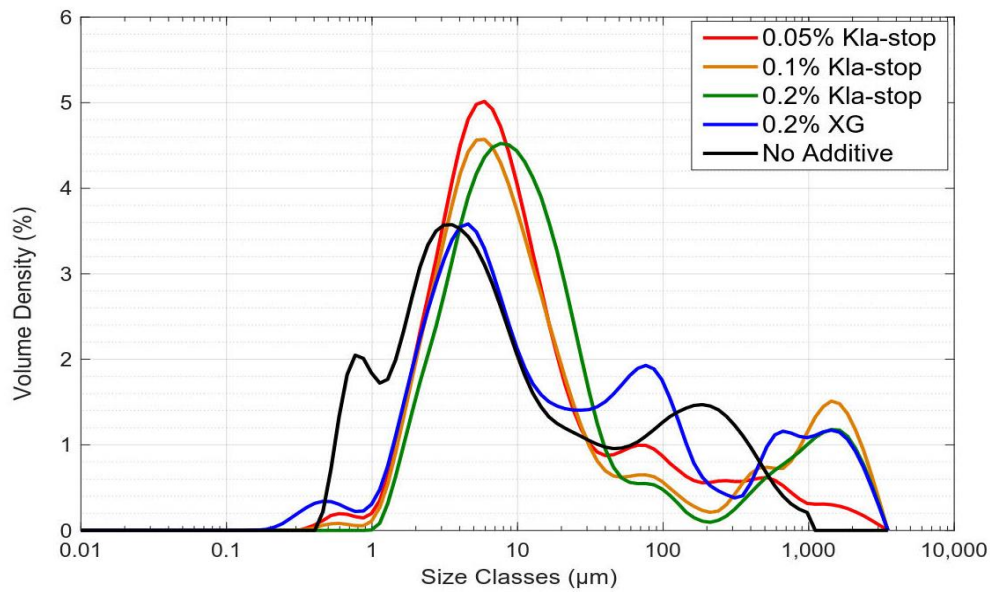


Figure 81. Xanthan Gum particle size results.

The largest volume density of the 0.2% XG test lies in the 1-10 µm size range as can be seen in Figure 82. This is similar to all concentrations of Kla-stop and even to the no additive test. Again here, 23.4% of the particles are in the 100-3500 µm size range and the cause of this again could be the formation of bubbles in the Mastersizer 3000 as explained earlier This is higher than any concentration of Kla-stop but it must also be noted that the 0.2% Kla-stop has a higher proportion of particles in the 10-100 µm size range. Thus, based on these observations, it can be concluded that XG possesses around the same inhibition efficiency as Kla-stop.

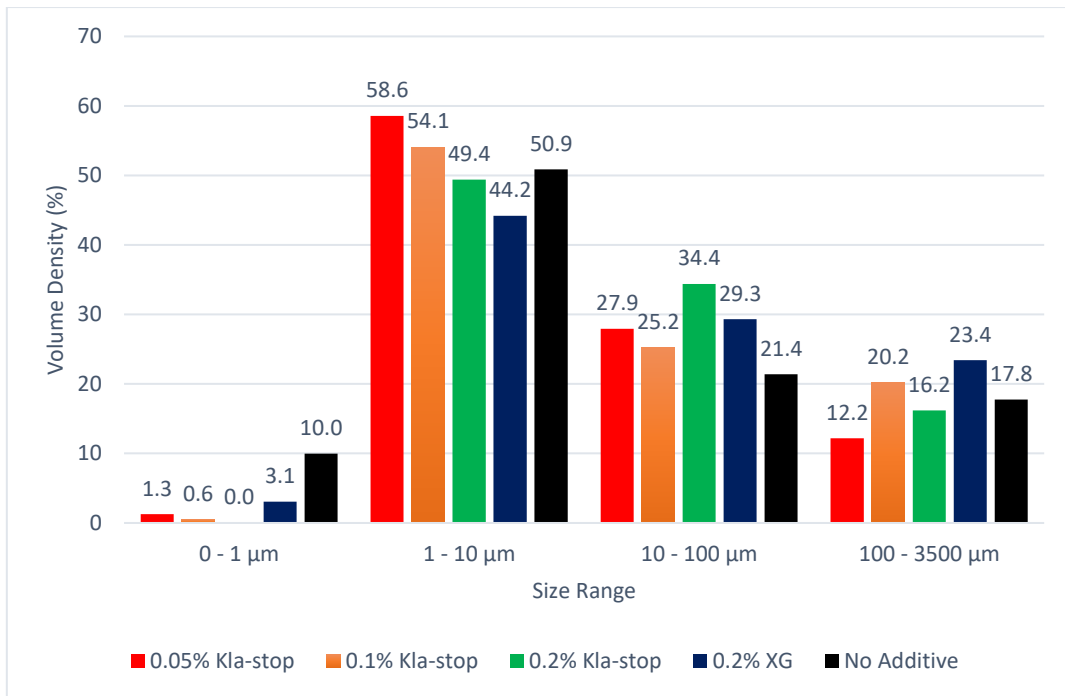


Figure 82. Xanthan Gum particle size distribution.

The benchmark of the tested industrial additives based on PSD's is listed in Table 9 . A benchmark of results from the FBRM particle count results was not completed as these results proved to be too erratic and at times were statistically insignificant. The best additive was selected based on how effective the additive was at keeping the particle size distribution larger (shifting more to the right in the results) and an optimum concentration is recommended based on the PSD results. As it can be clearly observed, the optimum concentration always tended to be the highest concentration that was tested. This information suggests that further testing should have been done with even higher concentrations so as to obtain more data to have quantitative comparisons. Only a certain amount of concentrations could be tested due to time restrictions and future research should have higher concentrations for each additive.

Table 9. Benchmark of industrial additives based on PSD's.

Rank #	Additive Name	Recommended Concentration
1	HMwPHPA	0.1%
2	Xtrahib	7%
3	LMwPHPA	0.1%
4	Kla-stop	0.2%
4	Xanthan Gum	0.1%

These results conform to the general hypothesis that a higher concentration of the additive will produce superior inhibition and maintain larger particle size. This ranking is based on the premise that the additive and concentration giving the larger average particle size range is most effecting while the additive giving the lower particle size range is least effective. This effect could also be observed if the additives caused particle aggregation and particle aggregation, for the purpose of this project, is desired as this would ultimately make it easier for the solids control unit to remove cuttings. HMwPHPA was the most effective additive and the least effective additives were Kla-stop and Xanthan Gum.

Chapter 5

Conclusion

5.1 Contribution

An experiment protocol was developed in this thesis to characterize the chemical degradation of cuttings, the process through which particles decompose to finer particles as a result of the clay-fluid reaction. The testing process generated valuable data and insight into fines behaviour with varying saline and polymer solutions. However it should be noted here that this testing is not completely representative of the actual drilling process as there were some uncertainties that are unanswered such as the pH of fluid sample and the effect of temperature.

In these experiments, the degree of clay agglomeration was recorded in terms of the changes in particle count, particle size distribution and changes in viscosity. There were two modes of experimentation with the first being for two-hours and the second being for forty-seven hours. The shorter duration simulated the exposure of cuttings in the annulus and the longer duration simulated the transient time of fluids at surface processing mud tanks

The experimental results showed that the results obtained from the particle size distribution and viscosity was more consistent and reliable than particle count measurements. This can be potentially attributed to the sensitivity and the condition of the particle tracking tool used in this thesis. Overall, it can be concluded that the FBRM results were inconsistent and unreliable and this could be attributed to the FBRM probe condition. The unit used was quite old but was the only device of the sort available for testing. It can be concluded that the FBRM results shown here are not reliable and are not recommended to be followed.

The particle size distribution can be affected as a result of the particle-fluid interaction. This may be dependent on the initial size and type of shale. As observed from Figure 12, at any viscosity, 100 micron particles are adequately handled by a hydrocyclone as all curves become asymptotic to 100% as size increases. So if the particles are removed within a few minutes of entering the hydrocyclone, what is left remaining is very small fine particles. Challenges, with regards to solids removal, only arise if particles are finer than 100 microns and this is indeed the case very

often as proven by the numerous plots shown in the results section of this research work. A general conceptual variation of the size distribution pertaining to the data obtained from this research projects testing is shown in Figure 83(a). As it is shown in the graph, the cutting disperses upon exposure to fluid shifting the distribution more to the left and forming smaller particles. This process is found to be time-dependent, where the concentration of finer particles increases at the expense of the concentration of coarser particles confirming that coarser particles are decomposing to finer particles as shown in Figure 83(b). The effect of inhibition on wet cuttings is also demonstrated in (a), which is the opposite of the effect of time on the size distribution.

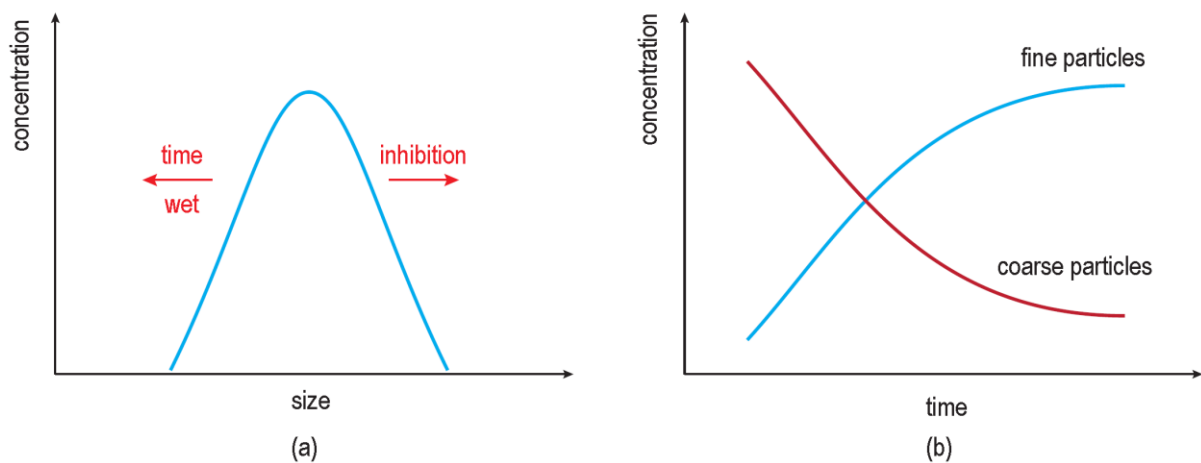


Figure 83. Conceptual variation of particle size distribution during the chemical degradation of cuttings: (a) variation of total size distribution; (b) variation of the proportion of fine and coarse particles.

The properties of the suspension fluid are affected by the disintegration of the cuttings. As it is conceptually shown in Figure 84, the fluid viscosity increases with time (assuming constant pH conditions). The increase in viscosity is due to the additional dispersion of the clay particles. This process is known as the increase in yield of bentonite in the field of drilling fluid engineering and this is when sodium montmorillonite is used as a viscosifying additive in drilling fluid. In research work performed at Drilling Mechanics Group of Curtin University, it was found that the filtration rate of the suspension fluid is also affected [95]. The clay-fluid interaction results in fine suspended cuttings, which form a less permeable mud cake in the API filtration experiment. Therefore, a smaller mud filtrate is achieved for a solution with

higher clay-fluid interaction as noted with the PHPA results. Similar to cutting size distribution and viscosity results, the fluid reaches a plateau within 24 hours.

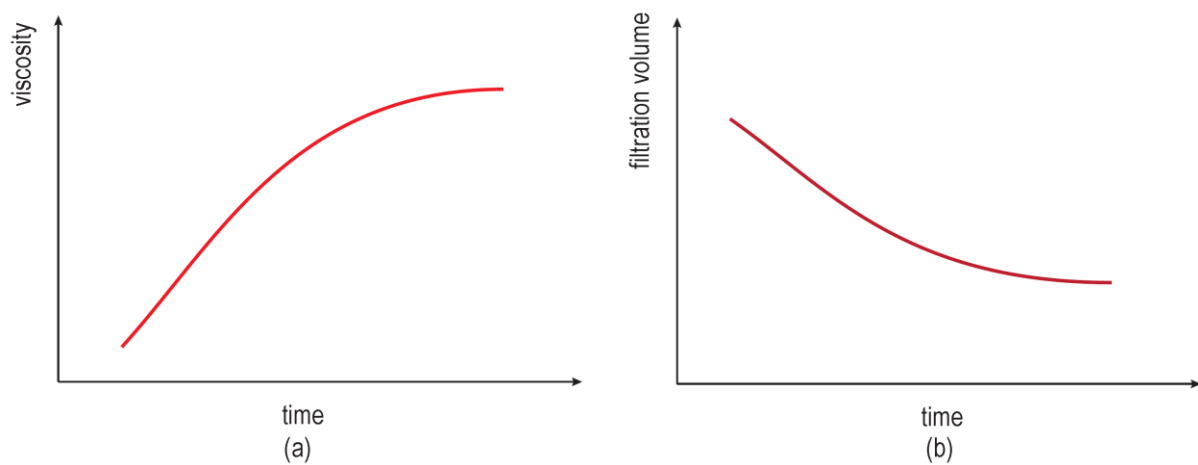


Figure 84. The variation of suspension fluid during the cutting degradation: (a) variation of viscosity; (b) variation of filtration rate.

The role of drilling fluid additives in degradation is studied using the developed test procedure. The selected additives were potassium chloride, a selection of natural and synthetic polymers and some other clay inhibitors. The experiments were performed at different concentrations, and the effectiveness of each additive in controlling fine particle formation was quantified. Based on particle size distributions alone, it was found that HMwPHPA was the most effective additive at maintaining a larger particle size range and it was also found that for all samples tested, a higher concentration resulted in the preferred larger particle size ranges.

5.2 Field Implications

Traditionally, drilling fluid chemistry is of major importance to stabilize shale formations which can lead to borehole instability, borehole collapse and stuck pipe. For this research project, various test protocols were developed to quantify the effectiveness of drilling fluid composition in controlling the drilling fluid-shale formation interaction. As representative shale samples were difficult to obtain, these experiments were performed on cuttings collected at the shale shaker. It can be argued that this analysis evaluates the fluid-rock interaction at a macro-scale aiming at the stability of the formation.

In this work, the research was focused on the stability of smaller shale particles with the goal of minimising formation of low gravity solids, i.e. fine solid particles which are difficult to remove from the drilling fluid using solid removal units. While the nature of the process is similar, the exposure of solids particles to drilling fluid is larger due to the smaller size of cuttings, i.e., smaller particles have higher surface area and therefore have higher exposure to fluid-rock interaction.

In parallel to other standard test protocols, the developed procedure in this research can be used as a criterion to design drilling fluids with the objective of quantifying the effectiveness of the drilling fluid in minimizing the formation of fine particles (low gravity solids). This test protocol was used in designing the drilling fluid properties of two coiled tube drilling field trials. The results show that the required concentration of shale inhibitor additive to control the shale instability is lower than the required concentration of additive to control the formation of low gravity solids. While the mechanism of the interaction is the same for both borehole stability and formation of low gravity solids, the surface area on which the fluid interacts with shale is different. In the time frame during which the stability was studied, the results suggest that a higher concentration of salts is required to minimise low gravity solid formation.

5.3 Recommendations and future work

Firstly, it must be emphasized here that much of the experimentation in this project had a narrow window of potential investigation. As stated earlier, the developed method only focused on the fluid interaction between the shale through the study of particle count and particle size and did not encompass structural effects, geo-mechanical effects and the impact of bottom-hole pressure. The effect of temperature was also not investigated, as all experimentation was done under isothermal conditions. Finally, another important aspect that was not investigated was the effect of pH – the acidity or alkalinity of the water based drilling fluid. The pH vs. time plot could affect the final results and should be investigated in future projects. Extending the scope of parametric analysis is of great importance. There are still a number of parameters which can potentially affect the disintegration of cuttings such as the initial particle size and the hardness of the sample.

Further research should be done to evaluate the effect of shear degradation. The shear can be simulated directly by experimenting with different impeller shear rate similar to previous work [96]. However, there is merit in simulating the dynamic condition of the well using a more controlled environment such as circulating fluid in a given pipe simulating the same level of shear the fluid is exposed to in the annulus. Also, similar experiments can be performed at a high shear rate simulating shear rates where the fluid is exposed in hydrocyclones to investigate if the inhibition/aggregation of particles can break with shear. Experiments at a smaller shear rate are relevant to simulate the condition of the fluid in the mud tanks.

It will be of added value to compare the results of the fluid design based on macro clay-rock interaction from the literature (similar to clay dispersion test and linear swelling meter) with clay-rock interaction developed in this work. It is essential to verify if similar trends can be achieved, or each procedure can potentially recommend a different fluid additive to control the clay-rock interaction.

In this work, the FBRM probe results were inconsistent and unreliable, which can be attributed to the probe condition. The probe being used for testing could have had defects as a result of aging. This is a risk and hidden danger of using outdated technology. Further work should be carried out with a newer unit with better sensitivity, and it is also recommended to use additional particle measurement techniques so as to obtain multiple sources of data.

The Mastersizer results also had the reoccurring issue of bubble peaks. These erroneous measurements have the potential to significantly impact the interpretation of the final results. This is especially the case if the operator of the instrument has not been trained to identify and minimize a bubble problem before collecting data. The final results reported in this research work are in alignment with the literature available on particle size analyzers. They both indicate that the repeatability and reproducibility of such tools and methods do not necessarily translate and reflect the accuracy of the measurement [88]. There is always a risk of producing repeatable erroneous data if a system to verify its accuracy is not scientifically established first. Depending on the background of the appropriate application, it is important that the results generated by a particle size analysis are first comprehensively understood. Furthermore, any results obtained from particle size analysers should include

another critical step. This step is to examine the sample under a microscope and verify if the obtained results correspond to the observed particle size. Such steps should be followed during the measurement of the particle size distribution of a material to guarantee that the measured output signal reflects the test sample rather than a source of contamination such as a bubble.

Appendix

Complete Safety Data Sheets of all additives are provided below



Safety Data Sheet POTASSIUM CHLORIDE

1. Identification of the substance/preparation and of the Company/undertaking

1.1 Product identifier

Product name	POTASSIUM CHLORIDE
Product code	MI10857
Synonyms	Potassium Chloride 88-99%
Denmark Pr. no.:	336939

1.2 Relevant identified uses of the substance or mixture and uses advised against

Recommended Use	Completion fluid additive. Drilling fluid additive.
Uses advised against	Consumer use

1.3 Details of the supplier of the safety data sheet

Supplier
M-I Australia Pty Ltd
ABN: 67 009 214 162
Level 5
256 St. George Tce
Perth
WA 6000
T = +61 08 9440 2900
F = +61 08 9322 3080
+47 51577424
MISDS@slb.com

1.4 Emergency Telephone Number

Emergency telephone - (24 Hour) Australia +61 2801 44558, Asia Pacific +65 3158 1074, China +86 10 5100 3039, Europe +44 (0) 1235 239 670, Middle East and Africa +44 (0) 1235 239 671, New Zealand +64 9929 1483, USA 001 281 561 1600

2. Hazards identification

2.1 Classification of the substance or mixture

Classification according to (EC) No. 1272/2008

Health hazards	Not classified
Environmental hazards	Not classified
Physical Hazards	Not classified

2.2 Label elements

Eye contact Remove contact lenses. Promptly wash eyes with lots of water while lifting eye lids.
Continue to rinse for at least 15 minutes. Get medical attention if any discomfort continues.

4.2 Most important symptoms and effects, both acute and delayed

General advice The severity of the symptoms described will vary dependant of the concentration and the length of exposure. If adverse symptoms develop, the casualty should be transferred to hospital as soon as possible.

Main symptoms

Inhalation Please see Section 11. Toxicological Information for further information.

Ingestion Please see Section 11. Toxicological Information for further information.

Skin contact Please see Section 11. Toxicological Information for further information.

Eye contact Please see Section 11. Toxicological Information for further information.

4.3 Indication of any immediate medical attention and special treatment needed

Notes to physician Treat symptomatically.

5. Fire-fighting measures

5.1 Extinguishing media

Suitable extinguishing media
Water Fog, Alcohol Foam, CO₂, Dry Chemical.

Extinguishing media which shall not be used for safety reasons
None known.

5.2 Special hazards arising from the substance or mixture

Unusual fire and explosion hazards
None known.

Hazardous combustion products
Fire or high temperatures create:, Chlorides.

5.3 Advice for firefighters

Special protective equipment for fire-fighters
As in any fire, wear self-contained breathing apparatus and full protective gear.

Special Fire-Fighting Procedures
Containers close to fire should be removed immediately or cooled with water.

6. Accidental release measures

6.1 Personal precautions, protective equipment and emergency procedures

Use personal protective equipment. See also section 8.

6.2 Environmental precautions

The product should not be allowed to enter drains, water courses or the soil.

Signal word

None

Hazard statements

This product is not classified as hazardous therefore no (H) hazard statements assigned.

Precautionary Statements - EU (§28, 1272/2008)

This product is not classified as hazardous therefore has no (P) precautionary statements assigned.

-

-

Contains

Potassium chloride

2.3 Other data

Not classified as PBT/vPvB by current EU criteria.

Australian statement of hazardous/dangerous nature

Classified as Non-Hazardous according to the criteria of NOHSC.
NON-HAZARDOUS SUBSTANCE. NON-DANGEROUS GOODS.

3. Composition/information on ingredients

3.1 Substances

Component	EC-No.	CAS-No	Weight % - range	Classification (67/548)	Classification (Reg. 1272/2008)	REACH registration number
Potassium chloride	231-211-8	7447-40-7	60-100	-	Not classified	01-2119539416-36-xxx

3.2 Mixtures

Not Applicable

4. First aid measures

4.1 First-Aid Measures

Inhalation	If inhaled, remove from area to fresh air. Get medical attention if respiratory irritation develops or if breathing becomes difficult.
Ingestion	Rinse mouth. Do not induce vomiting without medical advice. Never give anything by mouth to an unconscious person. Get medical attention if symptoms occur.
Skin contact	Wash off immediately with soap and plenty of water removing all contaminated clothes and shoes. Get medical attention immediately if symptoms occur.

Environmental exposure controls

Avoid release to the environment. Local authorities should be advised if significant spillages cannot be contained.

6.3 Methods and materials for containment and cleaning up

Methods for containment

Prevent further leakage or spillage if safe to do so.

Methods for cleaning up

Sweep up and shovel into suitable containers for disposal. After cleaning, flush away traces with water.

6.4 Reference to other sections

See section 13 for more information.

7. Handling and storage

7.1 Precautions for safe handling

Handling

Handle in accordance with good industrial hygiene and safety practice. Avoid contact with skin and eyes. Avoid dust formation. Wash thoroughly after handling.

Hygiene measures

Use good work and personal hygiene practices to avoid exposure. When using do not smoke, eat or drink. Wash hands before eating, drinking or smoking. Remove contaminated clothing.

7.2 Conditions for safe storage, including any incompatibilities

Technical measures/precautions Ensure adequate ventilation. Provide appropriate exhaust ventilation at places where dust is formed. Keep airborne concentrations below exposure limits.

Storage precautions Keep containers tightly closed in a dry, cool and well-ventilated place. Avoid contact with: Strong oxidizing agents Strong acids. Strong alkalies. Protect from moisture

Storage class Chemical storage.

Packaging material Use specially constructed containers only

7.3 Specific end uses

See Section 1.2.

8. Exposure controls/personal protection

8.1 Control parameters

Exposure limits NUI = Nuisance dust, TWA 4mg/m³ Respirable Dust, 10mg/m³ Total Dust.
No biological limit allocated

Component	EU OEL	Austria	Australia	Denmark
Potassium chloride	Not determined	Not determined	Not determined	Not determined

Component	Malaysia	France	Germany	Hungary
Potassium chloride	Not determined	Not determined	Not determined	Not determined

Component	New Zealand	Italy	Netherlands	Norway
Potassium chloride	Not Determined	Not determined	Not determined	Not determined

Component	Poland	Portugal	Romania	Russia
Potassium chloride	Not determined	Not determined	Not determined	5 mg/m ³ MAC

Component	Spain	Switzerland	Turkey	UK
Potassium chloride	Not determined	Not determined	Not determined	Not determined

Derived No Effect Level (DNEL)

Short term exposure systemic effects

Potassium chloride	
Dermal	910 mg/kg
Inhalation	5320 mg/m ³

Long term exposure systemic effects

Potassium chloride	
Dermal	303 mg/kg
Inhalation	1064 mg/m ³

Predicted No Effect Concentration (PNEC)

Potassium chloride	
Fresh water	0.1 mg/l
Sea water	0.1 mg/l
Impact on sewage treatment	10 mg/L
Intermittent release	10 mg/L

8.2 Exposure controls

All chemical Personal Protective Equipment (PPE) should be selected based on an assessment of both the chemical hazard present and the risk of exposure to those hazards. The PPE recommendations below are based on an assessment of the chemical hazards associated with this product. Where this product is used in a mixture with other products or fluids, additional hazards may be created and as such further assessment of risk may be required. The risk of exposure and need of respiratory protection will vary from workplace to workplace and should be assessed by the user in each situation.

Engineering measures to reduce exposure

Ensure adequate ventilation. Mechanical ventilation or local exhaust ventilation is required.

Personal protective equipment

Eye protection	Safety glasses with side-shields.
Hand protection	Use protective gloves made of: Rubber gloves, Frequent change is advisable.
Respiratory protection	No personal respiratory protective equipment normally required, In case of insufficient ventilation wear suitable respiratory equipment, Half mask with a particle filter P2 (European Norm EN 143 = former DIN 3181), At work in confined or poorly ventilated spaces, respiratory protection with air supply must be used.
Skin and body protection	Wear suitable protective clothing. Eye wash and emergency shower must be available at the work place.

10.2 Chemical stability

Stable under normal temperature conditions and recommended use.

10.3 Possibility of Hazardous Reactions

Hazardous polymerization
Hazardous polymerization does not occur.

10.4 Conditions to avoid

Avoid dust formation. Protect from moisture.

10.5 Incompatible materials

Strong oxidizing agents. Strong acids. Strong alkalies.

10.6 Hazardous decomposition products

See also section 5.2.

11. Toxicological information

11.1 Information on toxicological effects

Acute toxicity

Inhalation	Inhalation of dust in high concentration may cause irritation of respiratory system.
Eye contact	May cause slight irritation.
Skin contact	Prolonged contact may cause redness and irritation.
Ingestion	Ingestion may cause stomach discomfort.
Unknown acute toxicity	Not Applicable.

Component	LD50 Oral	LD50 Dermal	LC50 Inhalation
Potassium chloride	= 2600 mg/kg (Rat)	No data available	No data available

Sensitization This product does not contain any components suspected to be sensitizing.

Mutagenic effects This product does not contain any known or suspected mutagens.

Carcinogenicity This product does not contain any known or suspected carcinogens.

Reproductive toxicity This product does not contain any known or suspected reproductive hazards.

Routes of exposure None known.

Routes of entry No route of entry noted.

Hygiene measures

Wash hands before eating, drinking or smoking, Remove and wash contaminated clothing before re-use.



9. Physical and chemical properties

9.1 Information on basic physical and chemical properties

Physical state	Solid powder
Appearance	Dust
Odor	Odorless
Color	White - Light pink
Odor threshold	Not applicable

<u>Property</u>	<u>Values</u>	<u>Remarks</u>
pH	Not applicable	
pH @ dilution	~7	@ 1%
Melting/freezing point	768-773 °C / 1414-1423 °F	
Boiling point/range	1406-1413 °C / 2562-2575 °F	
Flash point	No information available	
Evaporation rate (BuAc =1)	No information available	
Flammability (solid, gas)	Not Applicable	
Flammability Limits in Air		
Upper flammability limit	Not applicable	
Lower flammability limit	Not applicable	
Vapor pressure	No information available	
Vapor density	No information available	
Specific gravity	No information available	
Bulk density	No information available	
Relative density	1.98	@ 20°C.
Water solubility	Soluble in water	
Solubility in other solvents	No information available	
Autoignition temperature	No information available	
Decomposition temperature	No information available	
Kinematic viscosity	No information available	
Dynamic viscosity	No information available	
Log Pow	No information available	
Explosive properties	Not Applicable	
Oxidizing properties	None known.	

9.2 Other information

Pour point	No information available
Molecular weight	No information available
VOC content(%)	None
Density	No information available

10. Stability and reactivity

10.1 Reactivity

No specific reactivity hazards associated with this product.

10.2 Chemical stability

Stable under normal temperature conditions and recommended use.

10.3 Possibility of Hazardous Reactions

Hazardous polymerization
Hazardous polymerization does not occur.

10.4 Conditions to avoid

Avoid dust formation. Protect from moisture.

10.5 Incompatible materials

Strong oxidizing agents. Strong acids. Strong alkalis.

10.6 Hazardous decomposition products

See also section 5.2.

11. Toxicological information

11.1 Information on toxicological effects

Acute toxicity

Inhalation	Inhalation of dust in high concentration may cause irritation of respiratory system.
Eye contact	May cause slight irritation.
Skin contact	Prolonged contact may cause redness and irritation.
Ingestion	Ingestion may cause stomach discomfort.
Unknown acute toxicity	Not Applicable.

Component	LD50 Oral	LD50 Dermal	LC50 Inhalation
Potassium chloride	= 2600 mg/kg (Rat)	No data available	No data available

Sensitization This product does not contain any components suspected to be sensitizing.

Mutagenic effects This product does not contain any known or suspected mutagens.

Carcinogenicity This product does not contain any known or suspected carcinogens.

Reproductive toxicity This product does not contain any known or suspected reproductive hazards.

Routes of exposure None known.

Routes of entry No route of entry noted.

Specific target organ toxicity (single exposure) Not classified
 Specific target organ toxicity (repeated exposure) Not classified.
 Aspiration hazard No hazard from product as supplied.

12. Ecological information

12.1 Toxicity

The product component(s) are not classified as environmentally hazardous. However, this does not exclude the possibility that large or frequent spills can have a harmful or damaging effect on the environment.

Listed on PLONOR list of OSPAR

Toxicity to algae
 This product is not considered toxic to algae.

Toxicity to fish
 This product is not considered toxic to fish.

Toxicity to daphnia and other aquatic invertebrates
 This product is not considered toxic to invertebrates.

Component	Toxicity to fish	Toxicity to algae	Toxicity to daphnia and other aquatic invertebrates
Potassium chloride	750 - 1020 mg/L LC50 (Pimephales promelas) = 96 h 1060 mg/L LC50 (Lepomis macrochirus) = 96 h	2500 mg/L EC50 (Desmodesmus subspicatus) = 72 h	83 mg/L EC50 (Daphnia magna) = 48 h 825 mg/L EC50 (Daphnia magna) = 48 h

12.2 Persistence and degradability

Not Applicable - Inorganic chemical.

12.3 Bioaccumulative potential

Not Applicable - Inorganic chemical.

12.4 Mobility in soil

Mobility
 Soluble in water.

12.5 Results of PBT and vPvB assessment

Not classified as PBT/vPvB by current EU criteria.

12.6 Other adverse effects.

None known.

13. Disposal considerations

13.1 Waste treatment methods

Waste from residues / unused products	Dispose of in accordance with local regulations.
Contaminated packaging	Empty containers should be taken for local recycling, recovery or waste disposal.
EWC Waste disposal No.	According to the European Waste Catalogue, Waste Codes are not product specific, but application specific. Waste codes should be assigned by the user based on the application for which the product was used. The following Waste Codes are only suggestions: EWC waste disposal No: 06 03 99

14. Transport information

14.1 UN Number

Not regulated

14.2 Proper shipping name

The product is not covered by international regulation on the transport of dangerous goods

14.3 Hazard class(es)

ADR/RID/ADN/ADG Hazard class	Not regulated
IMDG Hazard class	Not regulated
ICAO Hazard class/division	Not regulated

14.4 Packing group

ADR/RID/ADN/ADG Packing group	Not regulated
IMDG Packing group	Not regulated
ICAO Packing group	Not regulated

14.5 Environmental hazard

No

14.6 Special precautions

Not Applicable

14.7 Transport in bulk according to Annex II of MARPOL 73/78 and the IBC Code

Please contact MISDS@slb.com for info regarding transport in Bulk.

15. Regulatory information

15.1 Safety, health and environmental regulations/legislation specific for the substance or mixture

Germany, Water Endangering Classes (VwVwS) Hazardous to water/Class 1

Australian Standard for the Uniform Scheduling of Drugs and Poisons

Potassium chloride
Schedule 4

New Zealand hazard classification Not classified.

HSNO approval no. Not required.

Group number Not required.

Commission Regulation (EU) No 453/2010 of 20 May 2010 amending Regulation (EC) No 1907/2006 of the European Parliament and of the Council on the Registration, Evaluation, Authorisation and Restriction of Chemicals (REACH). Regulation (EC) No 1907/2006 of the European Parliament and of the Council of 18 December 2006 concerning the Registration, Evaluation, Authorisation and Restriction of Chemicals (REACH), establishing a European Chemicals Agency, amending Directive 1999/EC and repealing Council Regulation (EEC) No 793/93 and Commission Regulation (EC) No 1488/94 as well as Council Directive 76/769/EEC and Commission Directives 91/155/EEC, 93/67/EEC, 93/105/EC and 2000/21/EC, including amendments.

This safety data sheet complies with the requirements of Regulation (EC) No. 1272/2008.

National Code of Practice for the Preparation of Material Safety Data Sheets 2nd Edition [NOHSC: 2011 (2003)].

National Occupational Health and Safety Commission's Approved Criteria for Classifying Hazardous Substances [NOHSC:1008 (2004) 3rd Edition].

National Occupational Health and Safety Commission's Exposure Standards for Atmospheric Contaminants in the occupational Environment [NOHSC:1003 (1995)].

Safe Work Australia.

Standard for the Uniform Scheduling of Drugs and Poisons (SUSDP).

Not classified as Dangerous Goods by the criteria of the Australian Dangerous Goods Code (ADG Code) for transport by road or rail.

Dutch Mining Regulations: In accordance with Mining Regulations 9.2 and Chapter 4 of the Working Conditions Decree.

Occupational Safety and Health (Classification, Labelling and Safety Data Sheet of Hazardous Chemicals) Regulations 2013 [P.U.(A) 310/2013] (CLASS Regulations)

The Industry Code of Practice on Chemical Classification and Hazard Communication 2014 [P.U. (B) 128/2014] (ICOP) International inventories

USA (TSCA)	Complies
European Union (EINECS and ELINCS)	Complies
Canada (DSL)	Complies
Philippines (PICCS)	Complies
Japan (ENCS)	Complies
China (IECSC)	Complies
Australia (AICS)	Complies
Korean (KECL)	Complies
New Zealand (NZIoC)	Complies

Contact REACH@miswaco.slb.com for REACH information.

15.2 Chemical Safety Report

No information available

16. Other information

Prepared by	Global Regulatory Compliance - Chemicals (GRC - Chemicals) , Anne Karin (Anka) Fosse
Supersedes date	26/Feb/2013
Revision date	20/Jun/2015
Version	5
The following sections have been revised:	This SDS have been made in a new database and therefore a new layout. No changes with regard to classification have been made, Updated according to GHS/CLP.

Full text of H-Statements referred to under sections 2 and 3

This product is not classified as hazardous therefore no (H) hazard statements assigned.

Disclaimer

The information contained herein is considered in good faith as reliable of the date issued and is based upon on **measurements, tests or data derived from supplier's own study or furnished by others. In providing this SDS** information, Supplier makes no express or implied warranties as to the information or product; merchantability or fitness of purpose; any express or implied warranty; or non-infringement of intellectual property rights; and supplier assumes no responsibility for any direct, special or consequential damages, results obtained, or the activities of others. To the **maximum extent permitted by law, supplier's warranty obligations and buyer's sole remedies are as stated in separate** agreement between the parties.

Material Safety Data Sheet

Xanthan gum MSDS

Section 1: Chemical Product and Company Identification

Product Name: Xanthan gum	Contact Information:
Catalog Codes: SLX1045, SLX1099	Sciencelab.com, Inc. 14025 Smith Rd. Houston, Texas 77396
CAS#: 11138-66-2	US Sales: 1-800-901-7247 International Sales: 1-281-441-4400
RTECS: Not available.	Order Online: ScienceLab.com
TSCA: TSCA 8(b) inventory: Xanthan gum	CHEMTREC (24HR Emergency Telephone), call: 1-800-424-9300
CI#: Not available.	International CHEMTREC, call: 1-703-527-3887
Synonym:	For non-emergency assistance, call: 1-281-441-4400
Chemical Name: Not available.	
Chemical Formula: Not available.	

Section 2: Composition and Information on Ingredients

Composition:

Name	CAS #	% by Weight
Xanthan gum	11138-66-2	100

Toxicological Data on Ingredients: Xanthan gum LD50: Not available. LC50: Not available.

Section 3: Hazards Identification

Potential Acute Health Effects: Hazardous in case of skin contact (irritant), of eye contact (irritant), of ingestion, of inhalation.

Potential Chronic Health Effects:

CARCINOGENIC EFFECTS: Not available. MUTAGENIC EFFECTS: Not available. TERATOGENIC EFFECTS: Not available. DEVELOPMENTAL TOXICITY: Not available. Repeated or prolonged exposure is not known to aggravate medical condition.

Section 4: First Aid Measures

Eye Contact:

Check for and remove any contact lenses. Immediately flush eyes with running water for at least 15 minutes, keeping eyelids open. Cold water may be used. Do not use an eye ointment. Seek medical attention.

Skin Contact:

After contact with skin, wash immediately with plenty of water. Gently and thoroughly wash the contaminated skin with running water and non-abrasive soap. Be particularly careful to clean folds, crevices, creases and groin. Cold water may be used.

Cover the irritated skin with an emollient. If irritation persists, seek medical attention. Wash contaminated clothing before reusing.

Serious Skin Contact:

Wash with a disinfectant soap and cover the contaminated skin with an anti-bacterial cream. Seek medical attention.

Inhalation: Allow the victim to rest in a well ventilated area. Seek immediate medical attention.

Serious Inhalation: Not available.

Ingestion:

Do not induce vomiting. Loosen tight clothing such as a collar, tie, belt or waistband. If the victim is not breathing, perform mouth-to-mouth resuscitation. Seek immediate medical attention.

Serious Ingestion: Not available.

Section 5: Fire and Explosion Data

Flammability of the Product: May be combustible at high temperature.

Auto-Ignition Temperature: Not available.

Flash Points: Not available.

Flammable Limits: Not available.

Products of Combustion: Not available.

Fire Hazards in Presence of Various Substances:

Flammable in presence of open flames and sparks. Slightly flammable to flammable in presence of heat.

Explosion Hazards in Presence of Various Substances:

Risks of explosion of the product in presence of mechanical impact: Not available. Risks of explosion of the product in presence of static discharge: Not available.

Fire Fighting Media and Instructions:

SMALL FIRE: Use DRY chemical powder. LARGE FIRE: Use water spray, fog or foam. Do not use water jet.

Special Remarks on Fire Hazards: Not available.

Special Remarks on Explosion Hazards: Not available.

Section 6: Accidental Release Measures

Small Spill:

Use appropriate tools to put the spilled solid in a convenient waste disposal container. Finish cleaning by spreading water on the contaminated surface and dispose of according to local and regional authority requirements.

Large Spill:

Use a shovel to put the material into a convenient waste disposal container. Finish cleaning by spreading water on the contaminated surface and allow to evacuate through the sanitary system.

Section 7: Handling and Storage

Precautions:

Keep away from heat. Keep away from sources of ignition. Empty containers pose a fire risk, evaporate the residue under a fume hood. Ground all equipment containing material. Do not breathe dust. Wear suitable protective clothing. In case of insufficient ventilation, wear suitable respiratory equipment. If you feel unwell, seek medical attention and show the label when possible. Avoid contact with skin and eyes.

Storage:

Keep container dry. Keep in a cool place. Ground all equipment containing material. Keep container tightly closed. Keep in a cool, well-ventilated place. Combustible materials should be stored away from extreme heat and away from strong oxidizing agents.

Section 8: Exposure Controls/Personal Protection

Engineering Controls:

Use process enclosures, local exhaust ventilation, or other engineering controls to keep airborne levels below recommended exposure limits. If user operations generate dust, fume or mist, use ventilation to keep exposure to airborne contaminants below the exposure limit.

Personal Protection:

Splash goggles. Lab coat. Dust respirator. Be sure to use an approved/certified respirator or equivalent. Gloves.

Personal Protection in Case of a Large Spill:

Splash goggles. Full suit. Dust respirator. Boots. Gloves. A self contained breathing apparatus should be used to avoid inhalation of the product. Suggested protective clothing might not be sufficient; consult a specialist BEFORE handling this product.

Exposure Limits: Not available.

Section 9: Physical and Chemical Properties

Physical state and appearance: Solid.

Odor: Not available.

Taste: Not available.

Molecular Weight: Not available.

Color: Not available.

pH (1% soln/water): Not available.

Boiling Point: Decomposes.

Melting Point: Not available.

Critical Temperature: Not available.

Specific Gravity: 1.5 (Water = 1)

Vapor Pressure: Not applicable.

Vapor Density: Not available.

Volatility: Not available.

Odor Threshold: Not available.

Water/Oil Dist. Coeff.: Not available.

Ionicity (in Water): Not available.

Dispersion Properties: See solubility in water.

Solubility: Easily soluble in cold water.

Section 10: Stability and Reactivity Data

Stability: The product is stable.

Instability Temperature: Not available.

Conditions of Instability: Not available.
Incompatibility with various substances: Not available.
Corrosivity: Non-corrosive in presence of glass.
Special Remarks on Reactivity: Not available.
Special Remarks on Corrosivity: Not available.
Polymerization: No.

Section 11: Toxicological Information

Routes of Entry: Eye contact. Inhalation. Ingestion.
Toxicity to Animals:
LD50: Not available. LC50: Not available.
Chronic Effects on Humans: Not available.
Other Toxic Effects on Humans: Hazardous in case of skin contact (irritant), of ingestion, of inhalation.
Special Remarks on Toxicity to Animals: Not available.
Special Remarks on Chronic Effects on Humans: Not available.
Special Remarks on other Toxic Effects on Humans: Not available.

Section 12: Ecological Information

Ecotoxicity: Not available.
BOD5 and COD: Not available.
Products of Biodegradation:
Possibly hazardous short term degradation products are not likely. However, long term degradation products may arise.
Toxicity of the Products of Biodegradation: The products of degradation are more toxic.
Special Remarks on the Products of Biodegradation: Not available.

Section 13: Disposal Considerations

Waste Disposal:

Section 14: Transport Information

DOT Classification: Not a DOT controlled material (United States).
Identification: Not applicable.
Special Provisions for Transport: Not applicable.

Section 15: Other Regulatory Information

Federal and State Regulations: TSCA 8(b) inventory: Xanthan gum
Other Regulations: Not available..

Other Classifications:

WHMIS (Canada): Not controlled under WHMIS (Canada).

DSCL (EEC): R36/38- Irritating to eyes and skin.

HMIS (U.S.A.):

Health Hazard: 2

Fire Hazard: 1

Reactivity: 0

Personal Protection: E

National Fire Protection Association (U.S.A.):

Health: 2

Flammability: 1

Reactivity: 0

Specific hazard:

Protective Equipment:

Gloves. Lab coat. Dust respirator. Be sure to use an approved/certified respirator or equivalent. Splash goggles.

Section 16: Other Information

References: Not available.

Other Special Considerations: Not available.

Created: 10/11/2005 12:54 PM

Last Updated: 05/21/2013 12:00 PM

The information above is believed to be accurate and represents the best information currently available to us. However, we make no warranty of merchantability or any other warranty, express or implied, with respect to such information, and we assume no liability resulting from its use. Users should make their own investigations to determine the suitability of the information for their particular purposes. In no event shall ScienceLab.com be liable for any claims, losses, or damages of any third party or for lost profits or any special, indirect, incidental, consequential or exemplary damages, howsoever arising, even if ScienceLab.com has been advised of the possibility of such damages.

Material Safety Data Sheet

PHPA L

I. PRODUCT AND COMPANY IDENTIFICATION

Product Name: PHPA L
Chemical Name: PARTIALLY HYDROLIZED POLYACRYLAMIDE
Chemical Family: SODIUM ACRYLATE & ACRYLAMIDE
Chemical Formula: PROPRIETARY
Synonyms: DRILL P, PHPA

Date Revised: 7/2010
CAS#: NDA

NFPA Properties: Health: 0 Flammability: 1 Reactivity: 0 Contact: 1

Supplier:

NOV FluidControl
4310 N Sam Houston Parkway East
Houston, Texas 77032 USA
Office: (713) 482-0500
Fax: (713) 482-0695
Company website: www.nov.com

Emergency Telephone Number:

CHEMTREC: 1-800-424-9300 or International +1-703-527-3887

II. HAZARDOUS INGREDIENTS/IDENTITY INFORMATION

Hazardous Components	TWAPPM	TWA MG/M ³	TLV's (ACGIH)		CAS#	OTHER LIMITS	%
			STEL PPM	STEL MG/M ³			
1.							
2.							
3.							

III. PHYSICAL/CHEMICAL CHARACTERISTICS

Boiling Point °F: N/A	Color: WHITE
Specific Gravity: 0.8-1.0	Odor: NONE
Vapor Pressure: NDA	Appearance: VISCOUS LIQUID
Percent Volatility: NDA	pH:
Vapor Density: N/A	Viscosity: N/A
Evaporation Rate: N/A	Activity: 87-90 BY WT%
Solubility In Water: SOLUBLE	LC50: NDA
Melting Point °F: N/A	LD50: NDA

VII. SPILL & DISPOSAL PROCEDURES

Steps To Be Taken in Case Material is Released or Spilled --- Procedures For Clean – Up: WEAR SUITABLE PROTECTIVE CLOTHING. SWEEP UP WITH CLEAN EQUIPMENT AND PLACE IN APPROPRIATE CONTAINER. HYDRATING THIS MATERIAL WILL PRODUCE AN EXTREMELY SLICK/SLIPPERY SURFACE.

Waste Disposal Method: DISPOSE OF IN ACCORDANCE WITH ALL APPLICABLE FEDERAL, STATE AND LOCAL REGULATIONS.

Precautions To Be Taken In Handling & Storage: NONE

VIII. PROTECTIVE EQUIPMENT

Ventilation Type Required: MECHANICAL

Protective Gloves: RUBBER OR PLASTIC

Respiratory Protection: WEAR A NIOSH APPROVED MASK IF CONCENTRATION IS TO EXCEED TLV

Other Protective Equipment:

Comments:

IX. REGULATORY & TRANSPORTATION INFORMATION

US DOT Proper Shipping Name: "OIL – WELL TREATING COMPOUND"

US DOT Hazard Class:

ID Number:

Unregulated By DOT:

Special Transportation Note:

Labels Required:

DOT ID Number:

Freight Classification:

Regulated by DOT: NO

DISCLAIMER:

Although the information and recommendations set forth herein (hereinafter "Information") are presented in good faith and believed to be correct as of the date hereof, NOV FluidControl, makes no representations as to the completeness or accuracy thereof. Information is supplied upon the condition that the person receiving this MSDS will make own determination as to its suitability for their intended purpose prior to use. Since the product is within the exclusive control of the user, it is the user's obligation to determine the conditions of safe use of this product. Such conditions should comply with all Federal Regulations concerning the Product. NO REPRESENTATIONS OR WARRANTIES, EITHER EXPRESS OR IMPLIED, OF MERCHANTABILITY, FITNESS FOR A PARTICULAR PURPOSE OR ANY OTHER NATURE ARE MADE HERUNDER WITH RESPECT TO INFORMATION OR THE PRODUCT TO WHICH INFORMATION REFERS.

For further information contact:

NOV FluidControl
4310 N Sam Houston Parkway East
Houston, Texas 77032 USA
Office: (713) 482-0500
Fax: (713) 482-0695
Company website: www.nov.com

IV. FIRE & EXPLOSION HAZARD DATA

Extinguishing Agents: DRY CHEMICAL OR WATERSPRAY OR WATERFOG OR CO2 OR FOAM OR SAND & EARTH

Flash Point °F: N/A

Flammable Limits: N/A

LEL: N/A UEL: N/A

Special Firefighting Procedures: FIREFIGHTERS SHOULD WEAR PROPER PROTECTIVE EQUIPMENT AND SELF-CONTAINED (POSITIVE PRESSURE IF AVAILABLE) BREATHING APPARATUS WITH FULL FACEPIECE.

Unusual Fire & Explosion Hazards: NONE

Toxic Gases Produced: CARBON MONOXIDE, CARBON DIOXIDE

V. HEALTH HAZARD DATA

Routes of Entry: Inhalation: YES Skin: YES Ingestion: YES

Effects of Overexposure: DUST MAY IRRITATE EYES OR SKIN.

Toxicological Properties: NDA

Chronic & Acute Effects of Overexposure: NDA

Carcinogenicity: NTP: NO IARC Monographs: NO

OSHA Regulated: NO

Emergency First Aid Procedures

Eyes: IMMEDIATELY FLUSH WITH LARGE QUANTITIES OF WATER FOR AT LEAST 15 MINUTES AND CALL A PHYSICIAN.

Skin Contact: FLUSH WITH LARGE AMOUNTS OF SOAP & WATER FOR 15 MINUTES.

Inhalation: REMOVE TO FRESH AIR, IF BREATHING IS DIFFICULT, GIVE OXYGEN AND CALL A PHYSICIAN.

Ingestion: GIVE LARGE AMOUNTS OF WATER AND CALL A PHYSICIAN.



Safety Data Sheet KLA-STOP†

Quantity restrictions apply! Not to be used in quantities of 1 tonne or more within the EEA.

1. Identification of the substance/preparation and of the Company/undertaking

1.1 Product identifier

Product name KLA-STOP†
Product code MI10818

1.2 Relevant identified uses of the substance or mixture and uses advised against

Recommended Use Shale inhibitor.

Uses advised against Consumer use

1.3 Details of the supplier of the safety data sheet

Supplier
M-I Australia Pty Ltd
Level 5
256 St. George Terrace
Perth
WA 6000
T= 08 9440 2900
MISDS@slb.com

1.4 Emergency Telephone Number

Emergency telephone - (24 Hour) Australia +61 2801 44558, Asia Pacific +65 3158 1074, China +86 10 5100 3039, Europe +44 (0) 1235 239 670, Middle East and Africa +44 (0) 1235 239 671, New Zealand +64 9929 1483, USA 001 281 561 1600

2. Hazards identification

2.1 Classification of the substance or mixture

Classification according to (EC) No. 1272/2008

Health hazards

Skin corrosion/irritation	Category 1 Subcategory 1B
Serious eye damage/eye irritation	Category 1

Environmental hazards Not classified

Physical Hazards Not classified

2.2 Label elements



Signal word
DANGER

Hazard statements

H314 - Causes severe skin burns and eye damage

Precautionary Statements - EU (§28, 1272/2008)

P260 - Do not breathe dust/fume/gas/mist/vapors/spray

P280 - Wear protective gloves/ protective clothing/ eye protection/ face protection

P303 + P361 + P353 - IF ON SKIN (or hair): Remove/ Take off immediately all contaminated clothing. Rinse skin with water/ shower

P305 + P351 + P338 - IF IN EYES: Rinse cautiously with water for several minutes. Remove contact lenses, if present and easy to do. Continue rinsing

P310 - Immediately call a POISON CENTER or doctor/ physician

P501 - Dispose of contents/container in accordance with local regulations.

Supplementary precautionary statements

P264 - Wash face, hands and any exposed skin thoroughly after handling

P301 + P330 + P331 - IF SWALLOWED: rinse mouth. Do NOT induce vomiting

P304 + P340 - IF INHALED: Remove to fresh air and keep at rest in a position comfortable for breathing

P363 - Wash contaminated clothing before reuse

Classification according to EU Directives 67/548/EEC or 1999/45/EC

Indication of danger

C - Corrosive

R-code(s)

R34

Contains

Polyether amine

Polyether amine acetate

For the full text of the R-phrases and H-Statements mentioned in this Section, see Section 16.

2.3 Other data

Not classified as PBT/VPB by current EU criteria

Australian statement of hazardous/dangerous nature

Classified as Hazardous according to the criteria of NOHSC.

HAZARDOUS SUBSTANCE. DANGEROUS GOODS.

3. Composition/information on ingredients

3.1 Substances

3.2 Mixtures

Component	EC-No.	CAS-No	Weight % - range	Classification (67/548)	Classification (Reg. 1272/2008)	REACH registration number
Polyether amine	Polymer	9046-10-0	60-100	C;R34	Skin Corr. 1B (H314)	No data available
Polyether amine acetate		0-00-0	10-30	C; R34	Skin Corr. 1B(H314)	No data available

Comments

The product contains other ingredients which do not contribute to the overall classification.

4. First aid measures

4.1 First-Aid Measures

Inhalation	Keep at rest. Move the exposed person to fresh air at once. If breathing is difficult, (trained personnel should) give oxygen. Seek medical attention at once.
Ingestion	Do NOT induce vomiting. Get immediate medical attention. Rinse mouth. Never give anything by mouth to an unconscious person. If vomiting occurs spontaneously, minimize the risk of aspiration by properly positioning the affected person.
Skin contact	Promptly wash contaminated skin with soap or mild detergent and water. Promptly remove clothing if soaked through and wash as above. Burns: Flush with water immediately. While flushing, remove clothes which do not adhere to affected area. Call an ambulance. Continue flushing during transport to hospital. Chemical burns must be treated by a physician.
Eye contact	Remove contact lenses. Immediately flush eyes with water for 15 minutes while holding eyelids open. Seek medical attention.

4.2 Most important symptoms and effects, both acute and delayed

General advice	Seek medical attention for all burns, regardless how minor they may seem. The severity of the symptoms described will vary dependant of the concentration and the length of exposure. If adverse symptoms develop, the casualty should be transferred to hospital as soon as possible.
-----------------------	--

Main symptoms

Inhalation	Please see Section 11. Toxicological Information for further information.
Ingestion	Please see Section 11. Toxicological Information for further information.
Skin contact	Please see Section 11. Toxicological Information for further information.
Eye contact	Please see Section 11. Toxicological Information for further information.

4.3 Indication of any immediate medical attention and special treatment needed

Notes to physician	Treat symptomatically.
---------------------------	------------------------

5. Fire-fighting measures

5.1 Extinguishing media

Suitable extinguishing media

Water Fog, Alcohol Foam, CO₂, Dry Chemical.

Extinguishing media which shall not be used for safety reasons

None known.

5.2 Special hazards arising from the substance or mixture

Unusual fire and explosion hazards

None known.

Hazardous combustion products

Thermal decomposition can lead to release of toxic and corrosive gases/vapors.

5.3 Advice for firefighters

Special protective equipment for fire-fighters

As in any fire, wear self-contained breathing apparatus and full protective gear.

Special Fire-Fighting Procedures

Containers close to fire should be removed immediately or cooled with water.

Hazchem code ADG

X2

6. Accidental release measures

6.1 Personal precautions, protective equipment and emergency procedures

Keep people away from and upwind of spill/leak. Do not get on skin or clothing. Wash thoroughly after handling. Avoid contact with eyes. Do not breathe vapors or spray mist. Use personal protective equipment. See also section 8.

6.2 Environmental precautions

The product should not be allowed to enter drains, water courses or the soil.

Environmental exposure controls

Avoid release to the environment. Local authorities should be advised if significant spillages cannot be contained.

6.3 Methods and materials for containment and cleaning up

Methods for containment

Prevent further leakage or spillage if safe to do so. Dike far ahead of liquid spill for later disposal.

Methods for cleaning up

Contain and collect spillage with non-combustible absorbent material, (e.g. sand, earth, diatomaceous earth, vermiculite) and place in container for disposal according to local/national regulations (see Section 13).

6.4 Reference to other sections

See section 13 for more information.

7. Handling and storage

7.1 Precautions for safe handling

Handling

Handle in accordance with good industrial hygiene and safety practice. Keep away from heat and sources of ignition. Do not get in eyes, on skin or on clothing. Avoid spills and splashing during use. Do not breathe vapors or spray mist.

Hygiene measures

Use good work and personal hygiene practices to avoid exposure. When using do not smoke, eat or drink. Wash hands before eating, drinking or smoking. Remove contaminated clothing.

7.2 Conditions for safe storage, including any incompatibilities

Technical measures/precautions Ensure adequate ventilation.

Storage precautions Keep containers tightly closed in a dry, cool and well-ventilated place. Keep away from open flames, hot surfaces and sources of ignition. Avoid contact with: Acids

Storage class Corrosive storage.

Packaging material Use specially constructed containers only

7.3 Specific end uses

See Section 1.2.

8. Exposure controls/personal protection

8.1 Control parameters

Exposure limits Contains no substances with occupational exposure limit values
No biological limit allocated

Component	EU OEL	Austria	Australia	Denmark
Polyether amine	Not determined	Not determined	Not determined	Not determined
Polyether amine acetate	Not determined	Not determined	Not determined	Not determined

Component	Finland	France	Germany	Hungary
Polyether amine	Not determined	Not determined	Not determined	Not determined
Polyether amine acetate	Not determined	Not determined	Not determined	Not determined

Component	New Zealand	Italy	Netherlands	Norway
Polyether amine	Not Determined	Not determined	Not determined	Not determined
Polyether amine acetate	Not Determined	Not determined	Not determined	Not determined

Component	Poland	Portugal	Romania	Russia
Polyether amine	Not determined	Not determined	Not determined	Not determined
Polyether amine acetate	Not determined	Not determined	Not determined	Not determined

Component	Spain	Switzerland	Turkey	UK
-----------	-------	-------------	--------	----

8.2 Exposure controls

All chemical Personal Protective Equipment (PPE) should be selected based on an assessment of both the chemical hazard present and the risk of exposure to those hazards. The PPE recommendations below are based on an assessment of the chemical hazards associated with this product. Where this product is used in a mixture with other products or fluids, additional hazards may be created and as such further assessment of risk may be required. The risk of exposure and need of respiratory protection will vary from workplace to workplace and should be assessed by the user in each situation.

Engineering measures to reduce exposure

Ensure adequate ventilation. Mechanical ventilation or local exhaust ventilation is required.

Personal protective equipment

Eye protection	It is good practice to wear goggles when handling any chemical. Tightly fitting safety goggles. Face-shield.
Hand protection	Impervious gloves made of: Nitrile, Neoprene, Rubber, Be aware that liquid may penetrate the gloves. Frequent change is advisable.
Respiratory protection	In case of insufficient ventilation wear suitable respiratory equipment, Chemical respirator with ammonia and amines cartridge (K/P2, green filter), At work in confined or poorly ventilated spaces, respiratory protection with air supply must be used.
Skin and body protection	Wear suitable protective clothing, Eye wash and emergency shower must be available at the work place.

Hygiene measures Wash hands before eating, drinking or smoking, Remove and wash contaminated clothing before re-use.



9. Physical and chemical properties

9.1 Information on basic physical and chemical properties

Physical state	Liquid
Appearance	No information available
Odor	Ammoniacal
Color	Colorless
Odor threshold	Not applicable

<u>Property</u>	<u>Values</u>	<u>Remarks</u>
pH	No information available	
pH @ dilution	11.7	@ 5%
Melting/freezing point	-22 - -20 °C / -7.6 - -4 °F	
Boiling point/range	232 °C / 449.6 °F	
Flash point	128 °C / 262.4 °F	Closed cup
Evaporation rate (BuAc =1)		

Flammability Limits in Air		
Upper flammability limit	Not applicable	
Lower flammability limit	Not applicable	
Vapor pressure	> 1 mmHg	@ 100 °C
Vapor density	No information available	
Specific gravity	No information available	
Bulk density	No information available	
Relative density	1.03 - 1.04 sg	@ 20-25°C.
Water solubility	Miscible with water.	
Solubility in other solvents	No information available	
Autoignition temperature	230 °C / 446 °F	
Decomposition temperature	No information available	
Kinematic viscosity	5.46 cSt	
Dynamic viscosity	No information available	
Log Pow	-0.38 (Log Kow)	
Explosive properties	No information available	
Oxidizing properties	No information available	

9.2 Other information

Pour point	No information available
Molecular weight	No information available
VOC content(%)	25%
Density	No information available

10. Stability and reactivity

10.1 Reactivity

Corrosive.

10.2 Chemical stability

Stable under normal temperature conditions and recommended use.

10.3 Possibility of Hazardous Reactions

Hazardous polymerization

Not known.

10.4 Conditions to avoid

Avoid heat, flames and other sources of ignition.

10.5 Incompatible materials

Acids.

10.6 Hazardous decomposition products

See also section 5.2.

11. Toxicological information

11.1 Information on toxicological effects

Acute toxicity

Inhalation	Vapors may irritate throat and respiratory system. Inhaled corrosive substances can lead to a toxic edema of the lungs.
Eye contact	Causes burns. May cause irreversible damage to eyes.
Skin contact	Causes severe skin burns.
Ingestion	Ingestion may cause gastrointestinal irritation, nausea, vomiting and diarrhea.

Component	LD50 Oral	LD50 Dermal	LC50 Inhalation
Polyether amine	= 242 mg/kg (Rat)	= 360 mg/kg (Rabbit)	No data available
Polyether amine acetate	No data available	No data available	No data available

Sensitization	This product does not contain any components suspected to be sensitizing.
Mutagenic effects	This product does not contain any known or suspected mutagens.
Carcinogenicity	This product does not contain any known or suspected carcinogens.

Reproductive toxicity	This product does not contain any known or suspected reproductive hazards.
Routes of exposure	Skin contact. Eye contact. Inhalation.
Routes of entry	Skin contact. Eye contact. Inhalation.
Specific target organ toxicity (single exposure)	Not classified
Specific target organ toxicity (repeated exposure)	Not classified.
Aspiration hazard	No hazard from product as supplied.

12. Ecological information

12.1 Toxicity

The product component(s) are not classified as environmentally hazardous. However, this does not exclude the possibility that large or frequent spills can have a harmful or damaging effect on the environment.

Toxicity to algae
This product is not considered toxic to algae.

Toxicity to fish
This product is not considered toxic to fish.

Toxicity to daphnia and other aquatic invertebrates
This product is not considered toxic to invertebrates.

Component	Toxicity to fish	Toxicity to algae	Toxicity to daphnia and other aquatic invertebrates
Polyether amine	No information available	No information available	No information available
Polyether amine acetate	No information available	No information available	No information available

12.2 Persistence and degradability

Product is not biodegradable.

12.3 Bioaccumulative potential

Does not bioaccumulate.

Log Pow

-0.38 (Log Kow)

12.4 Mobility in soil

Mobility

The product is miscible with water. May spread in water systems.

12.5 Results of PBT and vPvB assessment

Not classified as PBT/vPvB by current EU criteria.

12.6 Other adverse effects.

None known.

13. Disposal considerations

13.1 Waste treatment methods

Waste from residues / unused products

Dispose of in accordance with local regulations.

Contaminated packaging

Empty containers should be taken for local recycling, recovery or waste disposal.

EWC Waste disposal No.

According to the European Waste Catalogue, Waste Codes are not product specific, but application specific. Waste codes should be assigned by the user based on the application for which the product was used. The following Waste Codes are only suggestions: EWC waste disposal No: 07 01 04 Waste Code: 7152 Organic waste without halogen.

14. Transport information

14.1 UN Number

UN/ID No. (ADR/RID/ADN/ADG)	UN2735
UN No. (IMDG)	UN2735
UN No. (ICAO)	UN2735

14.2 Proper shipping name

AMINES, LIQUID, CORROSIVE, N.O.S. (Contains Poly ether amine)

14.3 Hazard class(es)

ADR/RID/ADN Hazard class	8
IMDG Hazard class	8
ICAO Hazard class/division	8

14.4 Packing group

ADR/RID/ADN Packing Group	III
IMDG Packing group	III
ICAO Packing group	III



14.5 Environmental hazard

No

14.6 Special precautions

Hazard identification no (ADR)	80
EmS (IMDG)	F-A, S-B
Emergency action code	2X
Tunnel restriction code	(E)
Hazchem code ADG	X2

14.7 Transport in bulk according to Annex II of MARPOL 73/78 and the IBC Code

Please contact MISDS@slb.com for info regarding transport in Bulk.

15. Regulatory information

15.1 Safety, health and environmental regulations/legislation specific for the substance or mixture

Germany, Water Endangering Water endangering class = 1
Classes (VwVWS)

Australian Standard for the Uniform Scheduling of Drugs and Poisons
No Poisons Schedule number allocated

New Zealand hazard classification Corrosive

HSNO approval no. HSR002491

Group number 8.3A, 8.2C

Commission Regulation (EU) No 453/2010 of 20 May 2010 amending Regulation (EC) No 1907/2006 of the European Parliament and of the Council on the Registration, Evaluation, Authorisation and Restriction of Chemicals (REACH). Regulation (EC) No 1907/2006 of the European Parliament and of the Council of 18 December 2006 concerning the Registration, Evaluation, Authorisation and Restriction of Chemicals (REACH), establishing a European Chemicals Agency, amending Directive 1999/EC and repealing Council Regulation (EEC) No 793/93 and Commission Regulation (EC) No 1488/94 as well as Council Directive 76/769/EEC and Commission Directives 91/155/EEC, 93/67/EEC, 93/105/EC and 2000/21/EC, including amendments.

This safety data sheet complies with the requirements of Regulation (EC) No. 1272/2008.

National Code of Practice for the Preparation of Material Safety Data Sheets 2nd Edition [NOHSC: 2011 (2003)].

National Occupational Health and Safety Commission's Approved Criteria for Classifying Hazardous Substances [NOHSC:1008 (2004) 3rd Edition].

National Occupational Health and Safety Commission's Exposure Standards for Atmospheric Contaminants in the occupational Environment [NOHSC:1003 (1995)].

Safe Work Australia.

Standard for the Uniform Scheduling of Drugs and Poisons (SUSDP).

ADG Code – Australian Dangerous Goods Code.

Dutch Mining Regulations: In accordance with Mining Regulations 9.2 and Chapter 4 of the Working Conditions Decree.

International inventories

USA (TSCA)	Complies
European Union (EINECS and ELINCS)	Complies
Canada (DSL)	Complies
Philippines (PICCS)	Complies
Japan (ENCS)	Complies
China (IECSC)	Complies
Australia (AICS)	Complies
Korean (KECL)	Complies
New Zealand (NZIoC)	Complies

Restricted for use in Europe until REACH assessed. Please contact REACH@miswaco.slb.com if intended for use in Europe.

15.2 Chemical Safety Report

No information available

16. Other information

Prepared by	Global Regulatory Compliance - Chemicals (GRC - Chemicals) , Anne Karin (Anka) Fosse
Supersedes date	13/Sep/2013
Revision date	06/Feb/2015
Version	5

AMC SHALEHIB ULTRA™

CLAY & SHALE STABILISERS



Description

AMC SHALEHIB ULTRA™ is an amine based product that provides superior shale and clay inhibition in polymer based drilling fluids. Effective in formations containing shale and reactive clay AMC SHALEHIB ULTRA™ reduces the potential for bit balling, torque and drag as well as other clay and shale related issues. All this is delivered by a product that has a minimal chloride content, making it far more environmentally acceptable than potassium chloride, which is typically used for inhibition.

Application

AMC SHALEHIB ULTRA™ is a liquid inhibitor that acts as a clay hydration suppressant by restricting the space between clay platelets, preventing water molecules from entering which normally results in clay swelling. It is important to observe the condition of cuttings at the shakers – sticky or soft cuttings may indicate insufficient inhibition as a result of depleted AMC SHALEHIB ULTRA™.

Typical Physical Properties

Appearance:	Pale to dark amber liquid
Specific gravity:	1.0 – 1.1
pH:	9 – 11
Solubility:	Soluble in water

Recommended Treatment

AMC SHALEHIB ULTRA™ should be added to the system before drilling into the troublesome shale or hydratable clay section.

The recommended concentration is 1.0 – 3.5% by volume, with concentration ultimately depending on shale reactivity and the amount present in the section to be drilled.

AMC SHALEHIB ULTRA™ is consumed as the formation is drilled and a proper concentration must be maintained. For optimum results, monitor penetration rates, rheology, dilution and solids control and adjust hourly treatment as necessary.

Advantages

- Prevents swelling of clay and shales
- Provides excellent shale inhibition
- Low chloride content
- Environmentally acceptable
- Compatible with most water based systems
- Prevents bit balling
- Reduces torque and drag
- Maintains cuttings integrity.

Please Note: Several factors will dictate the most appropriate concentration rate. Please contact your nearest AMC representative for optimum results.

ASIA PACIFIC

Perth, Australia (Head Office)

T +61 8 9445 4000

E amc@imdexlimited.com

Indonesia

T +62 (0) 21 759 11244

AFRICA

South Africa

T +27 (11) 908 5595

EUROPE

Germany

T +49 4402 6950-0

United Kingdom

T +44 (0) 1273 405 975

SOUTH AMERICA

Argentina

T +54 (9) 261 426 1116

Brazil

T +55 (47) 3404 5920

Chile

T +56 (2) 2589 9300

Peru

T +51 (1) 322 8850

NORTH AMERICA

USA / Canada

T +801-364-0233

Mexico

T +52 (871) 169 2095

Bibliography

References

1. Christidis, G., *Industrial clays*. EMU Notes in Mineralogy, 2011. **9**: p. 341-414.
2. Bohor, B. and R.E. Hughes, *Scanning electron microscopy of clays and clay minerals*. Clays and Clay Minerals, 1971. **19**(1): p. 49-54.
3. Bloys, B., et al., *Designing and managing drilling fluid*. Oilfield Review, 1994. **6**(2): p. 33-43.
4. Khodja, M., et al., *Shale problems and water-based drilling fluid optimisation in the Hassi Messaoud Algerian oil field*. Applied Clay Science, 2010. **49**(4): p. 383-393.
5. Sadiq, R., et al., *Risk-based decision-making for drilling waste discharges using a fuzzy synthetic evaluation technique*. Ocean Engineering, 2004. **31**(16): p. 1929-1953.
6. Haut, R., et al. *Minimizing Waste during Drilling Operations*. in *Proc. 2007 AADE National Technical Conference and Exhibition*. 2007.
7. Bland, R., et al. *Low salinity polyglycol water-based drilling fluids as alternatives to oil-based muds*. in *SPE/IADC Asia Pacific Drilling Technology*. 1996. Society of Petroleum Engineers.
8. Young, S. and J. Friedheim. *Environmentally friendly drilling fluids for unconventional shale*. in *Offshore Mediterranean Conference and Exhibition*. 2013. Offshore Mediterranean Conference.
9. Sharma, V.P. and V. Mahto. *Studies on less expansive environmentally safe polymers for development of water based drilling fluids*. in *SPE Asia Pacific Oil & Gas Conference and Exhibition*. 2006. Society of Petroleum Engineers.
10. Zhou, J., *A New Application of Potassium Nitrate as an Environmentally Friendly Clay Stabilizer in Water-Based Drilling Fluid*. 2015.
11. Glaser, K.S., et al., *Seeking the sweet spot: Reservoir and completion quality in organic shales*. Oilfield Review, 2013. **25**(4): p. 16-29.
12. Aplin, A.C., A.J. Fleet, and J.H. Macquaker, *Muds and mudstones: Physical and fluid-flow properties*. Geological Society, London, Special Publications, 1999. **158**(1): p. 1-8.
13. Yaalon, D., *Mineral composition of the average shale: Clay Minerals Bull.*, v. 5. 1962.
14. Ballard, T.J., S.P. Beare, and T.A. Lawless, *Fundamentals of shale stabilisation: water transport through shales*. SPE Formation Evaluation, 1994. **9**(02): p. 129-134.
15. Zhang, Q., et al., *A review of the shale wellbore stability mechanism based on mechanical-chemical coupling theories*. Petroleum, 2015. **1**(2): p. 91-96.
16. CRC, D., *September 2017: DET CRC Technical Press Release: RoXplorer® Coiled Tubing Drill Rig Successfully Drills Consolidated and Unconsolidated Cover Rocks and Basement and Delivers Representative Samples*. 2017.
17. Nelson, M. *Removal of Fine Solids from Weighted Mud*. in *Drilling and Production Practice*. 1970. American Petroleum Institute.
18. Mohan, K.K., et al., *Water sensitivity of sandstones containing swelling and non-swelling clays*, in *Colloids in the Aquatic Environment*. 1993, Elsevier. p. 237-254.
19. Laird, D.A., *Influence of layer charge on swelling of smectites*. Applied clay science, 2006. **34**(1-4): p. 74-87.
20. Villar, M., R. Gómez-Espina, and L. Gutiérrez-Nebot, *Basal spacings of smectite in compacted bentonite*. Applied Clay Science, 2012. **65**: p. 95-105.
21. Dixon, J.B. and D.G. Schulze, *Soil mineralogy with environmental applications*. 2002: Soil Science Society of America Inc.
22. Sridharan, A. and P. Satyamurty, *Potential-distance relationships of clay-water systems considering the Stern theory*. Clays and Clay Minerals, 1996. **44**(4): p. 479-484.
23. Mojid, M. and H. Cho, *Estimating the fully developed diffuse double layer thickness from the bulk electrical conductivity in clay*. Applied clay science, 2006. **33**(3-4): p. 278-286.

24. Wilson, M., L. Wilson, and H. Shaw, *Clay mineralogy and shale instability: an alternative conceptual analysis*. Clay Minerals, 2014. **49**(2): p. 127-145.
25. Bailey, L., et al., *Effect of clay/polymer interactions on shale stabilization during drilling*. Langmuir, 1994. **10**(5): p. 1544-1549.
26. Anderson, R., et al., *Clay swelling—a challenge in the oilfield*. Earth-Science Reviews, 2010. **98**(3-4): p. 201-216.
27. Reid, P., B. Dolan, and S. Cliffe. *Mechanism of shale inhibition by polyols in water based drilling fluids*. in *SPE International Symposium on Oilfield Chemistry*. 1995. Society of Petroleum Engineers.
28. Van Olphen, H., *An introduction to clay colloid chemistry: for clay technologists, geologists, and soil scientists*. 1977.
29. Norrish, K., *The swelling of montmorillonite*. Discussions of the Faraday society, 1954. **18**: p. 120-134.
30. Khandal, R. and T.F. Tadros, *Application of viscoelastic measurements to the investigation of the swelling of sodium montmorillonite suspensions*. Journal of colloid and interface science, 1988. **125**(1): p. 122-128.
31. Madsen, F.T. and M. Müller-Vonmoos, *The swelling behaviour of clays*. Applied Clay Science, 1989. **4**(2): p. 143-156.
32. Kraehenbuehl, F., et al., *Study of the water-bentonite system by vapour adsorption, immersion calorimetry and X-ray techniques: I. Micropore volumes and internal surface areas, following Dubinin's theory*. Clay Minerals, 1987. **22**(1): p. 1-9.
33. Van Oort, E., *On the physical and chemical stability of shales*. Journal of Petroleum Science and Engineering, 2003. **38**(3-4): p. 213-235.
34. Van Oort, E., A. Hale, and F. Mody. *Manipulation of coupled osmotic flows for stabilisation of shales exposed to water-based drilling fluids*. in *SPE annual technical conference and exhibition*. 1995. Society of Petroleum Engineers.
35. van Oort, E., et al., *Transport in shales and the design of improved water-based shale drilling fluids*. SPE drilling & completion, 1996. **11**(03): p. 137-146.
36. Joel, O., U. Durueke, and C. Nwokoye, *Effect of KCl on rheological properties of shale contaminated water-based MUD (WBM)*. Global Journals Inc.(USA), 2012. **12**(1).
37. Bell, J., *Practical methods for estimating in situ stresses for borehole stability applications in sedimentary basins*. Journal of Petroleum Science and Engineering, 2003. **38**(3-4): p. 111-119.
38. Moore, P.L., *Drilling practices manual*. 1986.
39. Marthinussen, S.-A., *The Effect of Fluid Viscosity on Hydrocyclone Performance: Design and Commissioning of an Experimental Rig and Results*. 2011, The University of Bergen.
40. Chenevert, M. and S. Osisanya, *Shale/mud inhibition defined with rig-site methods*. SPE Drilling Engineering, 1989. **4**(03): p. 261-268.
41. Horsrud, P., et al. *Interaction between shale and water-based drilling fluids: laboratory exposure tests give new insight into mechanisms and field consequences of KCl contents*. in *SPE Annual Technical Conference and Exhibition*. 1998. Society of Petroleum Engineers.
42. Molenaar, M., J. Huyghe, and P. Van Den Bogert. *A constitutive model for swelling shales*. in *SPE/ISRM Rock Mechanics in Petroleum Engineering*. 1998. Society of Petroleum Engineers.
43. Huang, H., J. Azar, and A.H. Hale. *Numerical simulation and experimental studies of shale interaction with water-base drilling fluid*. in *IADC/SPE Asia Pacific Drilling Technology*. 1998. Society of Petroleum Engineers.
44. Basma, A.A., S.A. Barakat, and M. Omar, *Modeling time dependent swell of clays using sequential artificial neural networks*. Environmental & Engineering Geoscience, 2003. **9**(3): p. 279-288.
45. Zhong, H., et al., *Bis (hexamethylene) triamine as potential shale inhibitor in water-based drilling fluid*. Open Petroleum Engineering Journal, 2013. **6**(1): p. 49-56.

46. Qu, Y., et al., *Polyoxyalkyleneamine as shale inhibitor in water-based drilling fluids*. Applied Clay Science, 2009. **44**(3-4): p. 265-268.
47. Pham, H. and Q.P. Nguyen, *Effect of silica nanoparticles on clay swelling and aqueous stability of nanoparticle dispersions*. Journal of Nanoparticle Research, 2014. **16**(1): p. 2137.
48. Peng, B., et al., *Structure–property relationship of polyetheramines as clay-swelling inhibitors in water-based drilling fluids*. Journal of Applied Polymer Science, 2013. **129**(3): p. 1074-1079.
49. Ghimici, L. and S. Dragan, *Behaviour of cationic polyelectrolytes upon binding of electrolytes: effects of polycation structure, counterions and nature of the solvent*. Colloid and Polymer Science, 2002. **280**(2): p. 130-134.
50. Bol, G. *The effect of various polymers and salts on borehole and cutting stability in water-base shale drilling fluids*. in *SPE/IADC Drilling Conference*. 1986. Society of Petroleum Engineers.
51. Israelachvili, J.N., *Intermolecular and surface forces*. 2011: Academic press.
52. Karaborni, S., et al., *The swelling of clays: molecular simulations of the hydration of montmorillonite*. Science, 1996. **271**(5252): p. 1102-1104.
53. Stephens, M., S. Gomez-Nava, and M. Churan. *Laboratory methods to assess shale reactivity with drilling fluids*. in *American Association of Drilling Engineers. National Technical Conference & Exhibition, New Orleans, Louisiana*. 2009.
54. Blatt, H., R. Tracy, and B. Owens, *Petrology: igneous, sedimentary, and metamorphic*. 2006: Macmillan.
55. Folk, R.L., *Petrology of sedimentary rocks*. 1980: Hemphill Publishing Company.
56. Dubey, S. and A. Gudmundsson, *Field Study and Numerical Modeling of Fracture Networks: Application to Petroleum Reservoirs*. M&S: Schlumberger J. of Modeling, Design, and Simulation, 2012. **3**(1): p. 5-9.
57. Ronald, J., *Quantitative X-ray diffraction analysis using clay mineral standards extracted from the samples to be analysed*. Clay Minerals, 1967. **7**: p. 79.
58. Bish, D.L. and J.E. Post, *Quantitative mineralogical analysis using the Rietveld full-pattern fitting method*. American Mineralogist, 1993. **78**(9-10): p. 932-940.
59. Srodon, J., et al., *Quantitative X-ray diffraction analysis of clay-bearing rocks from random preparations*. Clays and Clay Minerals, 2001. **49**(6): p. 514-528.
60. Speakman, S.A., *Introduction to X-ray powder diffraction data analysis*. Center for Materials Science and Engineering at MIT, 2013.
61. Montañés, M., et al., *Evolution with exposure time of copper corrosion in a concentrated lithium bromide solution. Characterization of corrosion products by energy-dispersive X-ray analysis and X-ray diffraction*. Corrosion, 2006. **62**(1): p. 64-73.
62. Calabria, J.A., et al., *Determination of the cation exchange capacity of bentonite exposed to hyperalkaline fluid*. 2013.
63. Buckman, H.O. and N.C. Brady, *The nature and properties of soils*. Soil Science, 1960. **90**(3): p. 212.
64. Pittman, E. and J. Thomas, *Some applications of scanning electron microscopy to the study of reservoir rock*. Journal of Petroleum Technology, 1979. **31**(11): p. 1,375-1,380.
65. Roehl, E.A. and J.L. Hackett. *A laboratory technique for screening shale swelling inhibitors*. in *SPE Annual Technical Conference and Exhibition*. 1982. Society of Petroleum Engineers.
66. Ewy, R.T. and E.K. Morton. *Shale swelling tests using optimized water content and compaction load*. in *SPE Western Regional Meeting*. 2009. Society of Petroleum Engineers.
67. Hale, A., *Method to quantify viscosity effects on dispersion test improves testing of drilling-fluid polymers*. SPE Drilling Engineering, 1991. **6**(01): p. 44-50.
68. Temple, C. and A. Youngson, *Drilling fluids with improved shale inhibition and methods of drilling in subterranean formations*. 2010, Google Patents.

69. Wilcox, R., J. Fisk Jr, and G. Corbett, *Filtration method characterizes dispersive properties of shales*. SPE Drilling Engineering, 1987. **2**(02): p. 149-158.
70. Benoit, D., et al. *Obtaining Comparable and Relevant Formation Swelling Sensitivity Data from CST: Is this Even Possible?* in *SPE International Conference and Exhibition on Formation Damage Control*. 2016. Society of Petroleum Engineers.
71. Pagels, M., J.J. Hinkel, and D.M. Willberg. *Measuring capillary pressure tells more than pretty pictures*. in *SPE International Symposium and Exhibition on Formation Damage Control*. 2012. Society of Petroleum Engineers.
72. Pagels, M., J.J. Hinkel, and D.M. Willberg. *Moving Beyond the Capillary Suction Time Test*. in *SPE International Symposium and Exhibition on Formation Damage Control*. 2012. Society of Petroleum Engineers.
73. Patel, A.D. *Design and development of quaternary amine compounds: shale inhibition with improved environmental profile*. in *SPE International Symposium on Oilfield Chemistry*. 2009. Society of Petroleum Engineers.
74. Gomez, S. and W. He. *Laboratory method to evaluate fracture development in hard shale formations exposed to drilling fluids*. in *PaperAADE-06-DF-HO-38 presented at the AADE Fluids Technical Conference, Houston*. 2006.
75. Vanorio, T., *Recent advances in time-lapse, laboratory rock physics for the characterization and monitoring of fluid-rock interactions*. Geophysics, 2015. **80**(2): p. WA49-WA59.
76. Barati, P., et al., *Shale hydration inhibition characteristics and mechanism of a new amine-based additive in water-based drilling fluids*. Petroleum, 2017. **3**(4): p. 476-482.
77. Villabona-Estupiñán, S., J. de Almeida Rodrigues, and R.S.V. Nascimento, *Understanding the clay-PEG (and hydrophobic derivatives) interactions and their effect on clay hydration and dispersion: A comparative study*. Applied Clay Science, 2017. **143**: p. 89-100.
78. Scientific, H., *A guidebook to particle size analysis*. Horiba Instruments, Inc, 2012: p. 1-29.
79. Shimizu, T., et al. *Experimental Analysis of ESP Performance in Pipe Flows Including Methane Hydrate*. in *SPE/IATMI Asia Pacific Oil & Gas Conference and Exhibition*. 2015. Society of Petroleum Engineers.
80. Quintero, L. and T.A. Jones. *An alternative drill-in fluid system for low-pressure reservoirs*. in *SPE European Formation Damage Conference*. 2003. Society of Petroleum Engineers.
81. Ronaes, E., et al. *Remote real-time monitoring of particle size distribution in drilling fluids during drilling of a depleted HTHP reservoir*. in *Middle East Drilling Technology Conference & Exhibition*. 2009. Society of Petroleum Engineers.
82. Kartnaller, V., et al., *Laser beam backscattering as a new tool to study the effect of inhibitors on shale particles-water interactions: A real-time analysis*. APPLIED CLAY SCIENCE, 2017. **150**(1): p. 89-97.
83. Gomez, S.L. and A. Patel. *Shale inhibition: what works?* in *SPE International Symposium on Oilfield Chemistry*. 2013. Society of Petroleum Engineers.
84. Ali, S. and R. Bandyopadhyay, *Use of ultrasound attenuation spectroscopy to determine the size distribution of clay tactoids in aqueous suspensions*. Langmuir, 2013. **29**(41): p. 12663-12669.
85. Instruments, M., *Mastersizer 3000 user manual*. 2007, Malvern Instruments Worcestershire, United Kingdom.
86. Chhabra, R.P., *Bubbles, drops, and particles in non-Newtonian fluids*. 2006: CRC press.
87. Negro, C., et al., *Methodology for flocculant selection in fibre-cement manufacture*. Cement and Concrete Composites, 2006. **28**(1): p. 90-96.
88. Sabin, A., *Problems in particle size: laser diffraction observations*. Journal of GXP Compliance, 2011. **15**(4): p. 35-44.
89. Hoxha, B.B., et al., *Automated Particle Size Analysis using Advanced Analyzers*. 2016, AADE-16-FTCE-78, Houston Texas.

90. Fabris, A.J., *Mineral Systems Drilling Program in the southern Gawler Ranges, South Australia*. 2017: Department for the Premier and Cabinet.
91. Elimelech, M., J. Gregory, and X. Jia, *Particle deposition and aggregation: measurement, modelling and simulation*. 2013: Butterworth-Heinemann.
92. Clark, R., et al., *Polyacrylamide/potassium-chloride mud for drilling water-sensitive shales*. *Journal of Petroleum technology*, 1976. **28**(06): p. 719-727.
93. Fraser, L., *New method accurately analyzes PHPA's in muds*. *Oil Gas J.*;(United States), 1987. **85**(27).
94. Schlumberger, *Oilfield Glossary*.
95. Trifunoski, O., *Evaluation of the use of recycle material as lost circulation material*, in *Department of Petroleum Engineering*. 2017, Curtin University. p. 39.
96. Keinath, B., et al. *Investigation of produced oil-water emulsions and sensitivities to shear rate, water chemistry and oil field chemicals*. in *10th North American Conference on Multiphase Technology*. 2016. BHR Group.

Every reasonable effort has been made to acknowledge the owners of copyright material. I would be pleased to hear from any copyright owner who has been omitted or incorrectly acknowledged.